OH LIPIDS, THE PLACES WE HAVE GONE

by

De'Shovon Mone' Shenault

A Dissertation

Submitted to the Faculty of Purdue University

In Partial Fulfillment of the Requirements for the degree of

Doctor of Philosophy

Department of Chemistry

West Lafayette, Indiana

August 2023

THE PURDUE UNIVERSITY GRADUATE SCHOOL
STATEMENT OF COMMITTEE APPROVAL

Dr. Scott A McLuckey, Chair
Department of Chemistry

Dr. Julia Laskin
Department of Chemistry

Dr. Angeline M. Lyon
Department of Chemistry

Dr. Shalini T. Low-Nam
Department of Chemistry

Approved by:
Dr. Christine A. Hrycyna

Dedicated to my Heavenly Father Hashem; your plans & love for me is unmatched. I can't imagine what the future holds but excited for the ride.

Carmel Latte you are the best gift amazon couldn't deliver.

&

To my Grandmothers Genola Williams and Jessie Allen, I hope to be a blueprint to the younger generation and continue your legacy.

ACKNOWLEDGMENTS

In all things that I do I want to give you praise, glory and honor. Thank you, Hashem, for not just saving my life, but giving me a new life that outweighed my expectations. Never in my wildest dreams, I seen me becoming a scientist, let alone a doctor. Your love has transformed me into a better woman. I pray that I represent you in every area of my life. Thank you for allowing my life to represent scriptures: Yirmeyahu (Jeremiah), 1:5 "“Before I formed you in the belly I knew you, and before you came out of the womb I did set you apart – I appointed you a prophet to nations.”" and Yirmeyahu (Jeremiah) 29:10-14, "“For thus said יהוה, ‘When seventy years are completed, at Baḇel I shall visit you and establish My good word toward you, to bring you back to this place. For I know the plans I am planning for you,’ declares יהוה, ‘plans of peace and not of evil, to give you a future and an expectancy. Then you shall call on Me, and shall come and pray to Me, and I shall listen to you. And you shall seek Me, and shall find Me, when you search for Me with all your heart. And I shall be found by you,’ declares יהוה, ‘and I shall turn back your captivity, and shall gather you from all the nations and from all the places where I have driven you, declares יהוה. And I shall bring you back to the place from which I have exiled you.’" Hashem, your work is not finished, and I have so much more to do. Father, please continue to equip me for the task ahead. May I walk in your truth and continue to proclaim your name.

To my parents in the faith Corey and Regina Wilson, as tears stream down my face, “We Did It”. You have played a major role in my new life. I don’t know what I would have done without your support, encouragement, teaching, disciplining and love. May Hashem shower you with gifts past your expectations. I don’t have the words to express my love to you, but I pray one day I could repay you for your dedication in my life this last almost 11 years. I am so thankful that Iesha invited me to the Way Christian Ministries. The visit changed the trajectory of my life and thankful that I found you on the course. I look forward to the new skill that will develop inside of me and the fruit that I will produce.

Danny Dominque Smith (Carmel Latte), if you looked in the dictionary under the words Prince Charming, there would be a huge picture of you smiling with a plate of spinach & eggs with a side of potato patties. I never thought in my wildest dreams, our path will cross, and I will be becoming your wife. As a woman who went through so much hurt, disappointment and pain, the idea was never on my radar. I’m thankful that Hashem plan was different then mines. Thank you

for loving me the way you have. You have showered me with so much peace, trust, and stability. I don't think I would have made it through this last year without you. I pray that I can represent the woman you would be proud to call wife and mother of your children. Get ready for an amazing ride. Counting down the days to Mrs. Smith!

To my Daddy Wilbert Thomas-Jason and Stepmom Sylvia Alexander, when I was a small child, I would envision the kind of parents that I wanted. The things that they would teach me, the place we would go, and the memories that we will make. I'm thankful that I found that. Thank you for taking me under your wings and loving me like I was your own. Sylvia, I appreciate your heart and sacrifice over the years. Please know it hasn't been in vain. Daddy, I love you so much, even though you purposely drive me crazy, please know that I allow it. Thank you for not just helping me in school but wanting to be engaged with my work. Your love and encouragement pushed me when I wanted to quit. I truly hope you are proud of what you help produce. Your legacy has not fallen on death ears. Thank you for being the crazy daddy I would clear a room for.

To my family, my mother Elzena Shenault, sister Amorita Williams and brother Edward Williams, I hope I have represented the family in a positive light and open new door for the younger generation to come. Going through this experience has shown me the type of strive and tough skin you need to have in pursue your dreams. Thank you for allowing me to set the path. I pray that grandma's Genola and Jessie are pleased with the woman I have become. May they strength and dedication live on through me.

To my Laura O. Williams, thank you for being you. I know you say all the time that you don't do anything, but you honestly do more than enough. You have made this grad school experience worth having. Through so much loss, I am thankful to have kept you. You are not just a friend but a sister. I can't wait to see your dreams come true and get all that you deserve. I pray you truly understand how special you are to me. Dr. Williams, continue to shine bright and know that I am here rooting you ahead.

To my Jamaican honey Shanica M. Brown, when I say you are the true definition of what they call a Jamaican. To the future Dr. Shanica, you hold a special place in my heart. I love your crazy self. Thank you for all you have done for me. For the talks, goofy texts and all the home visits. You will always get a plate out of me. I can't wait to share in your success. Continue to be a free spirit.

To my KeKe (Kiera M. Estes), who knew that a run in at a card table would give me not just a little sister but a brother (Tyree Estes) and big sister (Tamara Estes) for life. Usually when you marry a person, you marry there family too but somehow in our relationship, we ended up marrying each other. Lord knows we have shared more laughs then tears. I love the person that you are. Never change or conform who you are. You are amazing just the way you are. I can't wait to call you Dr. Estes and see where the wind takes you.

To my E (Elissia T. Franklin), I am blessed to have crossed paths with you. You are an amazing woman and scientist; I hope you understand the greatness inside of you. I have always admired your drive and love for all things black. Continue to shine bright in the midst of darkness. Your future is brighter than you could ever imagine. I'm excite that I get to cheer on the outside. I love the woman you are and excited to see what your journey bring.

To Ant (Anthony Pitts-McCoy), as I write this message to you, I don't have the words to express my gratitude. With all my love, thank you. I truly thank you for helping me transition into graduate school and helping to sustain me here, it truly takes a village. I'm happy that you where apart of mine. I'm thankful that I had you as a mentor and friend. May Hashem open doors you want believe and shower you with endless possibilities.

To Femi (Oluwafemi Uzoma Ogunlalu), I owe a major debt to you. Femi, I can't thank you enough for just being you. I can't believe I get to honor you in this way. Femi, I truly thank you for every cume you stayed up and studied with me, when you had been done for months. For joining calls in another country to help me with my original proposal. For every cooking lesion and cultural understanding, but most of all, for every encouragement you gave and continue to give. I truly can't thank you enough. Dr. Femi, I appreciate you so much and can't wait to see where the Lord take you. Please know I will be there enjoying the ride with you and benefiting from the blessings.

To my brother from another mother, Edwin (Louis E Gonzalez) you are the best male friend a girl could ask for. Since day one, you have shown me the type of man and friend you can be, and I love you for it. You are such an amazing scientist, and any job would be blessed to have you. To my basement friend, and future Dr., thank you for the many laughs shared and endless tea given. I appreciate you and Aymi for always opening your doors and for all the snuggles the puppies gave. I can't wait to hear about your new puppy you get.

To my Shine Bright Like a Diamond (Diamond Ross), it gives me great pleasure to add you to my acknowledgement. Diamond, I don't have the words to express how thankful I am to be your friend. In just a short amount of time, you have become a sister, split from the same pea, embarking on a crazy journey together. I cannot thank you enough for every encouraging word given. Thank you for reinforcing who I am and the woman that I will become. For every laugh, tears shared with encouraging words. For every organization tip and book, I need to read. For preparing me for things I never thought to think of, I thank you. Diamond, I couldn't have done this program without you. Your love has pushed me to the finish line, and I am thankful to share this journey with you. I pray that your heart desires come to pass, and we share in this new chapter together. May Hashem grace blow you away this year and the ones to come.

To my Temi (Dr. Temitope Adeoye-Olenloa), who knew I would get a friend/sister for life from a paint and Thai night. The funny thing about that event, was the fact I planned on missing it. I was worn out from classes and didn't feel like being around people, but I am truly blessed that I came. You have seriously been an amazing person to me. I thank you for sharing the HeadsUP after school and teen mentoring program with me. Having the kids really increased my faith in my program and gave me the drive I needed. Temi, we have shared so much together, and I can't wait to share even more with you. Thank you for being an important part of my graduate career and spiritual faith. I love you more than you know, and I can't wait to share the married club with you. I pray endless blessings over you and provision in the steps you take. May I enjoy many more memories with you.

To the family and friends that I have lost in the physical world, the new generation to come and my godchildren (Jeremy Highsmith, Chrisette Willis, Keven Haley and Kanien Haley). May I be one example and not the end of your journey. Please know that you are physically and wonderfully made, the drive is already in you. Claim the journey and walk the path. It starts with you. Hashem has equipped you do his good work, know that I am here to push you along the way. You will do better things then me and I am excited to share in your accomplishment.

To all my mentors: Dr. Valerie Goss, Dr. Leroy Jones II, Dr. Chasity Love and Dr. Christopher Pulliam. The saying goes, it takes a village to raise a child, that also goes for the development of a scientist. It took all of you to educate, inspire, equip, push, and sometimes pull to the finish line. The many times I called and begged to quit the program, but you all encouraged me to stay. Thank you for all always tell me the truth, reading every paper and listening to presentations.

Your time was not spent in vain, and I am thankful to have you in my life. I pray many blessings over your life and look forward to being the doctor you knew I could be.

To the McLuckey group, past (John Lawler, Hsi-Chun Chao, Chris Harrilal, Abdirahman Abdillahi, Josh Johnson, Kenny Lee, Jay Bhanot, Nan Wang, Feifei Zhao, Caitlin Randolph, Mack Shih, Sarju Adhikari, Elissia T. Franklin, and Anthony Pitts-McCoy) and present (Ian Carrick, Kimberly C. Fabijanczuk, Nicole Michelle Brundridge, Sarah Twumwah Nsiah, Liangxuan Fu (Alex), Nicolas Josef Pizzala, Samantha A. Mehnert, Shelby Shannon Peterkin, Jordan Michael Fritz, and Joseph William Keating) students, it has been a pleasure sharing a space and ideas with you. You guys are awesome, and I wish you amazing futures to come. To Dr. Abdi, I thank you for being an amazing friend to me. I was lucky to have your wisdom and help transiting into the program. To future Dr. Nicole, you have been an amazing friend and office mate. I am so thankful for your friendship and look forward for fairytale story. To the future Dr. Sarah and Shelby, may you never forget who you are and conform to society idea of what your Blackness should sound or look like. You are here and no one can change that. Please TRUST your abilities and make beauty out of your mistakes, may it never leave your thoughts.

To my principal investigator Scott A. Mcluckey, Scott you believed in me when I didn't believe in myself. There were times when I found myself unworthy of being in your group. With the struggles faced as a young scientist, the unwarranted harassment from older grad student and the struggles of being a Black woman in a predominately white institution, yet you still encourage me to keep going. Thank you for showing me that I can be a great scientist. I appreciate all the talks we have had and the motivational speeches you gave. Thank you for being a great PI and I pray for much more success in the future. Thank you, Dr. Angeline Lyon, and Dr. Julia Laskin, for being great advisors and granting me my PhD candidacy. Angeline, I appreciate your trust and friendship during my graduate career. Thank you allowing me to oversee Chemistry Diversity Inclusion (CDI) and contribute to the world of science.

Lastly but not least, to De'Shovon Mone' Shenault, I am so proud of you. Seriously, I am beyond proud of you. Look at the woman you have become. On August 5, 2012, Hashem didn't just change your life, but he has given you a new one. My wildest dreams could not compare to the life that I have now, and I owe it all to you Hashem, my Elohim (King of the Universe). May I never forget my values, my abilities to do all things through him who strengthens me, to celebrate small success and to always smile and laugh. You have worked hard to get to this point and now

it’s time to reap the benefits of your SUCCESS. Promise me, that you will trust the strengthen in you. Promise me you will strive daily to be a better version of yourself. The baby in you is so proud of you and can’t wait to see were the scroll of life take you. Grab every moment by storm and take it all in. You have done enough.

TABLE OF CONTENTS

LIST OF TABLES

LIST OF FIGURES

LIST OF SCHEMES

CHAPTER 1. INTRODUCTION

1.1 Interlude

I titled my dissertation, “Oh Lipids, The Places We Have Gone.”, based off one of my favorite childhood books by Dr. Suess. I was reminded of the book, “Oh, the places you’ll go” by my mentor Dr. Valerie Goss and close friend Alicia Nesbary-Moore, at my farewell party to graduate school. Ironically, I received two of the same books, with similar meaning behind them, however, I would soon learn the meaning at the end of my journey. As many students, embarking on another chapter in life, I didn’t understand the magnitude of what this book would do for me and to me. So, I want to take you on my journey.

After my acceptance into graduate school, my tunnel vision only saw food chemistry as the end goal for my graduate career. I didn’t have a plan on how I would become a food scientist, nor the division or classes needed to accomplish this goal; but I knew one thing, when I said yes to Purdue University, I was on the path… Or so I thought. The real path started with my introduction into the world of analytical chemistry at recruitment weekend. I was clueless with what Purdue University had to offer as far as research or careers. So, during recruitment weekend I made sure I asked the questions needed to make a sound decision. I was given seminars and accolades regarding Purdue University being part of the Top 10 Universities in Analytical Chemistry and Engineering for the past decade. However, I didn’t understand at the time how Analytical Chemistry will be the steppingstone I needed to become the food chemist I dreamed about.

In the schedule given for recruitment weekend, faculty comingle with prospective students, to answer any questions they may have about the program or research. At the first luncheon, I had the pleasure of seating at the table with Dr. Graham Cooks (Dr. Cooks). During lunch, several people came to the table bowing and taking pictures with him, which left me a little puzzled. Who was the man I was seating next too? After a free moment to speak opened for Dr. Cooks, he kindly introduced himself to me. Greeting him with my name, he looked at me with slight confusion and asked, “do you know who I am?”. With even more confusion, I said “your name is Dr. Cooks, correct”. He immediately laughed and asked me a couple of questions about myself; what made me choose Purdue University and what was my interest.

Now it was my time to shine! I introduce myself as the new food chemist, I will become. The conversation was geared around my love for food and what journey I will take as a graduate student in the chemistry department. After listening for a couple of minutes, he asked me "how would I use mass spectrometry to solve this problem"? As a response, I asked him, "what is mass spectrometry"? Students at the table gasps and Dr. Cooks laughed and said we need to take a walk to the basement of Brown (Herbert C.) Laboratory of Chemistry at Purdue University. After traveling to Brown Laboratory, Dr. Cooks escorted me to the front of Scott McLuckey research board. This is where life got confusing for me. I was looking at a board of research and had no clue what it was saying, what he was saying or why I was here? However, I noticed one thing on the board that was familiar: lipids.

During the talk, I chuckled and said, "hey, this lab does food chemistry, I see lipids on the board". Dr. Cooks paused and said, "lipids are found in more than food, but in all organisms". I was shocked! I had no clue that lipids were everywhere. After leaving the conversation, I asked myself, "What is a Lipid and are they different from food lipids"? I thought I understood this question prior to acceptance into graduate school but only had a snapshot idea of the question. Then it hit me, I was entering the first stage of wonderland academy, but didn't know classes had started for me. Soon I will learn that recruitment weekend was the enrollment period, and like the little boy in the book, I was traveling down the path.

Leaving the basement of Brown Laboratory, I ran back to the hotel to do some investigation on lipids and the questions that were posed to me. I spent the night reading manuscripts, drawing mechanisms and pictures of mass spectrometers. Just to gain some understanding, but the more I searched, the more excited and confused I became. I knew if I could grab a meeting with Scott McLuckey during the 15-minute sessions, I am certain that my question would be answered. Unfortunately, after leaving the 15-minute session, oh the places I would go became more serious than I thought.

The research about lipids opened a newfound curiosity, which is scary but exciting at the same time. In looking back, I admire how easy it was for me to welcome the new path, even with so much uncertainty and struggles along the way. I believe the curiosity and physical drive I process was the push I needed to get the level of understanding I desired from lipids. While this new path token brought many challenges, confusion, pain, excitement, joy, with thrills, I understood more of the words Dr. Suess echoed in the background.

Oh Lipids, The Places We Have Gone!

Lipids I have brains in my head and research in my hand, you have steered me on the path, I am on my way. You have taken me through challenges, and paths untold, and allowed me to wrestle through things unknown. When things started to happen, you told me not to worry and pushed me right along.

Oh Lipids, The Places We Have Gone!

Lipids you have allowed me to sore and reach new heights. You allowed me to research and discover new sites. You promoted my discoveries and goofy presentations given, you allowed me to pass and take the lead. You understood the best wasn't the end for me and allowed me to search until no end.

Except when I didn't, and sometimes I couldn't. The bang-ups and hang-ups did happen to me too. When I fell into a slump, the discoveries weren't fun anymore, un-slumping myself wasn't uneasily done. I hit a place in the path that wasn't easy to steer. The light at the path wasn't easy to fear. Do I dare to keep going? Do I dare to stay? Do I dare to keep pushing because I am on my way? As I wait in the place of uncertainties and fears, I dare to allow curiosity to not steer.

Oh, to see I am not alone on the path. Waiting to see if my train will pass.

Waiting to pass the cumes. Waiting to be a candidate. Waiting to publish my manuscriptwhile waiting to write the last chapter… Waiting Waiting Waiting.

Waiting was good but it was also bad. Waiting promoted me and developed the new me.

I am ready for anything. I am strong and fierce. I has overcome challenges; I have overcome fears.

Oh Lipids, The Places We Have Gone!

This is not the end of our journey, nor the end of the ride. I have understood the path and accepted the strives. I have passed the test and published the papers. I have joined the lipid society by producing the data. I have trained and mentored, I have recruited and sored. I have succeeded, yes, I have succeeded indeed.

Today is the day... I am surely on my way.

As I end my graduate chapter with lipids, I look ahead to the new discoveries that mass spectrometry will take me, but before I leave...

Welcome to my dissertation! I am honored that you are here. I have designed my dissertation to take you through the world of lipids through my eyes, while showcasing my contribution to the world of Lipidomics. Thank you for reading. Welcome to lipids.

1.2 Overview

Biomolecules, also known as "natural biomaterial", are organic macro and micro- molecules that consist of lipids, nucleic acids, proteins, metabolites, carbohydrates and other chemical compositions, that play essential role in the stabilization, functionality, and survival of living organisms.[1,2] Biomolecules are important precursors for enzymatic catalysts, structural and transportive messenger, energy preservers, building and breaking of other biological components; while shaping and distributing nutrients in and out of the cell. [3,4] Due to their versatility and integrity of the biomolecules, it is critical to unravel the composition and functionality of biomolecules found in living systems; one particularly, the lipid.

Lipids are defined as "hydrophobic or amphipathic small molecules that may originate entirely or in part by carbanion-based condensations of thioesters and/or by carbocation-based condensations of isoprene units".[5] In spite of its simple definition, a complex assortment of lipids is observed in an organism, that serves many roles and function for existence of the system. A class of lipids that is located in all organisms is phospholipids. Phospholipids are the major building block of the lipid bilayer; with diverse roles that involve cellular signaling, vascular cell adhesion, scaffolding support, while supporting other bioactive molecules. Two classes of phospholipids most abundantly found in eukaryotic cells are: sphingomyelins and glycerophospholipids; while other lipids such as phosphoglycolipids are found in prokaryotic cells.[6,7,8] Lipids are crucial for the survival of the cell, aiding in transportation of nutrients and other ions through the membrane; making them essential for permeability in and out of the cell. For example, in eukaryotic cells, lipids "support potential for budding, tubulation, fission and fusion, characteristics that are essential for cell division, biological reproduction and intracellular membrane trafficking".[9,10]

Lipids are necessary in building and supplying the cells with material needed to sustain survival, while facilitating energy needed to maintain cell production. For example, triglycerides are a tri-esters fatty acid, with three acyl chain bound to the glycerol backbone. This subgroup of lipids, formally called "TAGs or TGs", convert unused calories into energy for usage on de-

mand.[11,12] While TGs are crucial for energy storage in the cell, other roles of insulation and protection of the vital organs are needed from TGs.[12,13] In considering the intensive list and functions that lipids possess, researchers are only scratching the surface on the many genres of lipids. To unravel and enhance efforts in endocrinology, diabetes, metabolism and/or nutrition; there are tools needed to enhance lipid analysis, while improving characterization and identification of lipid profiles. The limited research developed for lipids has shown challenges that the field that Lipidomics present.

1.3 Lipid Diversity

As mentioned above, lipids are extraordinary molecules found in all living organisms. Lipids can be categorized into 8 different classes, such as: fatty acyls (FAs), glycerolipids (GLs), glycerophospholipids (GPs), sphingolipids (SPs), sterol lipids (STs), prenol lipids (PRs), saccharolipids (SLs), and polyketides (PKs).[5] The category of lipids contains a diverse list of subclasses, with unique descriptions associated with each lipid class. These identifiers allow for classification of lipid identity, which varies by species.[14] PKs are a subclass of SMs that are biosynthesized by polyketide-synthesis.[15,16] SLs, also known as Lipid A, has six FAs linked directly to a sugar backbone; are comprised in the outer membrane of a gram-negative bacteria.[17] PRs and STs share a similar biosynthetic pathway, but differ in structural characteristics.[18] STs, commonly called cholesterol, are four membered hydrocarbon linked to a hydroxyl group. STs are commonly found in the cell membrane, where they build and maintain fluidity and temperature.[19,20] However, PRs are "synthesized for the five-carbon precursors: isopentenyl diphosphate and dimethylallyl diphosphate"[21], which transports electrons in and out of membrane to protein in the synthesis ATP.[22] Major components found in the cell membranes are GPs and SPs. While both contains fatty acids and are amphipathic, both differ in structural diversity. SPs are a class of lipid derived from a sphingosine, containing fatty acid connected to a aliphatic amino alcohol sphingosine base backbone.[23,24] Ironically, both SPs and GPs are considered polar lipids (PL), but GPs has two fatty acids at the sn-1 and sn-2 position, esterified to a glycerol backbone and phosphate group with varying head groups.[25,26] GLs are a subclass of lipids, containing long fatty acids esterified to a glycerol backbone with or without a alcohol bonded.[27] Lastly, FAs are long or short carboxylic acids, that vary in saturation or unsaturation of aliphatic chain.[28,29]

GPs are a unique class of lipids, commonly found in the cell membrane of the eukaryotic cell, displayed in Figure 1. As mentioned above, GPs have two fatty acids at the sn-1 and sn-2 position, esterified to a glycerol backbone and phosphate group with varying headgroups, represented in Figure 1(a). Differing in headgroup arrangements, the major classes of GPs are: glycerophosphate (PA), glycerophosphocholine (PC), glycerophosphoethanolamine (PE), glycerophosphoglycerol (PG), glycerophosphoserine (PS), and glycerophosphoinositol (PI), Figure 1(b). Other GPs, such as glycerophosphoglycerophosphates (PGP), glycerophosphoinositol monophosphates (PIP), glycerophosphoinositol bis-phosphates (PIP2), glycerophosphoinositol tris-phosphates (PIP3), glyceropyrophosphates (PPA), CDP-glycerols (CDP-DG), glycosylglycerophospholipids ([glycan]GP), glycerophosphoinositolglycans ([glycan]GP)PI, glycerophosphonocholines (PnC), and glycerophosphonoethanolamines (PnE), which is represented on a comprehensive list.[5,30] Cardiolipins constitute a unique subclass of phospholipids, located in the mitochondrial membrane; sharing two phosphatidic acids groups linked to a glycerol backbone, shown in Figure 1(c).[31,32] CL are important lipids that aid in the stabilization and support in the transporting of protein and electrons through the mitochondrial membrane.[33]

GPs and GLs share similar structural components, such as fatty acids linked to a glycerol backbone, but GLs differ from GPs, lacking a phosphate group and polar headgroup. GLs lipids are exceptional class of lipids, due to how many acyl chains can bind to the carbons on the glycerol backbone. The esterification of the acyl chains, can be displayed in category of (mono-, di- or triacylglycerol), producing three subclasses lipids called monoacylglycerol (MAGs), diacylglycerol (DAGs), and triacylglycerol (TAGs).[34] In the cell membrane, DAGs are an important precursor for the "biosynthesis and degradation of triglycerides, glycerophospholipids and glycerolglycolipids".[35] In the case of TAGs, one of the most important lipid from the GLs trio, is the main form of energy and fatty acid storage located in plants and animals.[36] TAGs are remarkable in regards to function, which is dependent on where the TAG is made. For example, in the adipose tissue, glucose is needed for the making of TAGs synthesis, after production of TAGs, TAGs transported to another part of the cell, to be used as fat cells for energy.[37] While these lipids are great in the varying functions that they process, the challenge comes with how the acyl chains are linked to the glycerol backbone, how many of the acyl chains, is each acyl chain different in structure or constitutional isomers. This is the trials that scientist face in understanding the structural dynamics of the lipid composition.

One of the major contributors to the structural diversity and complexity to all lipid classes are the fatty acids (FAs). FAs are the main lipid biomolecule found in all living organisms and playing an assortment of tasks.[38] By definition, FAs are defined as "carboxylic acids with long aliphatic chains which may be straight or branched, saturated or unsaturated".[28,29] FAs can be categories by either saturated or unsaturated fatty acids. Saturated fatty acids (SFAs) are fatty acids that doesn't contain any double bond, branching, cyclopropane or other functional groups.[39] Similar to unsaturated fatty acids (USFAs), the SFAs can range from 3 to 40 carbons linked to form fatty acid. When it comes to chain development, volatile fatty acids (C_1-C_5) contribute to the development of FAs (C_6-C_{24}), which later forms long-chain FAs (C_{25}-C_{40}).[40] In reference to unsaturated fatty acids, unsaturated fatty acids are normally formed by a biogenesis reaction called desaturation, which causes enzymes to carry out this sensitive and highly selective reaction, to form varying functional groups on the acyl chain.[41] Unsaturated fatty acids can be composed of double bonds, triple bonds, cyclopropanes, branching, sugars, trans and cis, and etc.[42–44] In understanding the complexity and beauty that lipids process, this work will focus on differentiating lipid isomers by class, subclass and acyl chain composition using mass spectrometry research with the aid of ion/ion chemistry.

1.4 Mass Spectrometry

Since the inception of mass spectrometry in 1912 by Francis Aston and J.J. Thompson[45–47], mass spectrometry has developed into one of the most multifaceted and powerful analytical methods known to man. Over the last century, researchers have dramatically changed the dynamics and mechanics of what mass spectrometer can do. With the expansion of research and never-ending questions that are addressed; mass spectrometers have developed into a more vigorous tools to solve problems. However, considering the question posed by Dr. Cooks, what is mass spectrometry? Mass spectrometry (MS) "is a high-throughput analytical detection technique used to get information about the molecular weights and chemical structures of the lipids, peptides, proteins, carbohydrates, oligonucleotides, natural products, drug metabolites and other molecules".[48,49] While there have been many improvement since development of the first mass spectrometer; as a mass spectrometrist, I will display the usefulness of the mass spectrometer in the lipid community and how we have addressed key problems posed throughout this dissertation.

1.4.1 Ionization

MS is composed of three major components: ion source (ionization), the mass analyzer, and the detector. The ion source converts the analyte of interest (solid, liquid or gas) into ions for analysis. The analysis of the ion can be determined by different types of mass analyzers developed. There are various methods that can be utilized for in solution ionization, such as: desorption electrospray ionization (DESI)[50], matrix assisted laser desorption ionization (MALDI)[51,52] and electrospray ionization (ESI)[53]. In this work, we will focus on ionization method (ESI), precisely nano-electrospray ionization (nESI), for analysis of lipid solutions.

1.4.2 History

As mentioned above, the start of any mass spectrometry evaluation, is the ionization. In considering any ionization method utilized, one must first consider the internal energy needed and molecular properties of the analyte of interest that undergoes ionization. Contingent on the internal energy needed, the ionization method can either be "hard" or "soft" for analysis.

Before the inception of the "soft" ionization; many known ionization techniques were not suitable for the ionization of lipids, peptides, proteins, and other biomolecular compounds. For example, electron ionization (EI) is the first ionization methods applied to compounds for analysis.[54–56] Considered as a "hard" ionization technique since its development in 1918, EI is extensively used in mass spectrometry, effectively in positive ion development studies for the understanding behind molecular and atomic structural formation.[57] However, there are several drawbacks to the employment of EI analysis, such as: high energy formed from the electron beam is needed for ionization, causing uncommon cleavages of bonds and inconsistent fragmentation, as well as, samples must be heat resistant for analysis. Additionally, due to extensive fragmentation of the analyte, spectra can be challenging to interpret.[58–60] In light of the drawbacks that "hard" ionization methods present, the birth of electrospray ionization by John Fenn was employed to improve upon the many challenges of utilizing "hard" ionization methods.

1.4.3 Electrospray ionization

Electrospray ionization (ESI), pioneered by John B. Fenn in the 1980s, is a soft ionization method that allows molecular weight determination of lipids, proteins, peptides, nucleic acids, and

other biomolecular compounds. The technique has been so beneficial to the field of mass spectrometry, and science in general, that in 2002 John B. Fenn won a Nobel Prize in Chemistry for his "development of soft desorption ionization methods for mass spectrometric analyses of biological macromolecules".[61,62] This revolutionized the abilities to analyze macro- and small-molecules in solid, liquids or gas forms.[63] Coupling electrospray ionization with tandem mass spectrometry (ESI-MS/MS) allowed for more detailed structural characterization of the analyte in questions. This technique soon opened doors for the examination of lipid classes in 1991. Lipid identities were soon reported, with the first manuscript from Weintraub and Pinckard for the analysis of platelet-activating factor (PAF).[64]

This "soft" ionization technique, ESI, utilizes atmospheric conditions to formulate ions, in the form of charged droplets for analysis. Shown in **Scheme 1.1**[65] is a schematic of ESI procedure. The ESI workflow begins with the analyte of interest loaded to the spray capillary at the interface of the mass spectrometer. A high electric field is formed between the end of the spray capillary and the interface of the mass spectrometer, which creates charged droplets at flow rates on the order of μL/min. Due to the strong force of the electric field, a Taylor cone is formed due to the charge on the solution surface and breaks up into charged droplets when the surface tension of the solvent is overcome. A stream of charged droplets is emitted from the Taylor cone, causing a droplet formation to occur. The ions within the droplet, undergoes two transitions; liquid to gas via droplet evaporation, until it reaches the Rayleigh limit. At the Rayleigh limit (the amount of charge that can be accommodated on the surface of a droplet) the droplet undergoes coulombic fission causing the droplet to decrease in size, until the evaporation ends leaving a charge analyte, which is represented in **Scheme 1.1**.[66,67] Lastly, the charged analyte is then transferred to the mass analyzer for evaluation.

1.4.4 Nano-electrospray Ionization

As addressed above, ESI is a "soft" ionization technique that is routinely used for the analysis of biomolecules. In the schematic shown in **Scheme 1.2**, ESI utilize a stainless-steel capillary (<0.2 mm) at a flow rate of 1-20 μL/min. Normally, high voltages (2-6 kV) are applied to the capillary to charge the analyte solution.[68,69] With the aid of the electric field, a Taylor cone is developed from the charge droplets, that undergoes evaporation of the analyte, which is later turned into charged aerosol that transfers to the orifice of the mass spectrometer.

Like ESI, nano-electrospray ionization (nESI) is a widely used method for the examination macro and micro-molecules in the mass spectrometer. Shown in **Scheme 1.3** is a typical setup of the nESI ionization of an analyte, where the analyte is loaded into a borosilicate glass capillary in front of the interface of the mass spectrometer to induce a Taylor cone.[65,70,71] However, nESI employs a lower flow rate in 20-50 nL/min, with a finer tip (1-4 μm diameter) and lower spray voltage between 0.7-1.1 kV, which allows for a lower sample size for analysis. Due to the utilization of capillary tips, nESI produces a much smaller droplet size, less than 200 nm diameter, compared to ESI (1-2μm diameter), which increases the sensitivity of the experiment. In addition, with the use of nESI, less sample is needed for experiments in comparison to ESI.[65,72]

1.5 Mass Analyzers

The mass analyzer is the most essential component of the mass spectrometer. In the past decade, many modifications to the mass analyzer have been made to increase the performance and detection of analytes in varying samples. However, what is the mass analyzer? Mass analyzer measures the ions generated from the ionization process, based on its mass-to-charge (m/z) ratio. Currently, there are six commercially available mass analyzer: quadrupole, time of flight, magnetic sector, Orbitrap (an electrostatic ion trap), quadrupole ion trap, and ion cyclotron resonance mass analyzer.[73] Although a detail discussion of the different analyzers is outside the scope of this dissertation, descriptions of the mass analyzers used for the analysis of lipids here are mentioned below.

1.5.1 Quadrupoles and Linear Quadrupole Ion Trap

The most popular type of mass analyzer is the quadrupole. Found on the benchtop of various sectors of research, quadrupole mass analyzers outrank other analyzer due to their design, speed, robustness, inexpensiveness, and dependability.[73] Quadrupoles have the abilities to filter, trap, separate and analyze ions in one sweep, making them the most valuable tool on the market.[74] As we progress through this section, experiments were analyzed using a linear quadrupole ion trap (LIT).

Design

The quadrupole mass analyzer consists of four metallic rods, parallel to each other. The opposing cylinder shape rods are connected by both the radio frequency (RF) and direct current (DC) applied to the rods (which is shown in positive (+) and negative (-) signs, located on the rods). As the ion pass through both the combined RF and DC potential, the ion undergoes a wave motion through the quadrupole in a z-direction. Each ion has a particular frequency that correlates to the stability through the quadrupole. Only stable ions are able to pass through the quadrupole. However, unstable ions undergo collision with the rods, which are later ejected out. Shown in **Scheme 1.4** is the schematic of a quadrupole mass analyzer.[73,75]

Ion Trapping and Stability

The stability of the ion is crucial for the quadrupole. To stabilize the ion, one must first start with the opposing DC (in phase) and RF (out phase) rods. These rods create a suitable field for ions to pass through. In order to store an ion, DC potentials must be added to trapping plates at the ends of the rod set. In principle, quadrupoles have the ability to store ions for extended periods of time; however, buffer gas and contaminants can lead to the loss of the ion of interest. Each ion in the quadrupole has its own mass-to-charge (m/z) ratio, causing a specific motion. This motion can be calculated by the Mathieu stability equation.[75,76] As mentioned, in order to isolate and stabilize the ion upon injection, two types of potentials are needed: the RF and DC potentials. In certain cases, ions can be trapped in a RF only trap, where the stability can be calculated by **Equation 1.1**, listed below, where the Mathieu stability equation can be expressed in terms of force, and the **q** value is related to the m/z of the ion. To determine the dimensionless quantities of "q" and "a" are comparative to that of RF and DC amplitudes.[75–78] The force induced by the RF potential can be derived by **Equation 1.1**:

$$q = \frac{4eV}{\mathrm{m}r_o^2\Omega^2} \qquad \textbf{(1.1)}$$

where ***e*** is the elementary charge (in Coulombs), ***V*** is the RF potential applied (in volts), ***m*** is the mass of the ion (in kg), $\mathbf{r_o}$ is the radius of the trap (in meters), and **Ω** is the radial frequency (in radians s^{-1}) of the RF potential.

The force induced by the DC potential can be derived from **Equation 1.2**. The value of **a** can be derived by equation below:

$$a = \frac{8eU}{mr_o^2\Omega^2} \tag{1.2}$$

where **U** is the DC potential (in volts). Both RF and DC equations can be represented in the Mathieu stability diagram, shown in **Figure 1.2**. **Figure 1.2** displays the shaded stable region for the ion. Overlapping of both **q** and **a** are considered the stable points for the ion of interest. In other regions, the ion is considered unstable. The instability of the ion can be depicted by the **q** axis by 0.908, which is commonly referred to as the low mass cutoff (LMCO).[79,80] Where **m** and **q** are inversely related; as the **q** value increase the smaller the mass becomes, crossing pass the LMCO point.

Ion Isolation

The isolation of the ion of interest is critical to any MS/MS experiment. All MS/MS experiments start with the ionization of the ion. During the ionization period, ions are transformed into charged droplets, where they receive energy to inject into the mass spectrometer for analysis. As the ion is received into the quadrupole by RF and DC potential, the stability of the ion is determined by the m/z needed to finish the experiment. While there are many ions free floating through the quadrupole, the ion of interest can be mass selected by its m/z using the **Equations 1.1** and **1.2** and held stable using the Mathieu Stability diagram, shown in **Figure 1.2** . Unwanted ions are ejected during the ion selection.

Two methods can be used to eject unwanted ions: dipole or quadrupole excitations. To eject a section of ions, a fixed dipole frequency (that corresponds to a given **q** value) is applied. To put the ions out of resonance, the trapping RF is changed which brings the unwanted ions to a

different m/z causing a RF sweep to occur out of the trap. Multiple m/z ratios can be ejected by applying different frequencies across a period, this is done with a broadband waveform.[81,82] Broadband waveform was first introduced in 1967 by Langmuir[83] on using quadrupole excitation to eject ions out of the trap.[81] This technique opens up new doors for scholars to transform the broadband waveform method. New approaches utilize: SWIFT methods[84,85], changing in frequency spacing[86,87], tunneling ions through ejection, altering the RF frequency to increase speed of ions or duty cycles[88], while incorporating these techniques on other traps instruments. This new method changed the scope of isolation, which is still done today. In this dissertation, broadband waveforms isolation is utilized to isolate different subclasses of lipids for characterization on our modified linear ion trap.

Mass Analysis (LIT) and Detection

The detection of the ion is the heart of the experiment. In a linear ion trap (LIT), ions are detected in two ways: first, by increasing the RF potential on the rods can either eject the ion out the trap or move them towards the detector. This is represented in the Mathieu stability diagram in **Figure 1.2**. The Mathieu stability diagram display the stable regions and boundary lines for an ion of interest. At a **q** axis of 0.908, DC potential **a = 0** and ions in that region are unstable. Considering the force induced by RF potential (**Equation 1.1**), ramping the RF from low to high m/z, can cause ejection of the ion. The second way: is ejecting ions using mass selective axial ejection (MSAE).[89] This is a common procedure in the workflow on hybrid instruments (which I will discuss below) and triple quadrupole. MSAE exploits the use of fringe fields, located at the exit of the quadrupole. Operating at RF-only, x, y and z are paired, allowing ions to flow through the quadrupole, reaching the exit lenses. The initial energy of the ion is transformed from radial to axial energy, causing a cone like reflection. As the axial kinetics of the ion increase, the ions are ejected radically towards the detector.[89,90] This method is ion specific, where the RF increases as each ion comes in resonance. In the experiments listed below, MSAE is applied as a detection technique for lipid analysis.

1.5.2 Hybrid Instruments

Tandem mass spectrometers can be either tandem-in-space, in which ions are continuously transmitted through the instrument and undergo ion isolation, fragmentation, and analyses in difference regions of space, or tandem-in-time, in which the various stages of the MS/MS experiment take place in the same place but are separated in time. Instruments the combine both transmission and trapping capabilities are referred to as 'hybrid' instruments. For example, the triple quadrupole (QqQ) mass spectrometer can be used in either a purely transmission mode or in a hybrid mode. Listed below are details describing capabilities of a hybrid QqQ mass spectrometer used in this work and how it was used to determine structural characteristics of lipids found in biological matrices.

Sciex 4000 Triple Quadrupole

Tandem mass spectrometry, often referred to as MS/MS or MS^n (where n describes the consecutive mass analysis stages), involves one or more MS stages are done consecutively to obtain structural elucidation of a particular species. Tandem mass spectrometry is normally done in stages. First, before any isolation of any particular ion (also known as the precursor ion) is performed, stage one (MS) has occurred. Second, after the precursor ion (m/z of interest) is isolated (from stage one) and fragmented, stage two (MS/MS) has occurred, producing a precursor ion for analysis. If an additional isolation and fragmentation of the product ion is needed, stage three (MS^3) has occurred. In an MS^n experiment, ions are generated from repeated isolation and fragmentation of a particular ions in a sequence.[75,91,92] To achieve these types of experiments, modified instruments are needed for analysis.

The most well-established tandem mass analyzer to date, is the triple quadrupole mass spectrometer. The triple quadrupole mass spectrometer (**QqQ**) embodies two dual quadrupoles (**Q**) with unique RF/DC attributes. Housed between the **Q**, is a single RF only quadrupole (**q**), making this triplet quadrupole capable of determining molecular structures. Shown in this work listed below, utilization of a hybrid triple quadrupole mass spectrometer, with modifications to the collision cell to perform ion/ion reactions (which will be explained in **Section 1.6.1-3**).

The Sciex 4000 Triple Quadrupole is a hybrid instrument with dual capabilities (which are mentioned above) that can perform unique experiments. Similar to stages in the Tandem mass

spectrometer, Sciex 4000 Triple Quadrupole also start in stages, which is represented in Scheme 1.5. In **Scheme 1.5**, the first quadrupole (**Q1**) performs as mass filter with abilities to isolate a particular m/z. The second quadrupole (q2) performs as a collision cell or also known as the storage cell, containing a particular gas. The gas particles (such as nitrogen or argon) can undergo energetic collisions with the ion of interest to produce fragmentation (this stage will be discussed more in **Section 1.6.1-3**). Lastly, the final quadrupole (**Q3**), considered a linear ion trap, can perform MS^n experiments. Examples of these experiments can be found in **Chapter 2-4**. **Scheme 1.5** displays a modified triple quadrupole with capabilities to perform ion/ion reaction (this stage will be discussed more in **Section 1.6.4**).

1.6 Tandem MS Techniques

1.6.1 Ion trap CID

The dissociation of ions in the gas-phase has been extensively studied over many decades. Within the context of tandem mass spectrometry, the most prominent means for inducing fragmentation is via energetic collisions. The overall process is usually referred to as collision-induced dissociation (CID) (also known as collision-activated dissociation (CAD)). CID is a commonly used method that allows structural elucidation of a particular macro or micro-molecules ion of interest.[93] CID is performed by converting some of the relative translational energy of the collision pair into internal energy to induce fragmentation.[94,95] In a linear ion trap, CID involves the of a buffer gas (located in the collision cell, **q2**), such as nitrogen, argon, or helium, to collide with the ion of interest to form fragments. As a result of energetic collisions with the gas, the ion will receive gain internal energy, which will be redistributed, and the ion will undergo bond breakage. The ion undergoes acceleration within the ion trap by a applying a frequency to opposing quadrupole rod that is in resonance the frequency of motion of the ion. The extent of acceleration is related to the voltage amplitude of the applied waveform. In the collision cell, **q2**, ions can be isolated, stored and/or undergo fragmentation. In **Chapter 2-4**, examples of CID are utilized for the fragmentation of lipids and formation of the ion/ion reaction.

1.6.2 Beam-type CID

A variety of conditions can be used to effect CID. An important approach involves the acceleration of the precursor ion into the collision cell. This is in contrast to the resonance acceleration of trapped ions that underlies ion trap CID. CID that occurs from accelerating ions into the collision cell is called beam-type (BT-CID). In a tandem mass spectrometer, BT-CID can be divided arbitrarily into high-energy or low-energy beam-type CID.[96] Depending on the nature of the analyte ion, collision conditions can yield a slew of different fragmentation patterns of a particular ion of interest. In an experiment using BT-CID, the collision energy is usually controlled by changing the potential on the rod offset higher or lower relative to the ion source to stimulate fragmentation. The potential applied to the rod offset affects the relative translational energy of the collision pair. In other words, modulating the potential (voltage) of the rod offset, modulates the collision energy. In a typical experiment, CID or BT-CID can be done under in the microsecond (BT-CID) to milli-second (ion trap CID) time scales, with energy applied ranging between 1 to hundreds of eV .[96,97]

1.6.3 Dipolar Direct CID

Dipolar Direct Current (DDC) Collisional Induced Dissociation (CID) is a broad-band ion trap CID approach. (This approach is not widely accessible with commercial instruments.) DDC is affected by applying a dipolar DC across two opposing electrodes in the quadrupole array to promote dissociation. By displacing ions from the center of the ion trap, where the quadrupolar field is very low, to a region with a stronger quadrupolar field, ions can absorb power from the trapping RF. The ions accelerated by the trapping RF can undergo energetic collisions with the bath gas resulting in what is often referred to as 'RF heating'. A schematic of the Sciex QTRAP 4000, triple quadrupole mass spectrometer is represented in **Figure 1.4**, displaying the DDC offset. DDC has been extensively used by our group.[98–102] It differs from conventional IT-CID in that it does not require the ions to be 'in resonance' (i.e., all ions are displaced from the center of the ion trap under DDC conditions) and therefore is not as tuning intensive as conventional IT-CID. The extent of ion heating is related to the ratio of the DDC voltage to that of the trapping RF. The change in ion temperature ($\Delta \mathbf{T_k}$) can be calculated by **Equation 1.3**[103104105]:

$$\Delta T_k = \frac{m_g \Omega^2 r_o^2}{24k} \left(\frac{V_{DDC}}{V_{RF}}\right)^2$$

(1.3)

Where $\mathbf{m_g}$ is the buffer gas, $\boldsymbol{\Omega}$ is the drive frequency, $\mathbf{r_o}$ is the radius of the trap (in meters), $\boldsymbol{k}$ is Boltzmann constant, $\boldsymbol{V_{DDC}}$ is the DDC voltage, and $\boldsymbol{V_{RF}}$ is the amplitude of the voltage applied. The temperature change is dependent on the extent of ion displacement from the center of the ion trap the ion displacement from the center of the trap can be calculated by **Equation 1.4**:

$$r_e = \frac{\Omega^2 r_o^3}{4e} m/z \frac{V_{DDC}}{V_{RF}^2}$$

(1.4)

Where $\mathbf{r_e}$ is displacement of the ion from the center of the trap (finite space). Equation 1.4 displays at higher m/z the displacement of the ion is affected. **Equation 1.4** can be altered to account for the high mass limit and shown in **Equation 1.5**:

$$\left(\frac{m}{z}\right)high = \frac{4e}{\Omega^2 r_o^3} \frac{V_{RF}^2}{V_{DDC}}$$

(1.5)

This dissociation method can be utilized with ions that are located in **q2** on Sciex QTRAP 4000, triple quadrupole mass spectrometer.

1.6.4 Ion/Ion Reaction

The gas-phase charge inversion chemistry, a form of ion/ion reaction (IIRXN), is one of the most remarkable reactions that has the power to make me smile. This simple but intriguing reaction has fueled my curiosity for the past five years, but "how did I get here?" In the basement of Brown Chemistry Laboratory, housed a poster of various biomolecule reactions that fell under three categories: instrument development, ion chemistry studies, and applications. While each

technique fell under one umbrella known as the ion/ion reactions. How does lipid add to the dance of ion/ion reaction? Confusing, but allow me to explain.

My first introduction to the ion/ion reaction started with a banner that hung from the McLuckey lab (near the meeting room). A diagram of the ion/ion reaction is represented in **Figure 1.5**. The mingling of the positive and negative ions where the basis of many of the research endeavors'[105–107], left me curious on how lipids played a role and moreover, "what is ion/ion reaction?" Gas-Phase ion/ion reaction involves two oppositely charged ions under attractive force blending together to form a new species of ions. This process takes place in a collision cell of a Sciex QTRAP 4000 hybrid triple quadrupole/linear ion trap mass spectrometer modified to perform ion/ion reactions.

A brief overview of a typical experiment involves alternately pulsed nano-electrospray ionization (nESI) to sequentially generate positive and negative ions. The anions are generated via negative ion mode nESI, mass selected during transit through **Q1**, and transferred to **q2** for storage. Next, the charge inversion (IIRXN) cation was generated via positive ion mode nESI. To facilitate the ion/ion reaction, cation and anions were simultaneously stored in a high-pressure collision cell, **q2**, resulting in the formation of charge-inverted species. During the ion/ion reaction, multiple reactions could possibly take place, depending on the natures of the analyte and reagent ions , including covalent modification, electron transfer reaction, proton transfer reaction, and etc. This ion/ion reaction has shown remarkable results, including sequencing, understanding structural diversity, molecular composition, and manipulation of ions in the gas-phase.[108–116] In **Chapters 2-3**, I will incorporate the ion/ion reaction to unravel structural elucidation of lipid species.

1.7 Mass Spectrometry-Based Lipidomic Methods

Since 1912[117], the underlying phenomena and mechanisms behind ion formation and detection, has continued to reach new heights in the world of mass spectrometry. Over the past decades, scientist have uncovered many truths, reaching back to the origin of life[118]. However, in regard to lipids, researchers are still scratching the surface, while developing new tools to detect lipids in and out of biological matrices. In considering this new advancement, blending of both lipids and mass spectrometry has been key in allowing novel discoveries to soar. To accomplish this task, lipidomic was developed. Lipidomics is described as "the full characterization of lipid molecular species and of their biological roles with respect to expression of proteins involved in

lipid metabolism and function, including gene regulation."[119] While there are many techniques out that allows the structural elucidation of lipids of interest, more soft ionization methods are needed to detect smaller lipid compositions.

1.7.1 Shotgun Lipidomics

The development of ESI-MS approaches has been key in the detection of lipids in a biological matrix. This "soft" ionization method allows the conversion of dissolved lipids into gaseous ions detectable by the mass spectrometer. In many cases, for true identification, prior separations are done before mass spectrometry to determine molecular species for analysis. However, Han and coworkers developed a technique that allows the direct fusion of intact lipids for analysis in the mass spectrometer, called shotgun lipidomics.[120–122] The shotgun lipidomic approach eliminates prior separation and perform a faster and robust platform to detect lipids of varying species.[123]

1.7.2 MS/MS

Many improvements have been done to the mass analyzer to allow detailed structural characterization of lipid species in biological samples. For example, the Sciex 4000 Triple Quadrupole hybrid mass spectrometer is a robust, inexpensive, dependable instrument with high degree of sensitivity. The Sciex 4000 Triple Quadrupole was useful in the probing lipids species in a complex mixture of different subclasses, such as Escherichia coli (*E. coli*) bacterium (example shown in **Chapters 2**).

In a typical linear ion trap experiment, the ion of interest is isolated and later probed to reveal unique physical characteristics. In any lipid experiment, it is crucial to predetermine subclass of lipid m/z before structural elucidation. In a complex mixture, such as eukaryotic cells, there are various lipid subclass represented in a sample, which is represented in **Figure 1.6**. To confidently identify subclasses within a mixture, precursor ion scans (PIS) and neutral loss scans (NLS) are employed to separate lipids based in their subclass.

In a MS/MS experiment, in the positive mode, glycerophospholipid (GPs) produces head group loss. While in the negative ion mode, fatty acyl chain, ketene loss, and neutral loss are represented. In either ion mode, MS/MS cannot determine the subclass of product ion alone, PIS and NLS are needed for concrete determination of m/z. In a mixture of varying subclasses of lipids, to

probe for phosphatidylcholine (PC), the PIS for m/z 184 Da is performed to determine any ions that shows loss of headgroup.[124] Additionally, in the same sample, a NLS of 141 Da is utilized to scan for any phosphatidylethanolamine (PE) in a sample. In the case of phosphatidylserines (PS) will have a NLS of 185, with PIS of 153 Da for phosphatidylglycerols (PG)[124]. These values are also represented in **Table 1.1**[124].

1.7.3 Phosphatidylglycerol Analysis

As mentioned above, phosphatidylglycerol (PGs) are a subclass of the glycerophospholipid (GPs), subclass located in the cell membrane. In the cell membrane, PGs are the second most abundant subclass located in the cell wall and found in the lung during gestation period (which later aid in the development of the lung).[33] Similar to other subclass of GPs lipids, PG are composed of two fatty acids at the sn-1 and sn-2 position, esterified to the glycerol backbone with a phosphate headgroup and glycerol moiety.[33] An example of GPs subclasses is shown in **Figure 1.1**.

PGs naturally contains a net negative charge while housed in the membrane surface, making them easy to ionize in the negative most of ESI. Analysis of PGs are different in terms of fragmentation in both positive and negative ion mode. In positive ion mode, PGs are protonated with a net charge of +1 and represented as $[M + H]^+$.[125] Under CID conditions in the positive ion mode, PGs displays headgroup loss $[M + H - 171]^+$. In the negative ion mode, PGs $[M - H]^-$, deprotonated PGs yields a slew of fragments corresponding to the glycerol moiety ($C_3H_6O_2$, m/z 153), sn-1 and sn-2 fatty acyl moieties (represented by $RCOO^-$ ion), neutral loss of sn-1 or sn-2 RCOOH group from $[M-H]^-$, loss of sn-1 or sn-2 acyl chain as ketene (RCH=C=O) from $[M-H]^-$, and other corresponding fragments.[30,33] An example of the fragmentation of PG 17:0/20:4 can be found in **Figure 1.7**.

1.7.4 Bis(monoacylglycerol)phosphate Analysis

A constitutional isomer phosphatidylglycerol (PGs) and bis(monoacylglycerol)phosphate (BMP) fatty acids are a unique lipid subclass of GPLs. Similar to PGs, BMP share the same chemical formula, exact mass, molecular weight, and m/z but differ in molecular configuration. As mentioned above, PGs are composed of two fatty acids at the sn-1 and sn-2 position, esterified to

a glycerol backbone with a phosphate and glycerol headgroup. However, BMP fatty acids exhibit a unique arrangement to the esterification of the fatty acids. On the BMP, two fatty acids are esterified to the glycerol backbone and phosphate head group in a sn-1:sn-1 arrangement for both fatty acids.[126] A schematic of PGs and BMP structures are shown in **Scheme 1.5**.

BMP are a beneficial lipid that diffuse material in and out of the endosomal compartment, while responsible for the transference and circulation in the cellular cholesterol. With such importance to the membrane, BMP are a challenge to analysis. In the gas-phase, MS and MS/MS alone are not able to differentiate constitutional isomers. Other systems like, liquid chromatography mass spectrometry (LC-MS), and hydrophilic interaction liquid chromatography (HILIC) has been used to separate these constitutional isomers, but limitations include high degree of solvents and long retentions times.[126] In **Chapter 4**, I will display the utility of the ion/ion reaction in the separation of constitutional isomers.

1.7.5 Phosphatidylethanolamine Analysis

Similar to PGs, phosphatidylethanolamine (PE) is a common lipid subclass, mainly composed in the mitochondrial membrane. Synthesized by phosphatidylserine decarboxylase (PSD) in the cell via two mechanisms.[26] PEs are one of the most abundant GPs and extremely special in relations to charge. Like many GPs, dependance on the location and need for the GPs in the cell will determine if there is a positive or negative charge on the lipid. However, PEs do not process a charge, but in a cell membrane, PEs can prompt a negative charge to boost membrane fusion.[26] Like other GPs, PEs are comprised of saturated or unsaturated acyl chains at the sn-1 and sn-2 position, which are bound to a glycerol backbone with a phosphate and ethanolamine headgroup. An example of PEs subclass is shown in **Figure 1.1.**

Analysis of PEs are different in terms of fragmentation in both positive and negative ion mode, due to the integration of the ethanolamine headgroup. In positive ion mode, PEs are protonated with a net charge of +1 and represented as $[M + H]^+$. However, ionization efficiency of PEs is particularly higher and lower depending on the polarity of the ionization. In the case for PEs, ionization in positive mode is favorable due to the primary amine but can be also ionized via negative mode if optimization of the analyte analysis. Under CID conditions in the positive ion mode, a NLS of 141 Da corresponds to the headgroup. Scanning through a mixture at with a NL of 141 Da can determine PEs present in a mixture for analysis. In the negative ion mode, PEs $[M – H]^-$,

deprotonated PEs yields a slew of fragments corresponding to the ethanolamine phosphate ion ($C_2H_8NO_4P$, m/z 141), sn-1 and sn-2 fatty acyl moieties (represented by $RCOO^-$ ion), neutral loss of sn-1 or sn-2 RCOOH group from $[M-H]^-$, loss of sn-1 or sn-2 acyl chain as ketene (RCH=C=O) from $[M - H]^-$, and other corresponding fragments.[30]

1.7.6 Saturated and Unsaturated fatty Acids Analysis

Lipids are distinct and universal class of molecules that play a crucial role in membrane composition, metabolic fuel, and cellular communication.[127] From the category of lipids, fatty acids (FAs) are notably the most common lipid class that doesn't get the recognition it deserves in comparison to other subclass lipids. Found in a genre of organisms, biological samples and etc.; FAs continue to soar beyond the basic building blocks. FAs demonstrates a wide variety of composition, in regard to the aliphatic chain length, geometry and degree of saturation. Similar to other classes of lipids, the arrangement of FAs can facilitate the biological and physical function needed for a particular sample. Variation in the saturation versus unsaturation of the FAs, can have adverse health effects, such as diabetes, cancer, and/or cardiovascular disease.[128] It is imperative to understand the composition of FAs.

Saturated fatty acids (SCFAs) are a group of lipids that doesn't contain any double bond, cyclopropane, branching or any constituted to the carbon-carbon chain. SCFAs can range from 4 – 40 carbons in a chain. SCFAs are generally found in meats, butter, dairy or other solids. Most cardiovascular, obesity, and diabetes cases are linked to high consumption of SCFAs. SCFAs risk factors have becomes a global issue in regard to health and safety of a population.[30,129]

Conversely, unsaturated fatty acids are a set of lipids that contain one or more double bonds in the fatty acyl chain. Unsaturated fatty acids can be monounsaturated (one double bond) or polyunsaturated (more than one double bond). Similar to SCFAs, unsaturated fatty acids can range from 4-30 carbon-carbon double bond. Unsaturated fatty acids are unique class of lipids due to diversity that each carbon chain can process.[130] For example, phytomonic acid, also known as 10-(2-hexylcyclopropyl)decanoic acid, is a 19-carbon fatty acid with a cyclo-group on the 10 carbons, which is similar in mass to its saturated counterpart nonadecanoic acid, better known as nonadecylic acid. Both sharing the same composition and carbon number but change in degree of unsaturation. Another example: phytanic acid or 3,7,11,15-tetramethyl hexadecenoic acid, is a branched chain fatty acid, composed of 20 carbons, but branching at the 3,7,11,15 carbon down

the chain. Similar in mass with isomer arachidic acid, these isomers can pose a challenge for scientist to identify and separate. In **Chapters 2 and 3,** I will display how the utility of the ion/ion reaction was able to separate these ions in the gas-phase without any prior separation or modification to the samples.

1.8 Thesis Overview

During recruitment weekend, I was given a question that changed the trajectory of my graduate career. The question posed by Dr. Graham Cooks, "how would I use mass spectrometry to solve this problem?", riddled my thoughts through the course of my graduate career. What are lipids and how do they relate to the body, is the same question many scientists in the world of mass spectrometry is trying to answer. As I have shown over the course of **Chapter 1**, since the invention of the mass spectrometer, scientists have dramatically changed the dynamics and mechanics of what a mass spectrometer can do. With many developments and newer technology, mass spectrometry is only scratching the surface in the lipid world.

How can I add to the fight? My objective for my graduate career was to explore new ways to evaluate and characterize various subclasses of lipids in and out of a biological sample. With the aid of the ion/ion reaction I was able to add to a well-known technique for the analysis of lipids. In **Chapters 2 – 4**, I will evaluate the use of the charge inversion reaction for the structural elucidation of saturated versus unsaturated isomers in a biological matrix.

1.9 References

(1) Voon, C. H.; Sam, S. T. 2 - Physical Surface Modification on the Biosensing Surface. In *Nanobiosensors for Biomolecular Targeting*; Gopinath, S. C. B., Lakshmipriya, T., Eds.; Micro and Nano Technologies; Elsevier, 2019; pp 23–50. https://doi.org/10.1016/B978-0-12-813900-4.00002-6.

(2) Kumar, J.; Narnoliya, L. K.; Alok, A. Chapter 6 - A CRISPR Technology and Biomolecule Production by Synthetic Biology Approach. In *Current Developments in Biotechnology and Bioengineering*; Singh, S. P., Pandey, A., Du, G., Kumar, S., Eds.; Elsevier, 2019; pp 143–161. https://doi.org/10.1016/B978-0-444-64085-7.00006-X.

(3) Suresh, R.; Pandiaraj, M.; Sankaralingam, M.; Giribabu, K. Chapter 6 - Graphene–Metal Chalcogenide Modified Electrochemical Sensors. In *Graphene-Based Electrochemical Sensors for Biomolecules*; Pandikumar, A., Rameshkumar, P., Eds.; Micro and Nano Technologies; Elsevier, 2019; pp 139–153. https://doi.org/10.1016/B978-0-12-815394-9.00006-6.

(4) Hoffman, A. S.; Hubbell, J. A. Chapter I.2.17 - Surface-Immobilized Biomolecules. In *Biomaterials Science (Third Edition)*; Ratner, B. D., Hoffman, A. S., Schoen, F. J., Lemons, J. E., Eds.; Academic Press, 2013; pp 339–349. https://doi.org/10.1016/B978-0-08-087780-8.00032-2.

(5) Fahy, E.; Subramaniam, S.; Murphy, R. C.; Nishijima, M.; Raetz, C. R. H.; Shimizu, T.; Spener, F.; van Meer, G.; Wakelam, M. J. O.; Dennis, E. A. Update of the LIPID MAPS Comprehensive Classification System for Lipids. *J. Lipid Res.* **2009**, *50* (Suppl), S9–S14. https://doi.org/10.1194/jlr.R800095-JLR200.

(6) Bevers, E. M.; Comfurius, P.; Dekkers, D. W.; Harmsma, M.; Zwaal, R. F. Transmembrane Phospholipid Distribution in Blood Cells: Control Mechanisms and Pathophysiological Significance. *Biol. Chem.* **1998**, *379* (8–9), 973–986.

(7) *A RAPID METHOD OF TOTAL LIPID EXTRACTION AND PURIFICATION*. https://cdnsciencepub.com/doi/abs/10.1139/o59-099 (accessed 2023-05-30).

(8) Blom, T. S.; Koivusalo, M.; Kuismanen, E.; Kostiainen, R.; Somerharju, P.; Ikonen, E. Mass Spectrometric Analysis Reveals an Increase in Plasma Membrane Polyunsaturated Phospholipid Species upon Cellular Cholesterol Loading. *Biochemistry* **2001**, *40* (48), 14635–14644. https://doi.org/10.1021/bi0156714.

(9) van Meer, G.; Voelker, D. R.; Feigenson, G. W. Membrane Lipids: Where They Are and How They Behave. *Nat. Rev. Mol. Cell Biol.* **2008**, *9* (2), 112–124. https://doi.org/10.1038/nrm2330.

(10) Cooper, G. M. Cell Membranes. In *The Cell: A Molecular Approach. 2nd edition*; Sinauer Associates, 2000.

(11) Tada, H.; Takamura, M.; Kawashiri, M. Chapter Five - Genomics of Hypertriglyceridemia. In *Advances in Clinical Chemistry*; Makowski, G. S., Ed.; Elsevier, 2020; Vol. 97, pp 141–169. https://doi.org/10.1016/bs.acc.2019.12.005.

(12) Dzoyem, J. P.; Kuete, V.; Eloff, J. N. 23 - Biochemical Parameters in Toxicological Studies in Africa: Significance, Principle of Methods, Data Interpretation, and Use in Plant Screenings. In *Toxicological Survey of African Medicinal Plants*; Kuete, V., Ed.; Elsevier, 2014; pp 659–715. https://doi.org/10.1016/B978-0-12-800018-2.00023-6.

(13) Carswell, K. A.; Lee, M.-J.; Fried, S. K. Culture of Isolated Human Adipocytes and Isolated Adipose Tissue. In *Human Cell Culture Protocols*; Mitry, R. R., Hughes, R. D., Eds.; Methods in Molecular Biology; Humana Press: Totowa, NJ, 2012; pp 203–214. https://doi.org/10.1007/978-1-61779-367-7_14.

(14) Schmelzer, K.; Fahy, E.; Subramaniam, S.; Dennis, E. A. The Lipid Maps Initiative in Lipidomics. In *Methods in Enzymology*; Lipidomics and Bioactive Lipids: Mass-Spectrometry–Based Lipid Analysis; Academic Press, 2007; Vol. 432, pp 171–183. https://doi.org/10.1016/S0076-6879(07)32007-7.

(15) Vinale, F.; Sivasithamparam, K.; Zeilinger, S.; Gutiérrez, S. Fungal Secondary Metabolism. In *Encyclopedia of Mycology*; Zaragoza, Ó., Casadevall, A., Eds.; Elsevier: Oxford, 2021; pp 54–63. https://doi.org/10.1016/B978-0-12-819990-9.00031-7.

(16) Korman, T. P.; Ames, B.; (Sheryl) Tsai, S.-C. 1.08 - Structural Enzymology of Polyketide Synthase: The Structure–Sequence–Function Correlation. In *Comprehensive Natural Products II*; Liu, H.-W. (Ben), Mander, L., Eds.; Elsevier: Oxford, 2010; pp 305–345. https://doi.org/10.1016/B978-008045382-8.00020-4.

(17) Merrill, A. H.; Vu, M. N. Glycolipids. In *Encyclopedia of Cell Biology*; Bradshaw, R. A., Stahl, P. D., Eds.; Academic Press: Waltham, 2016; pp 180–193. https://doi.org/10.1016/B978-0-12-394447-4.10022-7.

(18) Fahy, E.; Cotter, D.; Sud, M.; Subramaniam, S. Lipid Classification, Structures and Tools. *Biochim. Biophys. Acta BBA - Mol. Cell Biol. Lipids* **2011**, *1811* (11), 637–647. https://doi.org/10.1016/j.bbalip.2011.06.009.

(19) Fahy, E.; Subramaniam, S.; Brown, H. A.; Glass, C. K.; Merrill, A. H.; Murphy, R. C.; Raetz, C. R. H.; Russell, D. W.; Seyama, Y.; Shaw, W.; Shimizu, T.; Spener, F.; Meer, G. van; VanNieuwenhze, M. S.; White, S. H.; Witztum, J. L.; Dennis, E. A. A Comprehensive Classification System for Lipids1. *J. Lipid Res.* **2005**, *46* (5), 839–861. https://doi.org/10.1194/jlr.E400004-JLR200.

(20) Craig, M.; Yarrarapu, S. N. S.; Dimri, M. Biochemistry, Cholesterol. In *StatPearls*; StatPearls Publishing: Treasure Island (FL), 2023.

(21) Macabuhay, A.; Arsova, B.; Walker, R.; Johnson, A.; Watt, M.; Roessner, U. Modulators or Facilitators? Roles of Lipids in Plant Root–Microbe Interactions. *Trends Plant Sci.* **2022**, *27* (2), 180–190. https://doi.org/10.1016/j.tplants.2021.08.004.

(22) Zheng, Y.; Yang, Y.; Wang, M.; Hu, S.; Wu, J.; Yu, Z. Differences in Lipid Homeostasis and Membrane Lipid Unsaturation Confer Differential Tolerance to Low Temperatures in Two Cycas Species. *BMC Plant Biol.* **2021**, *21* (1), 377. https://doi.org/10.1186/s12870-021-03158-4.

(23) Jiang, X.-C.; Li, Z.; Yazdanyar, A. Chapter 6 - Sphingolipids and HDL Metabolism. In *The HDL Handbook (Second Edition)*; Komoda, T., Ed.; Academic Press: Boston, 2014; pp 133–158. https://doi.org/10.1016/B978-0-12-407867-3.00006-8.

(24) Castro-Gómez, P.; Garcia-Serrano, A.; Visioli, F.; Fontecha, J. Relevance of Dietary Glycerophospholipids and Sphingolipids to Human Health. *Prostaglandins Leukot. Essent. Fatty Acids* **2015**, *101*, 41–51. https://doi.org/10.1016/j.plefa.2015.07.004.

(25) Fonteh, A. N.; Chiang, A. J.; Arakaki, X.; Edminster, S. P.; Harrington, M. G. Accumulation of Cerebrospinal Fluid Glycerophospholipids and Sphingolipids in Cognitively Healthy Participants With Alzheimer's Biomarkers Precedes Lipolysis in the Dementia Stage. *Front. Neurosci.* **2020**, *14*, 611393. https://doi.org/10.3389/fnins.2020.611393.

(26) Vance, D. E.; Vance, J. E. CHAPTER 8 - Phospholipid Biosynthesis in Eukaryotes. In *Biochemistry of Lipids, Lipoproteins and Membranes (Fifth Edition)*; Vance, D. E., Vance, J. E., Eds.; Elsevier: San Diego, 2008; pp 213–244. https://doi.org/10.1016/B978-044453219-0.50010-6.

(27) Kenwood, B. M.; Merrill, A. H. Lipidomics. In *Encyclopedia of Cell Biology*; Bradshaw, R. A., Stahl, P. D., Eds.; Academic Press: Waltham, 2016; pp 147–159. https://doi.org/10.1016/B978-0-12-394447-4.10024-0.

(28) Wang, H.-M. D.; Li, X.-C.; Lee, D.-J.; Chang, J.-S. Potential Biomedical Applications of Marine Algae. *Bioresour. Technol.* **2017**, *244*, 1407–1415. https://doi.org/10.1016/j.biortech.2017.05.198.

(29) Venkata Mohan, S.; Rohit, M. V.; Chiranjeevi, P.; Chandra, R.; Navaneeth, B. Heterotrophic Microalgae Cultivation to Synergize Biodiesel Production with Waste Remediation: Progress and Perspectives. *Bioresour. Technol.* **2015**, *184*, 169–178. https://doi.org/10.1016/j.biortech.2014.10.056.

(30) *LIPID MAPS*. https://www.lipidmaps.org/ (accessed 2023-06-12).

(31) Lesnefsky, E. J.; Chen, Q.; Tandler, B.; Hoppel, C. L. Mitochondrial Bioenergetics in the Heart. In *Encyclopedia of Cardiovascular Research and Medicine*; Vasan, R. S., Sawyer, D. B., Eds.; Elsevier: Oxford, 2018; pp 365–380. https://doi.org/10.1016/B978-0-12-809657-4.99831-4.

(32) Mihara, K.; Otera, H. Mechanisms and Functions of Mitochondrial Dynamics. In *Encyclopedia of Cell Biology*; Bradshaw, R. A., Stahl, P. D., Eds.; Academic Press: Waltham, 2016; pp 279–292. https://doi.org/10.1016/B978-0-12-394447-4.20024-2.

(33) Stillwell, W. Chapter 5 - Membrane Polar Lipids. In *An Introduction to Biological Membranes (Second Edition)*; Stillwell, W., Ed.; Elsevier, 2016; pp 63–87. https://doi.org/10.1016/B978-0-444-63772-7.00005-1.

(34) Fantini, J.; Yahi, N. Chapter 1 - Chemical Basis of Lipid Biochemistry. In *Brain Lipids in Synaptic Function and Neurological Disease*; Fantini, J., Yahi, N., Eds.; Academic Press: San Diego, 2015; pp 1–28. https://doi.org/10.1016/B978-0-12-800111-0.00001-1.

(35) Goñi, F. M.; Alonso, A. Structure and Functional Properties of Diacylglycerols in Membranes1This Work Is Dedicated to Professor Vittorio Luzzati on Occasion of His 75th Birthday.1. *Prog. Lipid Res.* **1999**, *38* (1), 1–48. https://doi.org/10.1016/S0163-7827(98)00021-6.

(36) Xu, Y.; Brenna, J. T. Atmospheric Pressure Covalent Adduct Chemical Ionization Tandem Mass Spectrometry for Double Bond Localization in Monoene- and Diene-Containing Triacylglycerols. *Anal. Chem.* **2007**, *79* (6), 2525–2536. https://doi.org/10.1021/ac062055a.

(37) Zoidis, E.; Papamikos, V. Glucose: Metabolism and Regulation. In *Encyclopedia of Food and Health*; Caballero, B., Finglas, P. M., Toldrá, F., Eds.; Academic Press: Oxford, 2016; pp 233–238. https://doi.org/10.1016/B978-0-12-384947-2.00351-2.

(38) Makhutova, O. N.; Sushchik, N. N.; Gladyshev, M. I. Fatty Acid—Markers as Foodweb Tracers in Inland Waters. In *Encyclopedia of Inland Waters (Second Edition)*; Mehner, T., Tockner, K., Eds.; Elsevier: Oxford, 2022; pp 713–726. https://doi.org/10.1016/B978-0-12-819166-8.00094-3.

(39) Eshak, E. S.; Yamagishi, K.; Iso, H. Dietary Fat and Risk of Cardiovascular Disease. In *Encyclopedia of Cardiovascular Research and Medicine*; Vasan, R. S., Sawyer, D. B., Eds.; Elsevier: Oxford, 2018; pp 60–89. https://doi.org/10.1016/B978-0-12-809657-4.99603-0.

(40) Brondz, I. LIPIDS | Fatty Acids. In *Encyclopedia of Analytical Science (Second Edition)*; Worsfold, P., Townshend, A., Poole, C., Eds.; Elsevier: Oxford, 2005; pp 76–88. https://doi.org/10.1016/B0-12-369397-7/00310-1.

(41) Buist, P. H. 1.02 - Unsaturated Fatty Acids. In *Comprehensive Natural Products II*; Liu, H.-W. (Ben), Mander, L., Eds.; Elsevier: Oxford, 2010; pp 5–33. https://doi.org/10.1016/B978-008045382-8.00720-6.

(42) Kuksis, A. LIPIDS | Gas Chromatography. In *Encyclopedia of Separation Science*; Wilson, I. D., Ed.; Academic Press: Oxford, 2000; pp 3219–3237. https://doi.org/10.1016/B0-12-226770-2/02441-8.

(43) Moore, B. S.; Floss, H. G. 1.03 - Biosynthesis of Cyclic Fatty Acids Containing Cyclopropyl-, Cyclopentyl-, Cyclohexyl-, and Cycloheptyl-Rings. In *Comprehensive Natural Products Chemistry*; Barton, S. D., Nakanishi, K., Meth-Cohn, O., Eds.; Pergamon: Oxford, 1999; pp 61–82. https://doi.org/10.1016/B978-0-08-091283-7.00002-3.

(44) Kuksis, A. Gas Chromatography☆. In *Reference Module in Chemistry, Molecular Sciences and Chemical Engineering*; Elsevier, 2015. https://doi.org/10.1016/B978-0-12-409547-2.04805-8.

(45) *The Nobel Prize in Chemistry 1922*. NobelPrize.org. https://www.nobelprize.org/prizes/chemistry/1922/summary/ (accessed 2023-06-22).

(46) Thomson, J. J. XLVII. *On Rays of Positive Electricity*. *Lond. Edinb. Dublin Philos. Mag. J. Sci.* **1907**, *13* (77), 561–575. https://doi.org/10.1080/14786440709463633.

(47) Thomson, J. J. *Rays of Positive Electricity and Their Application to Chemical Analyses*; Longmans, Green and Company, 1921.

(48) Biemann, K. Laying the Groundwork for Proteomics: Mass Spectrometry from 1958 to 1988. *Int. J. Mass Spectrom.* **2007**, *259* (1), 1–7. https://doi.org/10.1016/j.ijms.2006.08.002.

(49) Büyükköroğlu, G.; Dora, D. D.; Özdemir, F.; Hızel, C. Chapter 15 - Techniques for Protein Analysis. In *Omics Technologies and Bio-Engineering*; Barh, D., Azevedo, V., Eds.; Academic Press, 2018; pp 317–351. https://doi.org/10.1016/B978-0-12-804659-3.00015-4.

(50) Takáts, Z.; Wiseman, J. M.; Gologan, B.; Cooks, R. G. Mass Spectrometry Sampling under Ambient Conditions with Desorption Electrospray Ionization. *Science* **2004**, *306* (5695), 471–473. https://doi.org/10.1126/science.1104404.

(51) Cramer, R. MALDI MS. *Methods Mol. Biol. Clifton NJ* **2009**, *564*, 85–103. https://doi.org/10.1007/978-1-60761-157-8_5.

(52) Karas, M.; Bachmann, D.; Bahr, U.; Hillenkamp, F. Matrix-Assisted Ultraviolet Laser Desorption of Non-Volatile Compounds. *Int. J. Mass Spectrom. Ion Process.* **1987**, *78*, 53–68. https://doi.org/10.1016/0168-1176(87)87041-6.

(53) Ho, C.; Lam, C.; Chan, M.; Cheung, R.; Law, L.; Lit, L.; Ng, K.; Suen, M.; Tai, H. Electrospray Ionisation Mass Spectrometry: Principles and Clinical Applications. *Clin. Biochem. Rev.* **2003**, *24* (1), 3–12.

(54) Märk, T. D.; Dunn, G. H. *Electron Impact Ionization*; Springer Science & Business Media, 2013.

(55) Nier, A. O. Some Reflections on the Early Days of Mass Spectrometry at the University of Minnesota. *Int. J. Mass Spectrom. Ion Process.* **1990**, *100*, 1–13. https://doi.org/10.1016/0168-1176(90)85063-8.

(56) Nier, A. O. A Mass Spectrometer for Isotope and Gas Analysis. *Rev. Sci. Instrum.* **2004**, *18* (6), 398–411. https://doi.org/10.1063/1.1740961.

(57) Mirsaleh-Kohan, N.; Robertson, W. D.; Compton, R. N. Electron Ionization Time-of-Flight Mass Spectrometry: Historical Review and Current Applications. *Mass Spectrom. Rev.* **2008**, *27* (3), 237–285. https://doi.org/10.1002/mas.20162.

(58) *Electrospray Ionization for Mass Spectrometry of Large Biomolecules*. https://doi.org/10.1126/science.2675315.

(59) Dole, M.; Mack, L. L.; Hines, R. L.; Mobley, R. C.; Ferguson, L. D.; Alice, M. B. Molecular Beams of Macroions. *J. Chem. Phys.* **2003**, *49* (5), 2240–2249. https://doi.org/10.1063/1.1670391.

(60) *Electrospray Ionization for Mass Spectrometry of Large Biomolecules | Science*. https://www.science.org/doi/abs/10.1126/science.2675315?casa_token=wDeV43AJcacAAAAA:8DeSxQTU4t-hL9OTAE9o3f28H-4E8lj7EUr-QKwEriMmZoQSTH7GN5eK-FK8tvd3OYFeymaHK-S5X6ME1 (accessed 2023-06-26).

(61) Yamashita, M.; Fenn, J. B. Electrospray Ion Source. Another Variation on the Free-Jet Theme. *J. Phys. Chem.* **1984**, *88* (20), 4451–4459. https://doi.org/10.1021/j150664a002.

(62) *The Nobel Prize in Chemistry 2002*. NobelPrize.org. https://www.nobelprize.org/prizes/chemistry/2002/fenn/facts/ (accessed 2023-06-26).

(63) Lui, T.-Y.; Chen, X.; Zhang, S.; Hu, D.; Dominic Chan, T.-W. Peptide Oxidation Induced by Liquid–Solid Contact Electrification as Revealed in Liquid Microjunction-Surface Sampling Probe Mass Spectrometry. *Anal. Chem.* **2023**, *95* (23), 9060–9067. https://doi.org/10.1021/acs.analchem.3c01411.

(64) Weintraub, S. T.; Pinckard, R. N.; Hail, M.; Gaskell, S. J. Electrospray Ionization for Analysis of Platelet-Activating Factor. *Rapid Commun. Mass Spectrom.* **1991**, *5* (7), 309–311. https://doi.org/10.1002/rcm.1290050702.

(65) Wilm, M.; Mann, M. Analytical Properties of the Nanoelectrospray Ion Source. *Anal. Chem.* **1996**, *68* (1), 1–8. https://doi.org/10.1021/ac9509519.

(66) Wilm, M. Principles of Electrospray Ionization. *Mol. Cell. Proteomics* **2011**, *10* (7). https://doi.org/10.1074/mcp.M111.009407.

(67) Wilm, M. S.; Mann, M. Electrospray and Taylor-Cone Theory, Dole's Beam of Macromolecules at Last? *Int. J. Mass Spectrom. Ion Process.* **1994**, *136* (2), 167–180. https://doi.org/10.1016/0168-1176(94)04024-9.

(68) *Calibration of ion spray mass spectra using cluster ions - Anacleto - 1992 - Organic Mass Spectrometry - Wiley Online Library*. https://analyticalsciencejournals.onlinelibrary.wiley.com/doi/abs/10.1002/oms.1210270603?casa_token=0ZpJ06M7ZgQAAAAA:mgHVrX9qsjTbVM-ROGym0nSPoNik_3pjVLo256Q7oSl4PcIoAxY9poP4GCFj6t8lQHqBQUkK-BVXJubnRkA (accessed 2023-06-27).

(69) Banerjee, S.; Mazumdar, S. Electrospray Ionization Mass Spectrometry: A Technique to Access the Information beyond the Molecular Weight of the Analyte. *Int. J. Anal. Chem.* **2012**, *2012*, 282574. https://doi.org/10.1155/2012/282574.

(70) Yuill, E. M.; Sa, N.; Ray, S. J.; Hieftje, G. M.; Baker, L. A. Electrospray Ionization from Nanopipette Emitters with Tip Diameters of Less than 100 Nm. *Anal. Chem.* **2013**, *85* (18), 8498–8502. https://doi.org/10.1021/ac402214g.

(71) Pal, S.; Kulkarni, A. A. Quantitative Comparison of Strategies to Delay Clogging in Straight Capillaries. *Chem. Eng. Sci.* **2019**, *199*, 88–99. https://doi.org/10.1016/j.ces.2019.01.015.

(72) Karas, M.; Bahr, U.; Dülcks, T. Nano-Electrospray Ionization Mass Spectrometry: Addressing Analytical Problems beyond Routine. *Fresenius J. Anal. Chem.* **2000**, *366* (6), 669–676. https://doi.org/10.1007/s002160051561.

(73) Haag, A. M. Mass Analyzers and Mass Spectrometers. In *Modern Proteomics – Sample Preparation, Analysis and Practical Applications*; Mirzaei, H., Carrasco, M., Eds.; Advances in Experimental Medicine and Biology; Springer International Publishing: Cham, 2016; pp 157–169. https://doi.org/10.1007/978-3-319-41448-5_7.

(74) Miller, P. E.; Denton, M. B. The Quadrupole Mass Filter: Basic Operating Concepts. *J. Chem. Educ.* **1986**, *63* (7), 617. https://doi.org/10.1021/ed063p617.

(75) March, R. E. An Introduction to Quadrupole Ion Trap Mass Spectrometry. *J. Mass Spectrom.* **1997**, *32* (4), 351–369. https://doi.org/10.1002/(SICI)1096-9888(199704)32:4<351::AID-JMS512>3.0.CO;2-Y.

(76) Mathieu, É. Mémoire sur le mouvement vibratoire d'une membrane de forme elliptique.

(77) Schwartz, J. C.; Senko, M. W.; Syka, J. E. P. A Two-Dimensional Quadrupole Ion Trap Mass Spectrometer. *J. Am. Soc. Mass Spectrom.* **2002**, *13* (6), 659–669. https://doi.org/10.1016/S1044-0305(02)00384-7.

(78) McLachlan, N. W. *Theory and Application of Mathieu Functions*; Clarendon Press, 1947.

(79) *Tandem Mass Spectrometry | Science*. https://www.science.org/doi/10.1126/science.7280693 (accessed 2023-06-27).

(80) McLafferty, F. W. Tandem Mass Spectrometry (MS/MS): A Promising New Analytical Technique for Specific Component Determination in Complex Mixtures. *Acc. Chem. Res.* **1980**, *13* (2), 33–39. https://doi.org/10.1021/ar50146a001.

(81) Douglas, D. J.; Frank, A. J.; Mao, D. Linear Ion Traps in Mass Spectrometry. *Mass Spectrom. Rev.* **2005**, *24* (1), 1–29. https://doi.org/10.1002/mas.20004.

(82) Douglas, D. J. Multipole Inlet System for Ion Traps. US5179278A, January 12, 1993. https://patents.google.com/patent/US5179278A/en (accessed 2023-06-28).

(83) Langmuir, R. V. Quadrupole Mass Filter with Means to Generate a Noise Spectrum Exclusive of the Resonant Frequency of the Desired Ions to Deflect Stable Ions. US3334225A, August 1, 1967. https://patents.google.com/patent/US3334225A/en (accessed 2023-06-28).

(84) Körner, R.; Wilm, M.; Morand, K.; Schubert, M.; Mann, M. Nano Electrospray Combined with a Quadrupole Ion Trap for the Analysis of Peptides and Protein Digests. *J. Am. Soc. Mass Spectrom.* **1996**, *7* (2), 150–156. https://doi.org/10.1016/1044-0305(95)00626-5.

(85) Marshall, A. G.; Wang, T. C. L.; Ricca, T. L. Tailored Excitation for Fourier Transform Ion Cyclotron Mass Spectrometry. *J. Am. Chem. Soc.* **1985**, *107* (26), 7893–7897. https://doi.org/10.1021/ja00312a015.

(86) Julian, R. K.; Cooks, R. Graham. Broad-Band Excitation in the Quadrupole Ion Trap Mass Spectrometer Using Shaped Pulses Created with the Inverse Fourier Transform. *Anal. Chem.* **1993**, *65* (14), 1827–1833. https://doi.org/10.1021/ac00062a006.

(87) Guan, Shenheng.; Marshall, A. G. Stored Waveform Inverse Fourier Transform Axial Excitation/Ejection for Quadrupole Ion Trap Mass Spectrometry. *Anal. Chem.* **1993**, *65* (9), 1288–1294. https://doi.org/10.1021/ac00057a029.

(88) Louris, J. N.; Taylor, D. M. Method and Apparatus for Ejecting Unwanted Ions in an Ion Trap Mass Spectrometer. US5324939A, June 28, 1994. https://patents.google.com/patent/US5324939A/en (accessed 2023-06-28).

(89) Londry, F. A.; Hager, J. W. Mass Selective Axial Ion Ejection from a Linear Quadrupole Ion Trap. *J. Am. Soc. Mass Spectrom.* **2003**, *14* (10), 1130–1147. https://doi.org/10.1016/S1044-0305(03)00446-X.

(90) Soyk, M. W.; Zhao, Q.; Houk, R. S.; Badman, E. R. A Linear Ion Trap Mass Spectrometer with Versatile Control and Data Acquisition for Ion/Ion Reactions. *J. Am. Soc. Mass Spectrom.* **2008**, *19* (12), 1821–1831. https://doi.org/10.1016/j.jasms.2008.08.020.

(91) Louris, J. N.; Cooks, R. Graham.; Syka, J. E. P.; Kelley, P. E.; Stafford, G. C.; Todd, J. F. J. Instrumentation, Applications, and Energy Deposition in Quadrupole Ion-Trap Tandem Mass Spectrometry. *Anal. Chem.* **1987**, *59* (13), 1677–1685. https://doi.org/10.1021/ac00140a021.

(92) *Quadrupole Mass Spectrometry and Its Applications - 1st Edition*. https://shop.elsevier.com/books/quadrupole-mass-spectrometry-and-its-applications/dawson/978-0-444-41345-1 (accessed 2023-06-29).

(93) *Mass Spectrometry: Principles and Applications, 3rd Edition | Wiley*. Wiley.com. https://www.wiley.com/en-be/Mass+Spectrometry%3A+Principles+and+Applications%2C+3rd+Edition-p-9780470033104 (accessed 2023-06-30).

(94) McLuckey, S. A. Principles of Collisional Activation in Analytical Mass Spectrometry. *J. Am. Soc. Mass Spectrom.* **1992**, *3* (6), 599–614. https://doi.org/10.1016/1044-0305(92)85001-Z.

(95) Wells, J. M.; McLuckey, S. A. Collision-Induced Dissociation (CID) of Peptides and Proteins. *Methods Enzymol.* **2005**, *402*, 148–185. https://doi.org/10.1016/S0076-6879(05)02005-7.

(96) Xia, Y.; Liang, X.; McLuckey, S. A. Ion Trap versus Low-Energy Beam-Type Collision-Induced Dissociation of Protonated Ubiquitin Ions. *Anal. Chem.* **2006**, *78* (4), 1218–1227. https://doi.org/10.1021/ac051622b.

(97) *A new technique for decomposition of selected ions in molecule ion reactor coupled with ortho-time-of-flight mass spectrometry - Dodonov - 1997 - Rapid Communications in Mass Spectrometry - Wiley Online Library*. https://analyticalsciencejournals.onlinelibrary.wiley.com/doi/abs/10.1002/(SICI)1097-0231(19971015)11:15%3C1649::AID-RCM67%3E3.0.CO;2-T?casa_token=6fr1d5mcZ18AAAAA:4zoLxV5GmcP8hCqHuoP1VXS34r0eHQiuHLY6xf-YAMp-Wu2K9pDy45nkUg1MtUy3KW3zJMM32WOn1nDOMw (accessed 2023-06-30).

(98) Prentice, B. M.; Santini, R. E.; McLuckey, S. A. Adaptation of a 3-D Quadrupole Ion Trap for Dipolar DC Collisional Activation. *J. Am. Soc. Mass Spectrom.* **2011**, *22* (9), 1486–1492. https://doi.org/10.1007/s13361-011-0183-z.

(99) Wang, L.; Xu, F.; Ding, C.-F. Dipolar Direct Current Driven Collision-Induced Dissociation in a Digital Ceramic-Based Rectilinear Ion Trap Mass Spectrometer. *Anal. Chem.* **2013**, *85* (3), 1271–1275. https://doi.org/10.1021/ac3031256.

(100) Prentice, B. M.; McLuckey, S. A. Dipolar DC Collisional Activation in a "Stretched" 3-D Ion Trap: The Effect of Higher Order Fields on Rf-Heating. *J. Am. Soc. Mass Spectrom.* **2012**, *23* (4), 736–744. https://doi.org/10.1007/s13361-011-0303-9.

(101) Prentice, B. M.; Xu, W.; Ouyang, Z.; McLuckey, S. A. DC Potentials Applied to an End-Cap Electrode of a 3D Ion Trap for Enhanced MSn Functionality. *Int. J. Mass Spectrom.* **2011**, *306* (2), 114–122. https://doi.org/10.1016/j.ijms.2010.09.022.

(102) Webb, I. K.; Londry, F. A.; McLuckey, S. A. Implementation of Dipolar Direct Current (DDC) Collision-Induced Dissociation in Storage and Transmission Modes on a Quadrupole/Time-of-Flight Tandem Mass Spectrometer. *Rapid Commun. Mass Spectrom.* **2011**, *25* (17), 2500–2510. https://doi.org/10.1002/rcm.5152.

(103) Kelly, R. T.; Tolmachev, A. V.; Page, J. S.; Tang, K.; Smith, R. D. The Ion Funnel: Theory, Implementations, and Applications. *Mass Spectrom. Rev.* **2010**, *29* (2), 294–312. https://doi.org/10.1002/mas.20232.

(104) Tolmachev, A. V.; Chernushevich, I. V.; Dodonov, A. F.; Standing, K. G. A Collisional Focusing Ion Guide for Coupling an Atmospheric Pressure Ion Source to a Mass Spectrometer. *Nucl. Instrum. Methods Phys. Res. Sect. B Beam Interact. Mater. At.* **1997**, *124* (1), 112–119. https://doi.org/10.1016/S0168-583X(97)00068-2.

(105) Tolmachev, A. V.; Kim, T.; Udseth, H. R.; Smith, R. D.; Bailey, T. H.; Futrell, J. H. Simulation-Based Optimization of the Electrodynamic Ion Funnel for High Sensitivity Electrospray Ionization Mass Spectrometry. *Int. J. Mass Spectrom.* **2000**, *203* (1), 31–47. https://doi.org/10.1016/S1387-3806(00)00265-7.

(106) *Recent developments in the ion/ion chemistry of high-mass multiply charged ions - Pitteri - 2005 - Mass Spectrometry Reviews - Wiley Online Library*. https://analyticalsciencejournals.onlinelibrary.wiley.com/doi/full/10.1002/mas.20048 (accessed 2023-06-30).

(107) Ogorzalek Loo, R. R.; Udseth, H. R.; Smith, R. D. A New Approach for the Study of Gas-Phase Ion-Ion Reactions Using Electrospray Ionization. *J. Am. Soc. Mass Spectrom.* **1992**, *3* (7), 695–705. https://doi.org/10.1016/1044-0305(92)87082-A.

(108) McLuckey, S. A.; Stephenson, J. L. Ion/Ion Chemistry of High-Mass Multiply Charged Ions. *Mass Spectrom. Rev.* **1998**, *17* (6), 369–407. https://doi.org/10.1002/(SICI)1098-2787(1998)17:6<369::AID-MAS1>3.0.CO;2-J.

(109) Shenault, D. M.; McLuckey, S. A.; Franklin, E. T. Localization of Cyclopropyl Groups and Alkenes within Glycerophospholipids Using Gas-Phase Ion/Ion Chemistry. *J. Mass Spectrom.* **2023**, *58* (4), e4913. https://doi.org/10.1002/jms.4913.

(110) Randolph, C. E.; Foreman, D. J.; Betancourt, S. K.; Blanksby, S. J.; McLuckey, S. A. Gas-Phase Ion/Ion Reactions Involving Tris-Phenanthroline Alkaline Earth Metal Complexes as Charge Inversion Reagents for the Identification of Fatty Acids. *Anal. Chem.* **2018**, *90* (21), 12861–12869. https://doi.org/10.1021/acs.analchem.8b03441.

(111) Randolph, C. E.; Blanksby, S. J.; McLuckey, S. A. Toward Complete Structure Elucidation of Glycerophospholipids in the Gas Phase through Charge Inversion Ion/Ion Chemistry. *Anal. Chem.* **2020**, *92* (1), 1219–1227. https://doi.org/10.1021/acs.analchem.9b04376.

(112) Randolph, C. E.; Foreman, D. J.; Blanksby, S. J.; McLuckey, S. A. Generating Fatty Acid Profiles in the Gas Phase: Fatty Acid Identification and Relative Quantitation Using Ion/Ion Charge Inversion Chemistry. *Anal. Chem.* **2019**, *91* (14), 9032–9040. https://doi.org/10.1021/acs.analchem.9b01333.

(113) Randolph, C. E.; Shenault, D. M.; Blanksby, S. J.; McLuckey, S. A. Localization of Carbon–Carbon Double Bond and Cyclopropane Sites in Cardiolipins via Gas-Phase Charge Inversion Reactions. *J. Am. Soc. Mass Spectrom.* **2021**, *32* (2), 455–464. https://doi.org/10.1021/jasms.0c00348.

(114) Randolph, C. E.; Shenault, D. M.; Blanksby, S. J.; McLuckey, S. A. Structural Elucidation of Ether Glycerophospholipids Using Gas-Phase Ion/Ion Charge Inversion Chemistry. *J. Am. Soc. Mass Spectrom.* **2020**, *31* (5), 1093–1103. https://doi.org/10.1021/jasms.0c00025.

(115) Franklin, E. T.; Betancourt, S. K.; Randolph, C. E.; McLuckey, S. A.; Xia, Y. In-Depth Structural Characterization of Phospholipids by Pairing Solution Photochemical Reaction with Charge Inversion Ion/Ion Chemistry. *Anal. Bioanal. Chem.* **2019**, *411* (19), 4739–4749. https://doi.org/10.1007/s00216-018-1537-1.

(116) Randolph, C. E.; Marshall, D. L.; Blanksby, S. J.; McLuckey, S. A. Charge-Switch Derivatization of Fatty Acid Esters of Hydroxy Fatty Acids via Gas-Phase Ion/Ion Reactions. *Anal. Chim. Acta* **2020**, *1129*, 31–39. https://doi.org/10.1016/j.aca.2020.07.005.

(117) Randolph, C. E.; Blanksby, S. J.; McLuckey, S. A. Enhancing Detection and Characterization of Lipids Using Charge Manipulation in Electrospray Ionization-Tandem Mass Spectrometry. *Chem. Phys. Lipids* **2020**, *232*, 104970. https://doi.org/10.1016/j.chemphyslip.2020.104970.

(118) Griffiths, J. A Brief History of Mass Spectrometry. *Anal. Chem.* **2008**, *80* (15), 5678–5683. https://doi.org/10.1021/ac8013065.

(119) Holden, D. T.; Morato, N. M.; Cooks, R. G. Aqueous Microdroplets Enable Abiotic Synthesis and Chain Extension of Unique Peptide Isomers from Free Amino Acids. *Proc. Natl. Acad. Sci.* **2022**, *119* (42), e2212642119. https://doi.org/10.1073/pnas.2212642119.

(120) Naudí, A.; Cabré, R.; Jové, M.; Ayala, V.; Gonzalo, H.; Portero-Otín, M.; Ferrer, I.; Pamplona, R. Chapter Five - Lipidomics of Human Brain Aging and Alzheimer's Disease Pathology. In *International Review of Neurobiology*; Hurley, M. J., Ed.; Omic Studies of Neurodegenerative Disease: Part B; Academic Press, 2015; Vol. 122, pp 133–189. https://doi.org/10.1016/bs.irn.2015.05.008.

(121) Wang, M.; Han, X. Multidimensional Mass Spectrometry-Based Shotgun Lipidomics. In *Mass Spectrometry in Metabolomics: Methods and Protocols*; Raftery, D., Ed.; Methods in Molecular Biology; Springer: New York, NY, 2014; pp 203–220. https://doi.org/10.1007/978-1-4939-1258-2_13.

(122) Han, X.; Gross, R. W. Shotgun Lipidomics: Multidimensional MS Analysis of Cellular Lipidomes. *Expert Rev. Proteomics* **2005**, *2* (2), 253–264. https://doi.org/10.1586/14789450.2.2.253.

(123) Han, X.; Yang, K.; Cheng, H.; Fikes, K. N.; Gross, R. W. Shotgun Lipidomics of Phosphoethanolamine-Containing Lipids in Biological Samples after One-Step in Situ Derivatization. *J. Lipid Res.* **2005**, *46* (7), 1548–1560. https://doi.org/10.1194/jlr.D500007-JLR200.

(124) Hu, C.; Duan, Q.; Han, X. Strategies to Improve/Eliminate the Limitations in Shotgun Lipidomics. *PROTEOMICS* **2020**, *20* (11), 1900070. https://doi.org/10.1002/pmic.201900070.

(125) Hsu, F.-F. Mass Spectrometry Based Shotgun Lipidomics-a Critical Review from the Technical Point of View. *Anal. Bioanal. Chem.* **2018**, *410* (25), 6387–6409. https://doi.org/10.1007/s00216-018-1252-y.

(126) Yeagle, P. L. Chapter 12 - Lipid–Protein Interactions in Membranes. In *The Membranes of Cells (Third Edition)*; Yeagle, P. L., Ed.; Academic Press: Boston, 2016; pp 291–334. https://doi.org/10.1016/B978-0-12-800047-2.00012-7.

(127) Vosse, C.; Wienken, C.; Cadenas, C.; Hayen, H. Separation and Identification of Phospholipids by Hydrophilic Interaction Liquid Chromatography Coupled to Tandem High Resolution Mass Spectrometry with Focus on Isomeric Phosphatidylglycerol and Bis(Monoacylglycero)Phosphate. *J. Chromatogr. A* **2018**, *1565*, 105–113. https://doi.org/10.1016/j.chroma.2018.06.039.

(128) Naudí, A.; Cabré, R.; Jové, M.; Ayala, V.; Gonzalo, H.; Portero-Otín, M.; Ferrer, I.; Pamplona, R. Lipidomics of Human Brain Aging and Alzheimer's Disease Pathology. *Int. Rev. Neurobiol.* **2015**, *122*, 133–189. https://doi.org/10.1016/bs.irn.2015.05.008.

(129) Murphy, R. C. *Tandem Mass Spectrometry of Lipids: Molecular Analysis of Complex Lipids*; Royal Society of Chemistry, 2014.

(130) Grundy, S. M. Cholesterol: Factors Determining Blood Levels. In *Encyclopedia of Human Nutrition (Third Edition)*; Caballero, B., Ed.; Academic Press: Waltham, 2013; pp 335–340. https://doi.org/10.1016/B978-0-12-375083-9.00051-9.

(131) Pelley, J. W. 10 - Fatty Acid and Triglyceride Metabolism. In *Elsevier's Integrated Review Biochemistry (Second Edition)*; Pelley, J. W., Ed.; W.B. Saunders: Philadelphia, 2012; pp 81–88. https://doi.org/10.1016/B978-0-323-07446-9.00010-6.

1.10 Figures

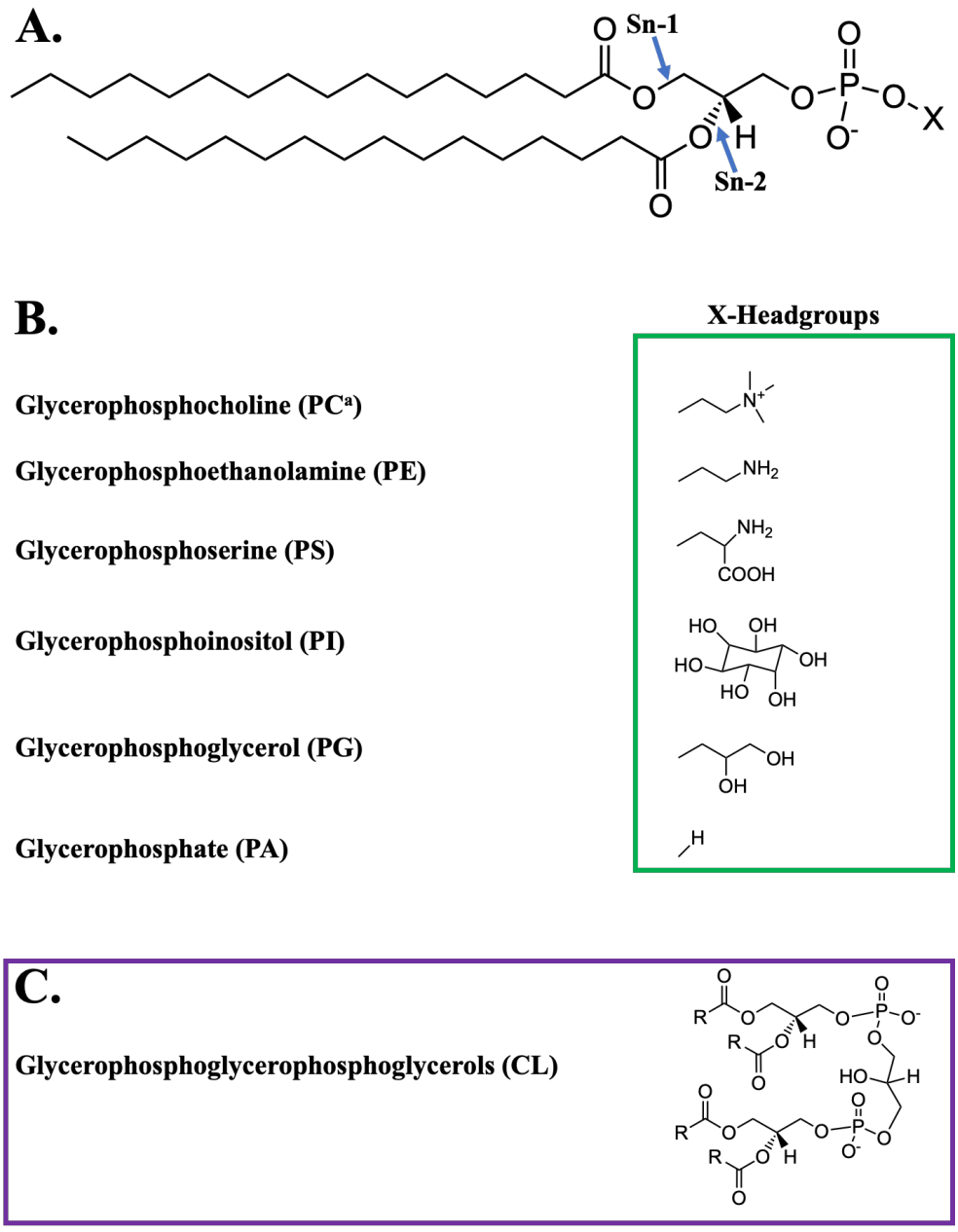

Figure 1.1 - The glycerophospholipid (GPs). (a) A diagram illustrating the GPs structure; GPs has two fatty acids at the sn-1 and sn-2 position, esterfied to a glycerol backbone and phosphate group with varying headgroups. (b) the different variation of headgroups are represented by the major classes of GPs; glycerophosphate (PA), glycerophosphocholine (PC), glycerophosphoethanolamine (PE), glycerophosphoglycerol (PG), glycerophosphoserine (PS), and glycerophosphoinositol (PI). (c) cardiolipid are a unique subclass of phospholipids, sharing two phosphatidic acids groups linked to a glycerol backbone.

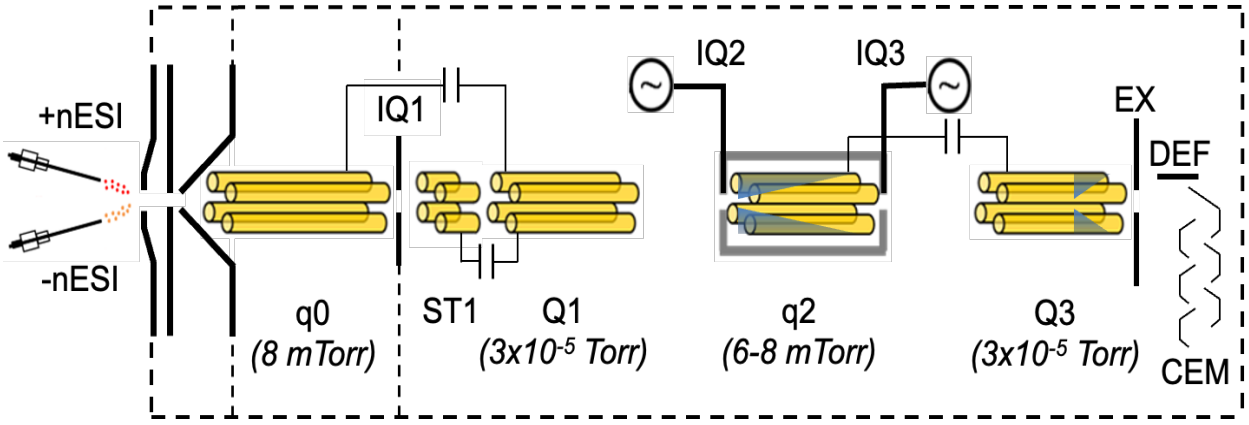

Figure 1.2 - A schematic of a Sciex 4000 Quadrupole modified for Ion/Ion reactions.

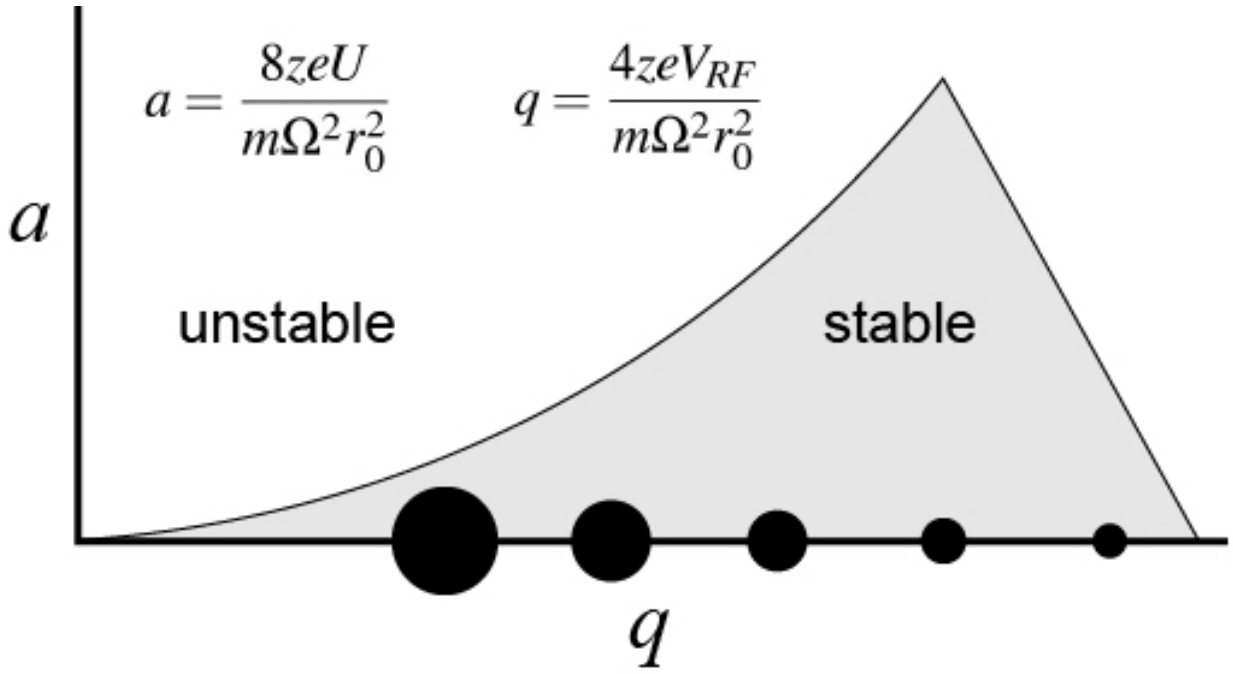

Figure 1.3 – Mathieu stability diagram depicted by Aston Labs: Ion Trap Development at Purdue University. Reconstructed by Dr. Graham Cooks lab. https://aston.chem.purdue.edu/research/ion-trap.html.

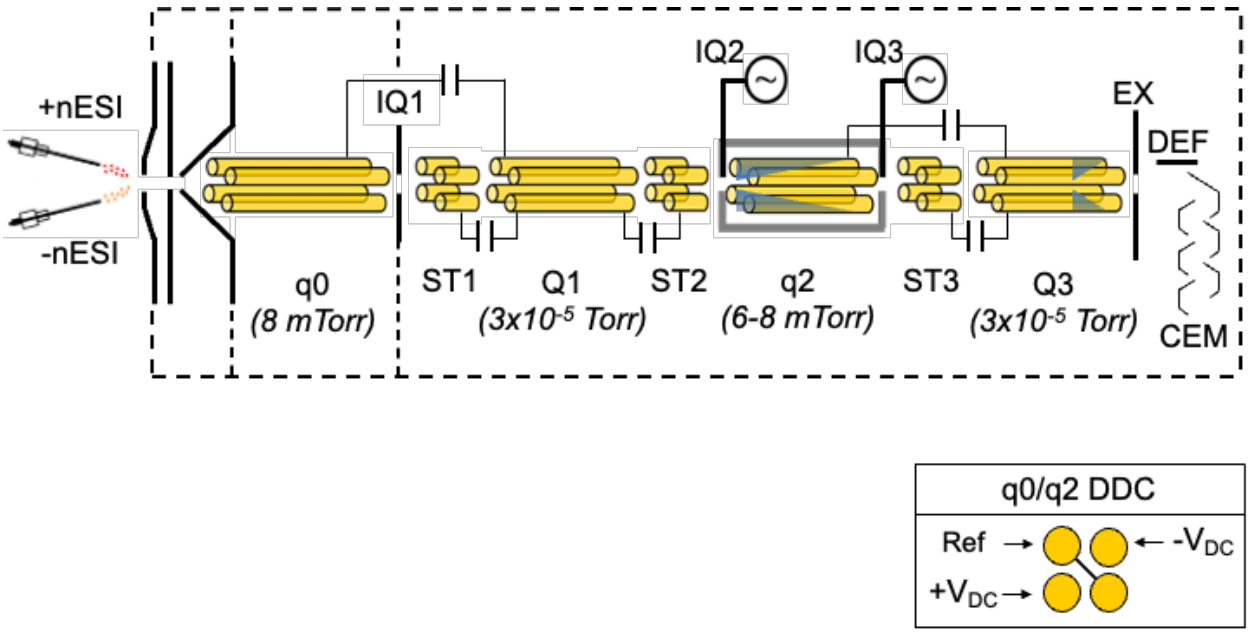

Figure 1.4 – Schematic of Sciex QTRAP 4000, triple quadrupole mass spectrometer with DDC offset.

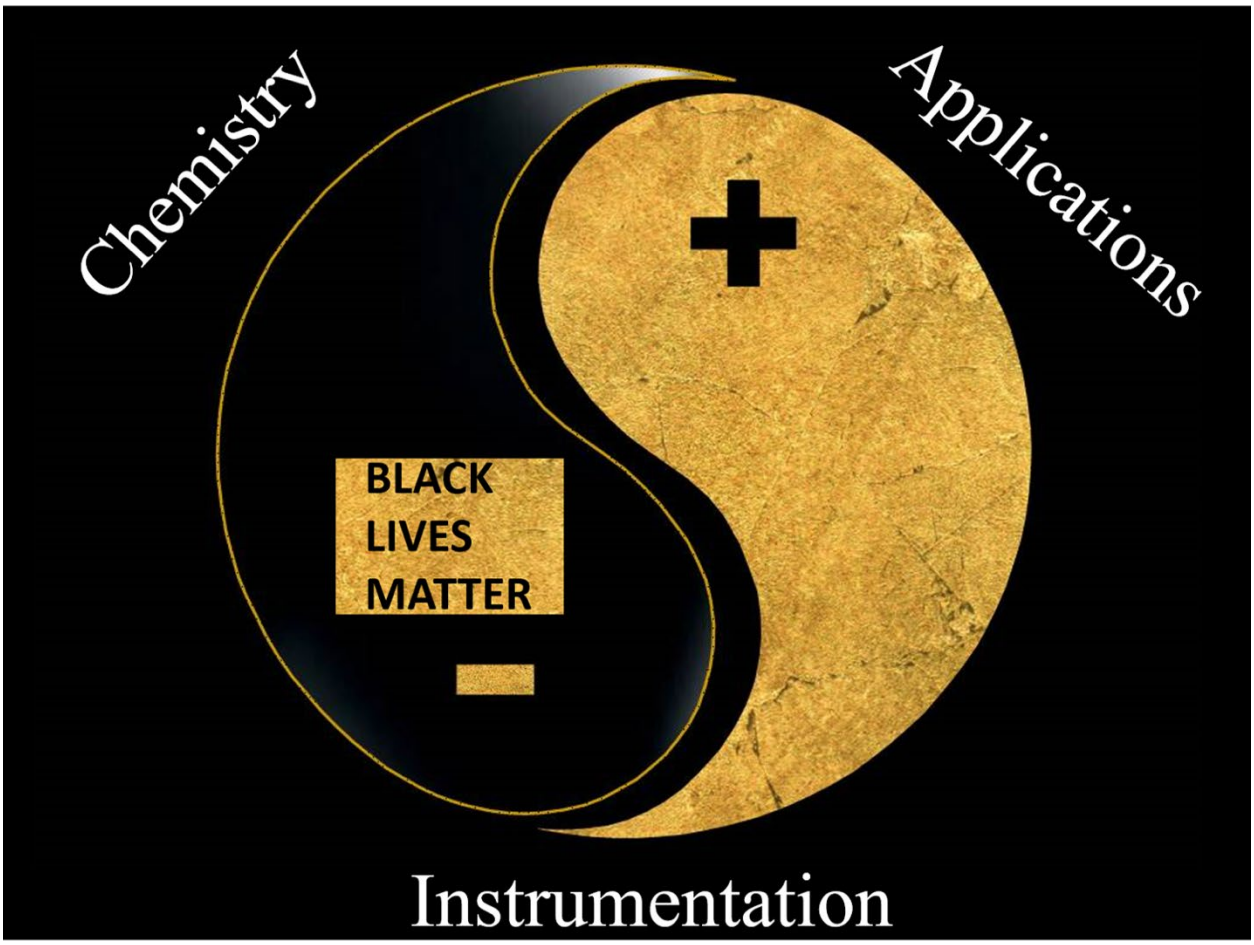

Figure 1.5 – Diagram of the ion/ion reaction in the McLuckey laboratory.

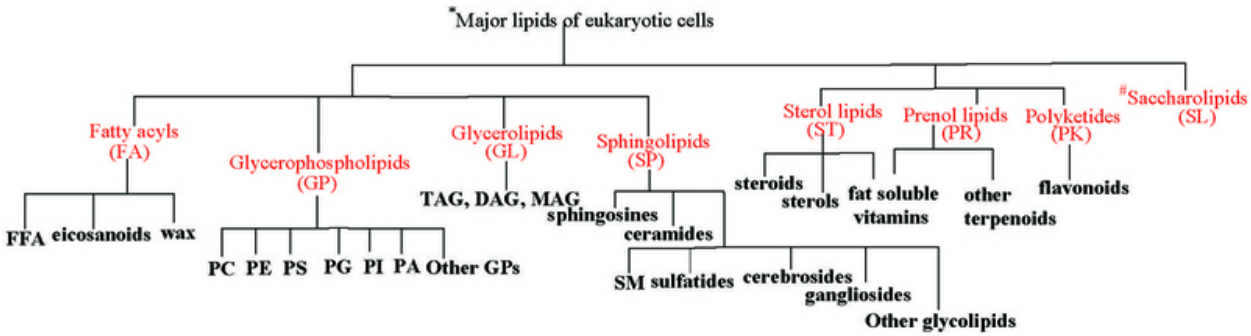

Figure 1.6 – Different classes and subclasses of of lipids found in eukaryotic cells.

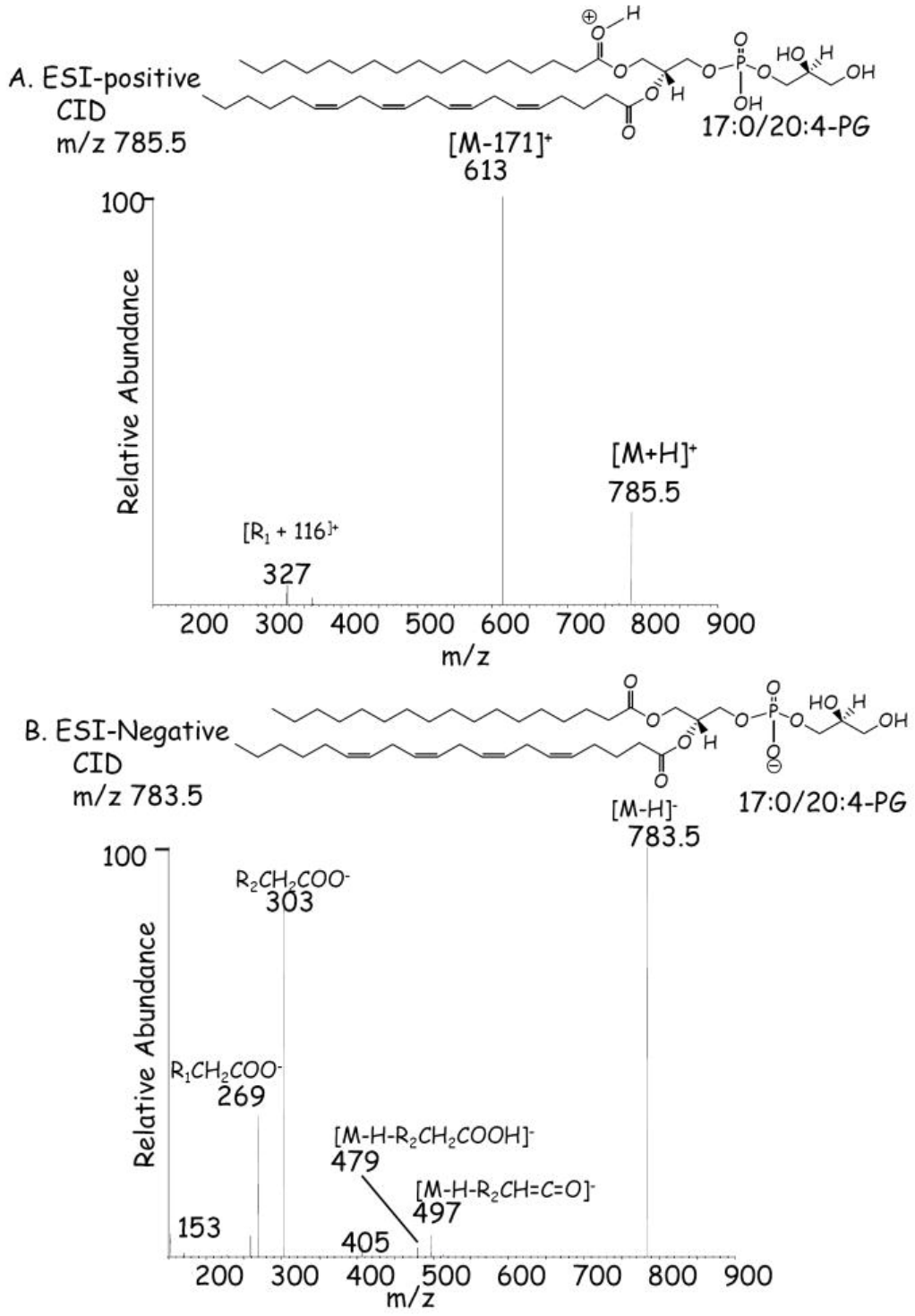

Figure 1.7 - Negative and Positive CID mass spectra of PG (17:0/20:4, ionized via ESI. (a) CID spectra of protonated PG 17:0/20:4 [M + H]+ ion at 785.5 m/z. (b) CID spectra of deprotonated PG 17:0/20:4 [M - H]- ion at 783.5 m/z. Reconstructed from Murphy RC, Axelsen PH. Mass spectrometric analysis of long-chain lipids. Mass Spectrom Rev. 2011 Jul-Aug;30(4):579-99. doi: 10.1002/mas.20284. Epub 2010 Nov 8. PMID: 21656842; PMCID: PMC3117083.

1.11 Schemes

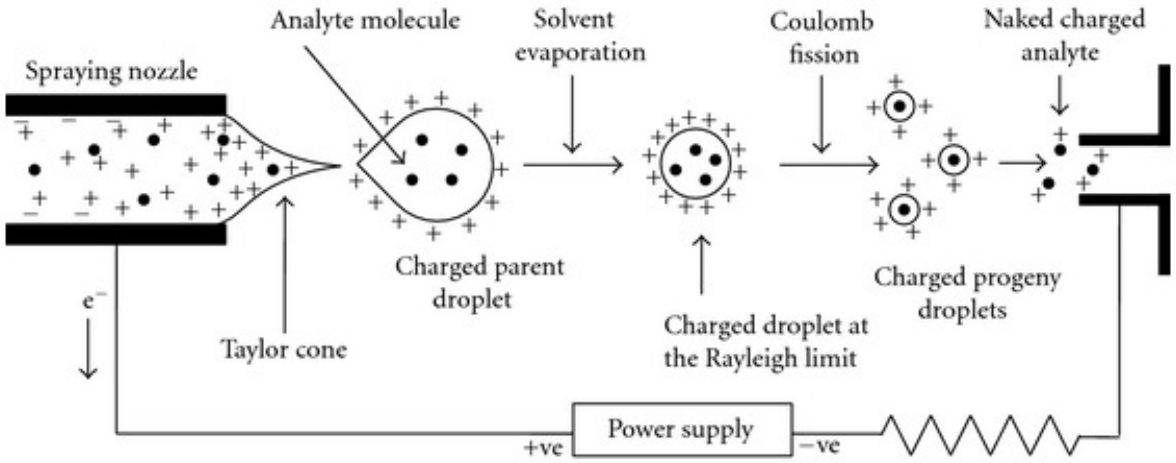

Scheme 1.1 - The schematic respresenting the elsectrospray ionization of a analyte. Reconstructed from Banerjee, S. and Mazumdar, S. Int. J. of Anal. Chem., 2012 (8), 1-40 (2012).

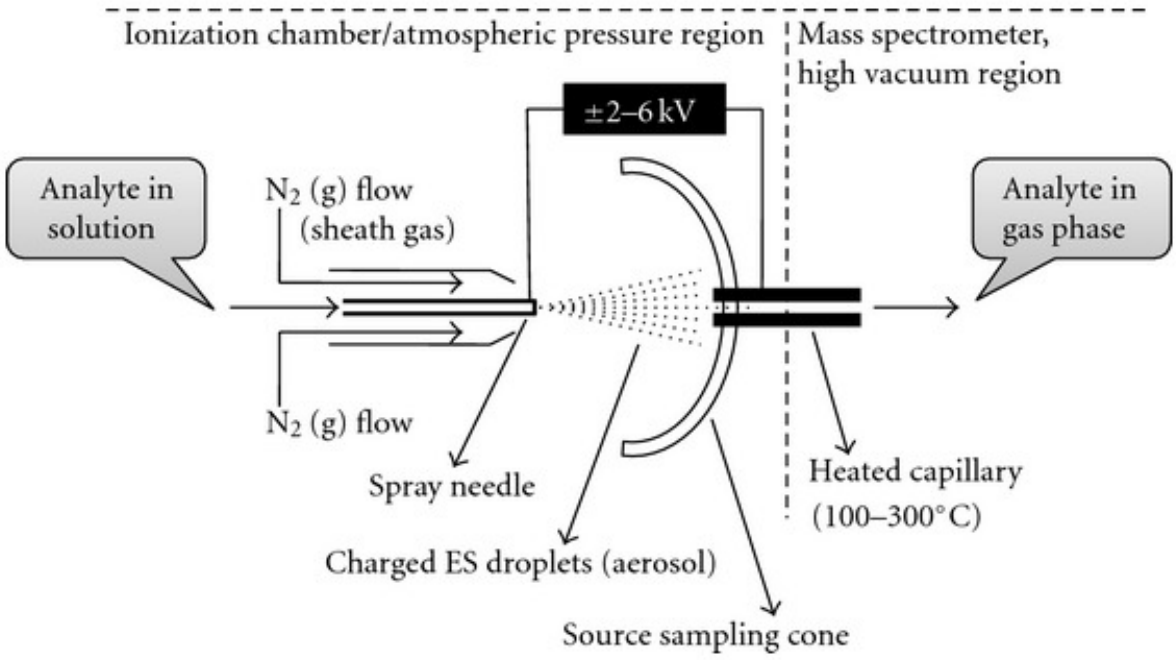

Scheme 1.2 - The schematic representing the electrospray ionization ion source. Reconstructed from Banerjee, S. and Mazumdar, S. Int. J. of Anal. Chem., 2012 (8), 1-40 (2012).

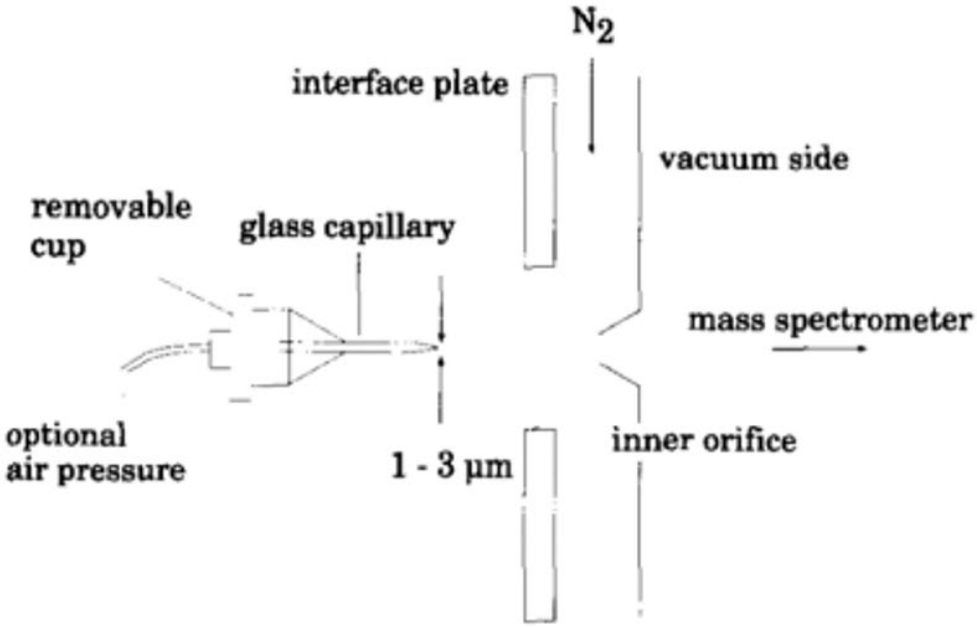

Scheme 1.3 - Nano-electrospray ionization (nESI) schematic that illustrates the utilization of tips for analysis. Reconstructed from Wilm, M.S. and Mann, M, Int. J. of Mass Spectrom. and Ion Process., 136(2), 167-180 (1994).

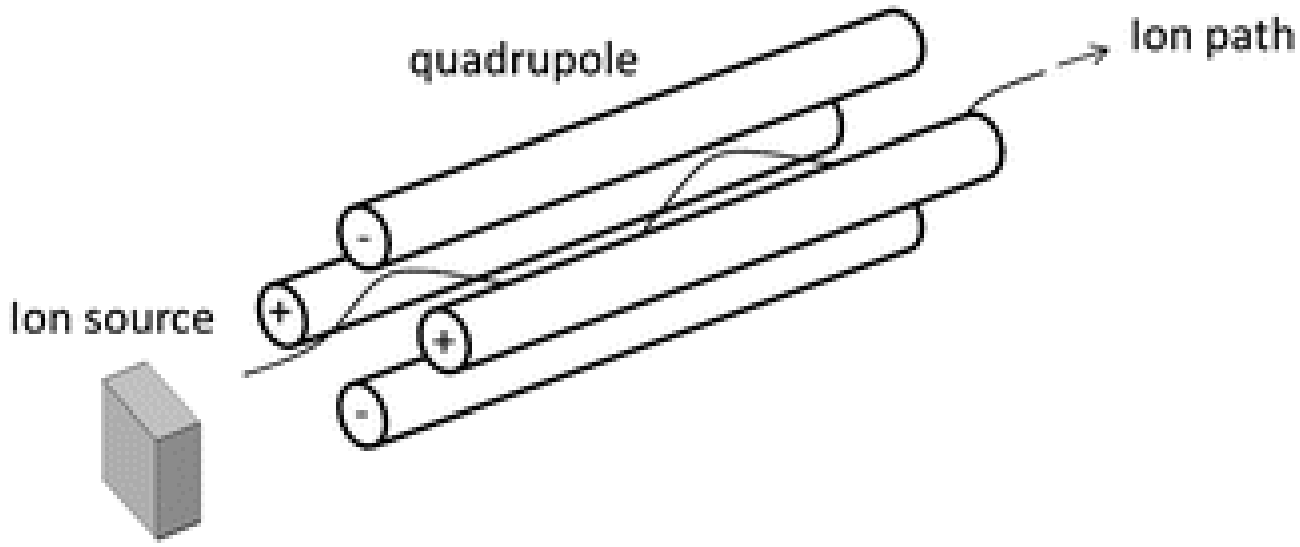

Scheme 1.4 – Schematic of the quadrupole mass analyzer. Reconstructed from Haag, A.M. (2016). Mass Analyzers and Mass Spectrometers. In: Mirzaei, H., Carrasco, M. (eds) Modern Proteomics – Sample Preparation, Analysis and Practical Applications. Advances in Experimental Medicine and Biology, vol 919. Springer, Cham. https://doi.org/10.1007/978-3-319-41448-5_7

PG 18:1(9Z)/18:1(9Z)

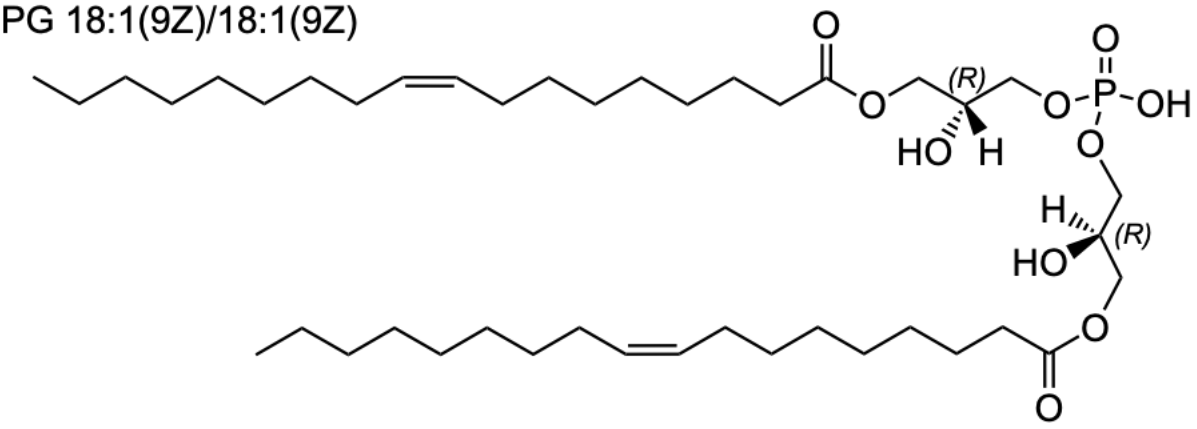

Chemical Formula: $C_{42}H_{79}O_{10}P$
Exact Mass: 774.54
Molecular Weight: 775.06
m/z: 774.54 (100.0%), 775.54 (45.4%), 776.55 (12.7%), 777.55 (2.5%), 775.55 (1.3%)

BMP 18:1(9Z)/18:1(9Z)

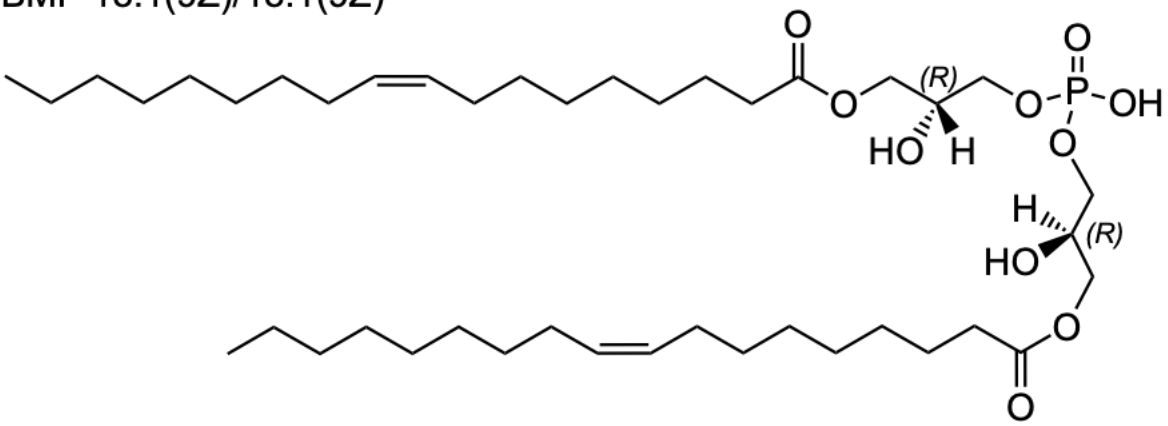

Chemical Formula: $C_{42}H_{79}O_{10}P$
Exact Mass: 774.54
Molecular Weight: 775.06
m/z: 774.54 (100.0%), 775.54 (45.4%), 776.55 (12.7%), 777.55 (2.5%), 775.55 (1.3%)

Scheme 1.5 – A schematic of phosphatidylglycerol (PGs) and bis(monoacylglycerol)phosphate (BMP) structures.

1.12 Tables

Table 1.1 - Precursor Ion Scans (PIS) and Netural Loss Scan (NLS) for lipid class m/z in positive in negative ion mode. Reconstructed by Hsu FF. Mass spectrometry-based shotgun lipidomics - a critical review from the technical point of view. Anal Bioanal Chem. 2018 Oct;410(25):6387-6409. doi: 10.1007/s00216-018-1252-y. Epub 2018 Aug 9. PMID: 30094786; PMCID: PMC6195124.

Lipid class	Detected ion type	scan mode	Fragment type	*optimal CE	References	Comments
PC	$[M + H]^+$	PIS 184	$[phosphocholine + H]^+$	34 eV	12	Excellent sensitivity
SM	$[M + H]^+$	PIS 184	$[phosphocholine + H]^+$	38 eV	12	Excellent sensitivity
PS	$[M + H]^+$	NLS 185	loss of phosphoserine	32 eV	12	Moderate sensitivity
PE	$[M + H]^+$	NLS 141	loss of phosphoethanolamine	32 eV	12	Moderate sensitivity, discriminates against plasmalogen PE; overlaps with $[M + Na]^+$
Cer	$[M + H - H_2O]^+$	PIS 264	$[LCB + H - 2H_2O]^+$	32 eV	79	Good sensitivity
Cer	$[M + Li]^+$	NLS 48	loss of $[H_2O + HCHO]$	45 eV	78	Good sensitivity for all LCB/nFA-Cer; not very specific; discriminates against LCB/αhFA-Cer
PC	$[M + Li]^+$	NLS 183	loss of phosphocholine	35 eV	83	Good sensitivity; favors polyunsaturated-FA containing PC
SM	$[M + Li]^+$	NLS 183	loss of phosphocholine	40 eV	58,67	Good sensitivity
SM	$[M + Li]^+$	NLS 59	loss of trimethylamine	30eV	58,67	Good sensitivity
SM	$[M + Li]^+$	NLS 213 1	loss of [phosphocholine + HCHO]	52eV	58,67	Good sensitivity
PS	$[M + Li]^+$	NLS 191	loss of [phosphoserine Li salt]	35 eV	9	Good sensitivity
PE	$[M - H + 2Li]^+$	NLS 129	loss of [phosphoethanolamine Li salt $- H_2O$]	32 eV	69	Good sensitivity and fidelity; dilithiated ions are less readily formed
PG	$[M - H + 2Li]^+$	PIS 167	$[phosphoglycerol - H + 2Li]^+$	45eV	9	Good sensitivity and fidelity; dilithiated ions are difficult to form
GlcCer	$[M + Li]^+$	NLS 210	loss of [Glc + HCHO]	65eV	59	Good sensitivity
PE	$[M + Na]^+$	PIS 164	$[phosaphethanolamine + Na]^+$	35eV	75	Good sensitivity; discriminates against plasmalogen PE
PG	$[M - H]^-$	PIS 153	$[phosphoglycerol - H_2O - H]^-$	35 eV	12	Poor sensitivity; not specific, co-present with all other phospholipids, and CL
PS	$[M - H]^-$	NLS 87	loss of $[serine - H_2O]$	25eV	9,12	Excellent sensitivity
PE	$[M - H]^-$	PIS 196	$[phosphoethanolamine - H + C_3H_4O]^-$	55eV	12,76	Poor sensitivity
PE	$[M + Cl]^-$	NLS 36	loss of $H^{35}Cl$	25eV	75	Excellent sensitivity; $[M + Cl]^-$ ions not readily formed
PI	$[M - H]^-$	PIS 241	$[phosphoinositol - H_2O - H]^-$	45eV	12, 65	Excellent sensitivity

Table 1.1 continued

Lipid class	Detected ion type	scan mode	Fragment type	*optimal CE	References	Comments
Cer	$[M-H]^-$	NLS 256	loss of $[C_{13}H_{27}CH{=}CHCHO + H_2O]$	32 eV	62, this paper	Excellent sensitivity; sphingosine (d18:1) ceramide only; discriminates against d18:1/αhFA-Cer
Cer	$[M-H]^-$	NLS 327	loss of [sphingosine + CO]	32 eV	62	Excellent sensitivity; specifically detect d18:1/αhFA-Cer
sulfatide	$[M-H]^-$	PIS 97	$H_2PO_4^-$	65eV	63,64	Good sensitivity
PIP	$[M-H]^-$	PIS 321	[inositol bisphosphoric acid $-H_2O-H]^-$	50eV	65	Moderate sensitivity
	$[M-H]^-$	PIS 241	[phosphoinositol $-H_2O-H]^-$	50eV	65	Good sensitivity; co-present with PI, PIP_2
PIP2	$[M-H]^-$	PIS 401	[inositol trisphosphoric acid $-H_2O-H]^-$	50eV	65	Moderate sensitivity
	$[M-H]^-$	PIS 241	[phosphoinositol $-H_2O-H]^-$	50eV	65	Good sensitivity; co-present with PI, PIP
IPC	$[M-H]^-$	PIS 241	[phosphoinositol $-H_2O-H]^-$	45eV	68	Good sensitivity
CL	$[M-H]^-$	PIS 153	[phosphoinositol $-H_2O-H]^-$	50eV	66	Poor sensitivity; not specific, co-present with all other phospholipids
	$[M-2H]^{2-}$	PIS 153	[phosphoinositol $-H_2O-H]^-$	25eV	66	Poor sensitivity; unique doubly charged ion pattern easy to identify

*Collison energy (CE) was optimized for overall fidelity and sensitivity

CHAPTER 2. LOCALIZATION OF CYCLOPROPYL GROUPS AND ALKENES WITHIN GLYCEROPHOSPHOLIPIDS USING GAS-PHASE ION/ION CHEMISTRY

Reprinted by permission from John Wiley and Sons: Journal of Mass Spectrometry. Shenault, DM, McLuckey, SA, Franklin, ET. Localization of cyclopropyl groups and alkenes within glycerophospholipids using gas-phase ion/ion chemistry. J Mass Spectrom. 2023; 58(4):e4913. doi:10.1002/jms.4913.

2.1 Abstract

Shotgun lipid analysis using electrospray ionization tandem mass spectrometry (ESI-MS/MS) is a common approach for the identification and characterization of glycerophohspholipids GPs. ESI-MS/MS, with the aid of collision-induced dissociation (CID), enables the characterization of GP species at the headgroup and fatty acyl sum compositional levels. However, important structural features that are often present, such as carbon–carbon double bond(s) and cyclopropane ring(s), can be difficult to determine. Here, we report the use of gas-phase charge inversion reactions that, in combination with CID, allow for more detailed structural elucidation of GPs. CID of a singly deprotonated GP, $[GP - H]^-$, generates FA anions, $[FA - H]^-$. The fatty acid anions can then react with doubly charged cationic magnesium tris-phenanthroline complex, $[Mg(Phen)_3]^{2+}$, to form charge inverted complex cations of the form $[FA - H + MgPhen_2]^+$. CID of the complex generates product ion spectral patterns that allow for the identification of carbon–carbon double bond position(s) as well as the sites of cyclopropyl position(s) in unsaturated lipids. This approach to determining both double bond and cyclopropane positions is demonstrated with GPs for the first time using standards and is applied to lipids extracted from *Escherichia coli*.

2.2 Introduction

Lipids constitute a large class of bio-molecules that play crucial roles in membrane composition, metabolism, and cellular communication.[1] Glycerophospholipids (GPs) constitute a common lipid class and are the major components of the membrane bilayer, aiding in energy storage and membrane organization.[2,3] Of the total GP content found in the *Escherichia coli* (*E. coli*) bacterial membrane, for example, 70% to 90% are composed of the GP subclasses phosphatidyleth-

anolamines (PEs), phosphatidylglycerols (PGs), and cardiolipins (CLs).[4] A typical GP is composed of a glycerol backbone with two fatty acyl (FA) chains attached at the *sn*-1 and *sn*-2 positions via an ester linkage, and one of a variety of head-groups (e.g., ethanolamine, choline, serine, inositol, or glycerol) linked via an esterified phosphate to the glycerol backbone at the *sn*-3 position.[5, 6] The complexity of the FA chains of GPs can vary, for example, on the basis of acyl chain length, nature of unsaturation (i.e., double bonds versus cyclopropane rings), extents of unsaturation, site(s) of unsaturation, and stereochemistry (e.g., cis- vs. trans-double bonds).[7]

Electrospray ionization tandem mass spectrometry (ESI-MS/MS) has been used to address the structural complexity of GPs. Activation methods such as collision-induced dissociation (CID) or higher-energy collisional dissociation, are commonly used for the structural elucidation of GPs.[8, 9] These methods applied to ions produced via ESI typically provide head-group and acyl chain composition, but are limited in localizing alterations (e.g., sites of unsaturation, cyclization, or oxidation) within the fatty acyl chain.[10] Furthermore, determining the cis/trans stereochemistry of the double bonds in lipids is problematic for widely available techniques in lipidomics,[11] although cis/trans isomers have been separated using ion mobility spectrometry and distinguished using ozone-induced dissociation (OzID) when applied to lipid standards.[11]

Although less common than double bonds, cyclopropane rings can also be present in GPs and can have significant biological relevance. Cyclopropane-containing fatty acids (CFAs), for example, are commonly found in bacteria, such as *E. coli*, *Streptococcus*, and *Salmonella*.[12] CFAs are generated by adding a methylene group, originating from S′-adenosyl-L-methionine, across the C=C bond of an unsaturated fatty acid in bacterial phospholipids.[13-15] The synthetic pathway of CFA has been extensively studied in *E. coli*,[16] and it has been reported that CFAs increase the resistance of *E. coli* to acid stress due to their influence on membrane fluidity.[17, 18] It is therefore important to be able to identify the presence of CFAs and to localize the position(s) of the cyclopropane rings in order to understand their roles.[19]

Gas-chromatography mass spectrometry constitutes the gold standard for the elucidation of lipids containing CFAs but can be time-consuming and is limited to volatile lipid samples.[20, 21] Various approaches, such as condensed-phase derivatization with the Paternò–Büchi (PB) reaction[22] and ozone-induced dissociation (OzID),[23] have been shown to be capable of determining the site(s) of unsaturation but are not appropriate for localizing cyclopropane moieties.[22, 23] Electron-based MS/MS techniques have been described for GP characterization, including double bond

localization.[24-27] An ultraviolent photodissociation (UVPD) method combined with CID, recently described by Brodbelt et al., demonstrated the localization of both C=C double bonds and cyclopropane rings in GPs derived from a bacterial extract.[10, 28] However, UVPD generally yields low dissociation efficiencies, which makes challenging the determination of relatively low-level components in biological matrices.

In this work, we demonstrate for the first time the use of gas-phase charge inversion ion/ion reactions in conjunction with CID for the localization of cyclopropane and double bond sites in GPs. Charge inversion reactions have been demonstrated for the partial structural characterization of GPs, including the localization of double bonds, present in biological matrices.[29, 30] In brief, CID of a singly deprotonated GP, $[GP-H]^-$, generates deprotonated FA anions, $[FA-H]^-$, from the fatty acyl chains. The mass of an FA anion reveals the carbon number and degree of unsaturation but CID of the anions does not reveal sites of unsaturation. The FA anions can be reacted with the doubly charged magnesium tris-phenanthroline complex, $[Mg(Phen)_3]^{2+}$, to form cations, $[FA-H+MgPhen]^+$. Subsequent CID of this ion results in charge-remote fragmentation along the aliphatic chain of the FA, which allows for the localization of double bonds and cyclopropane sites.[31] Recently, we reported the charge inversion of FA anions generated from cardiolipins to identify carbon–carbon double (C=C) bond position(s) as well as the site(s) of cyclopropyl position(s).[31, 32] We demonstrate here the application of a similar strategy to localize both cyclopropane moieties and double bonds within the fatty acyl chains in a mixture comprised primarily of PE, and PG GPs. Specifically, standards of GPs with CFAs are used to demonstrate the process while GPs extracted from *E. coli* are used to demonstrate the capability of the workflow in characterizing both double bond and cyclopropane isomers in a biological matrix.

2.3 Experimental Section

2.3.1 Nomenclature

The shorthand notation for lipid structures proposed by Liebisch et al. is adapted throughout this work when applicable.[33] GP classes are identified by their headgroups and abbreviated as such: for example, phosphatidylcholine (PC), phosphatidylethanolamine (PE), and phosphatidylglycerol (PG). GP standards have identified head groups, fatty acyl carbon numbers, C=C location, degrees of unsaturation, and stereo-orientation. For example, PC 16:0/18:1(9Z) represents a GP

with a PC headgroup, a FA 16:0 and FA 18:1 fatty acyl chain at the *sn*-1 and *sn*-2 positions, respectively, where the separator "/" indicating that the *sn*-positions are known. The separator "_" is used when the *sn*-positions are not known. The number before and after ":" indicate the carbon chain length and degree of unsaturation, respectively. C=C position and geometry is specified using "9Z" nomenclature meaning that the double bond is at the 9th carbon of the fatty acyl chain with cis geometry. When the C=C geometry is unknown, Δ-nomenclature followed by the carbon position number is used, that is, PC 16:0/18:1(Δ9). C=Cs with a cyclopropane modification are described using the nomenclature proposed by Blevins et al. where "c" specifies a known cyclopropane at that position.[10] For example, PC 16:0/18:1(c9) represents a cyclopropane motif at the 9th carbon along the fatty acyl chain of the *sn*-2 chain.

2.3.2 Chemicals

PE 16:1/17:1(c9) (16:0–17:0 cyclo PE (1-palmitoyl-2-cis-9,10-methylenehexadecanoyl-*sn*-glycero-3-phosphoethanolamine)), 17:1 Lyso PC (1-(10Z-heptadecenoyl)-2-hydroxy-*sn*-glycero-3-phosphocholine) standards and *E. coli* Total Lipid Extract (product #100500) were purchased from Avanti Polar Lipids (Alabaster, AL). Cis-10 nonadecanoic acid (10Z-nonadecenoic acid) (19:1(10Z)), phytomonic acid (19:1(c11)), FA 16:0, and FA 16:1(9Z) standards were purchased from Cayman Chemical Company (Ann Arbor, MI). Magnesium chloride, 1,10-phenanthroline (Phen), and HPLC Grade methanol were purchased from Thermo Fisher Scientific (Waltham, MA).

2.3.3 Sample Preparations

The lipid standards were dissolved in methanol and dilute to a final concentration of 10 μM. Similarly, a solution of the *E. coli* lipid extract (total) was prepared by dissolving the extract in methanol and diluted to a final concentration of 50 μM in methanol. Tris-phenanthroline magnesium complexes were prepared by mixing 1:1 (mol/mol) magnesium chloride with 1,10-phenanthroline (Phen) in 50:50 methanol:water and diluted with methanol to a final concentration of 20 μM.

2.3.4 Mass Spectrometry

All experiments were performed using a QTRAP 4000 hybrid triple quadrupole/linear ion-trap system (Sciex, Concord, ON, Canada). As previously reported,[34] this instrument has been modified to allow for the storage of anionic and cationic species simultaneously. Oppositely charged ions were generated from separate nano-ESI emitters in an alternately pulsed fashion.[35] FA standards were generated as anions using nano-ESI (−1700 V), mass selected with Q1, and transferred to the high-pressure collision cell, q2, where they were stored. Tris-phenanthroline magnesium cations, $[Mg(Phen)_3]^{2+}$, were produced by nano-ESI (+1200 V), mass isolated by Q1, and transferred to q2 to be mutually stored with the lipid fragment anions for 0.3 s.[31] The resulting cationic products, $[FA - H + Mg(Phen)_2]^+$, were transferred to Q3 where they were each mass-selected and subjected to CID. This initial CID step served to remove one of the Phen ligands to yield a $[FA - H + MgPhen]^+$ ion. Ion isolation and activation of each $[FA - H + MgPhen]^+$ ion was performed by single frequency resonance excitation at a q value of 0.383. Mass analysis was performed using mass selective axial ejection.[36] The GP anions were generated using nano-ESI (−1700 V), mass selected with Q1, and transferred to the high pressure collision cell, q2, where they were stored and subsequently collisionally activated (q = 0.25) to produce fatty acyl chain fragment anions $[FA - H]^-$. The procedure described above for the anions of the FA standards to generate and characterize $[FA - H + MgPhen]^+$ ions was used for the FA anions generated from the GP anions.

2.4 Results and Discussion

2.4.1 Distinguishing cyclopropane moieties from carbon–carbon double bonds in fatty acyl chains

Anions of model FA anions were generated by nano-ESI, converted to $[FA - H + MgPhen]^+$ ions via ion/ion reaction, and subjected to CID to illustrate the behavior of saturated, double-bond containing, and cyclopropane containing FA ions of the form $[FA - H + MgPhen]^+$. **Figure 2.1** highlights regions of the CID product ion spectra of (a) $[16:0 - H + MgPhen]^+$, (b) $[16:1(9Z) - H + MgPhen]^+$, and (c) and $[17:1(c9) - H + MgPhen]^+$ that show the distinctive dissociation behaviors of a saturated FA, a FA with single double bond, and a FA with a cyclopropane, respectively. With the exception of the *m/z* 262 ion, which is common

to the product ion spectra of all $[FA - H + MgPhen]^+$ ions and corresponds to $[\bullet CH_2CO_2^- + Mg^{2+}Phen]^+$, all product ions containing FA fragments are even-electron. In the case of the saturated FA cations, all of the neutral losses that are complementary to the even-electron product ions are alkanes (**Figure 2.1A**).

This indicates that a hydrogen transfer from the charged product to the neutral product, resulting in a double bond in the charged fragment, is the dominant process for each of the observed backbone cleavages, with the exception of the process leading to *m/z* 262. When a double bond is present, cleavages at and adjacent to the double bond are inhibited relative to cleavages one bond further away from the double bond (see **Figure 2.1B**).[37] Furthermore, spacings of 12 Da are observed between the fragments on either side of the double bond and the low-abundance fragments arising from the double bond location (compare *m/z* 359 with *m/z* 371 and *m/z* 357 with *m/z* 345) in **Figure 2.1B**.[33] The proposed products from the dissociation reactions of $[16{:}0 - H + MgPhen]^+$ leading to these ions are provided in **Scheme 2.1**. Fragmentation of the CFA ion (**Figure 2.1C**) is distinct from that of the saturated FA ion (**Figure 2.1A**) and double bond-containing FA ion (**Figure 2.1B**). In this case, multiple doublets are observed (e.g., *m/z* 357/359, *m/z* 371/373, *m/z* 385/387, and *m/z* 399/401), which reflect competing cleavage mechanisms for the relevant FA bonds involving and in the vicinity of the cyclopropyl group that result in a hydrogen transfer either to or from the charged product (see **Scheme 2.2**). This series of doublets constitutes a signature for the presence of a cyclopropyl group.

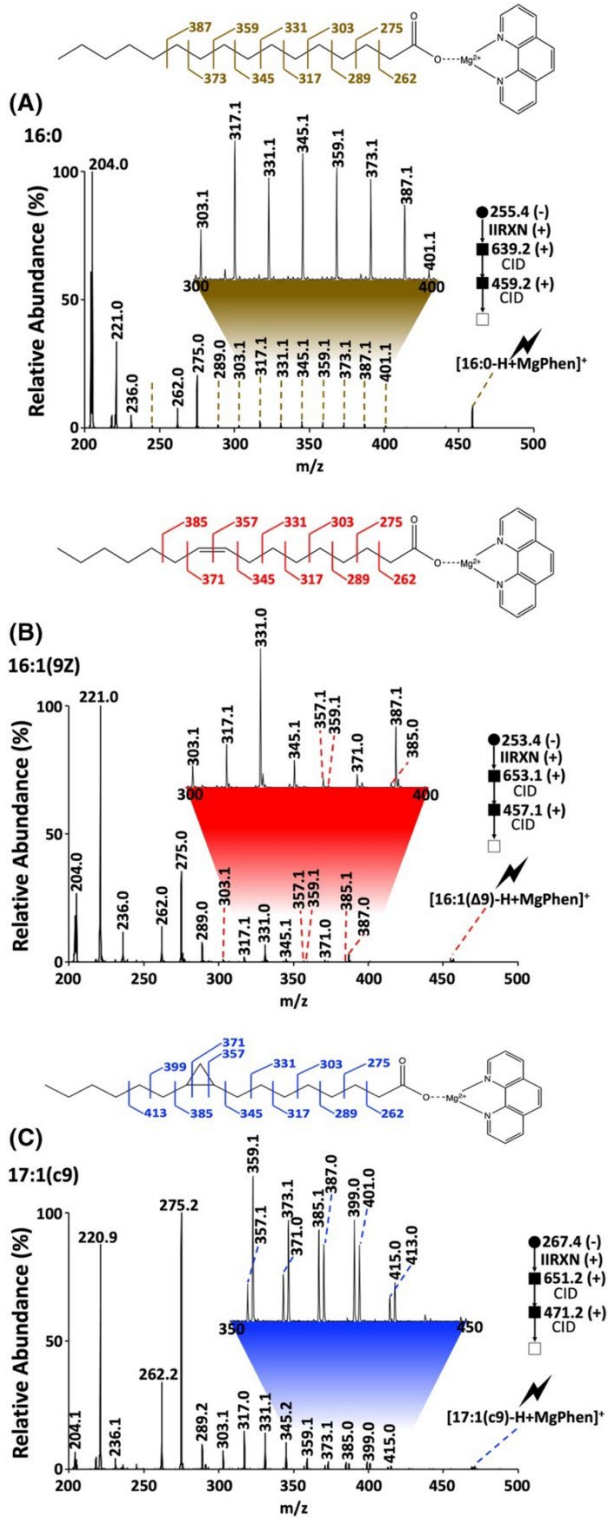

Figure 2.1 - The CID product ion spectra of (a) [16:0 − H + MgPhen]+, (b) [16:1(9Z) − H + MgPhen]+, and (c) [17:1(c9) − H + MgPhen]+. Filled and open circles (●/○) represent selected/unselected anions, respectively, and filled and open squares (■/□) represent selected and unselected cations. Lightning bolts (🗲) indicate the precursor ion subjected to collisional activation.

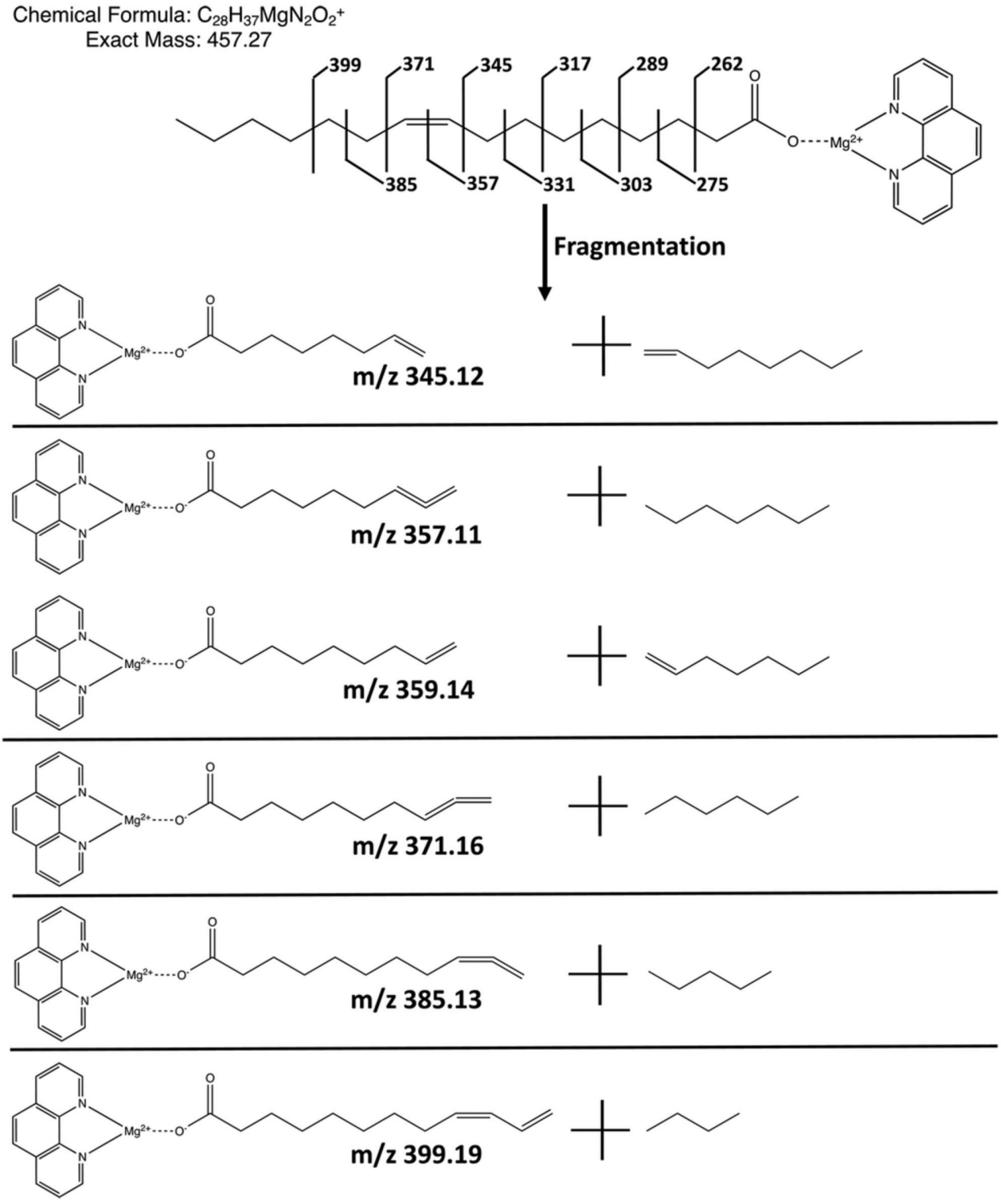

Scheme 2.1- Proposed products from cleavages in the double bond region of [16:1(9Z) − H + MgPhen]+.

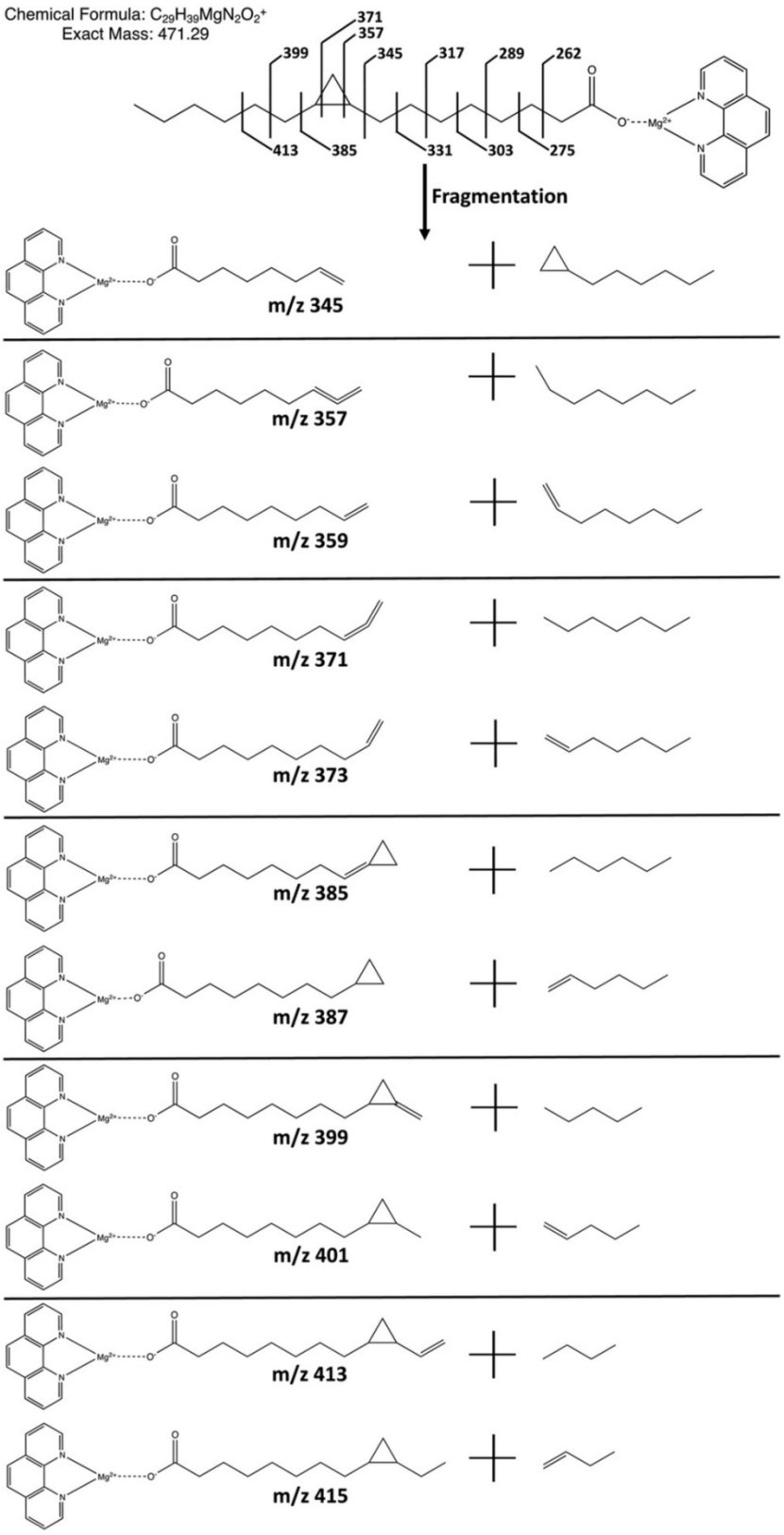

Scheme 2.2 - Proposed products from cleavages in the double bond region of [16:1(9Z) − H + MgPhen]+.

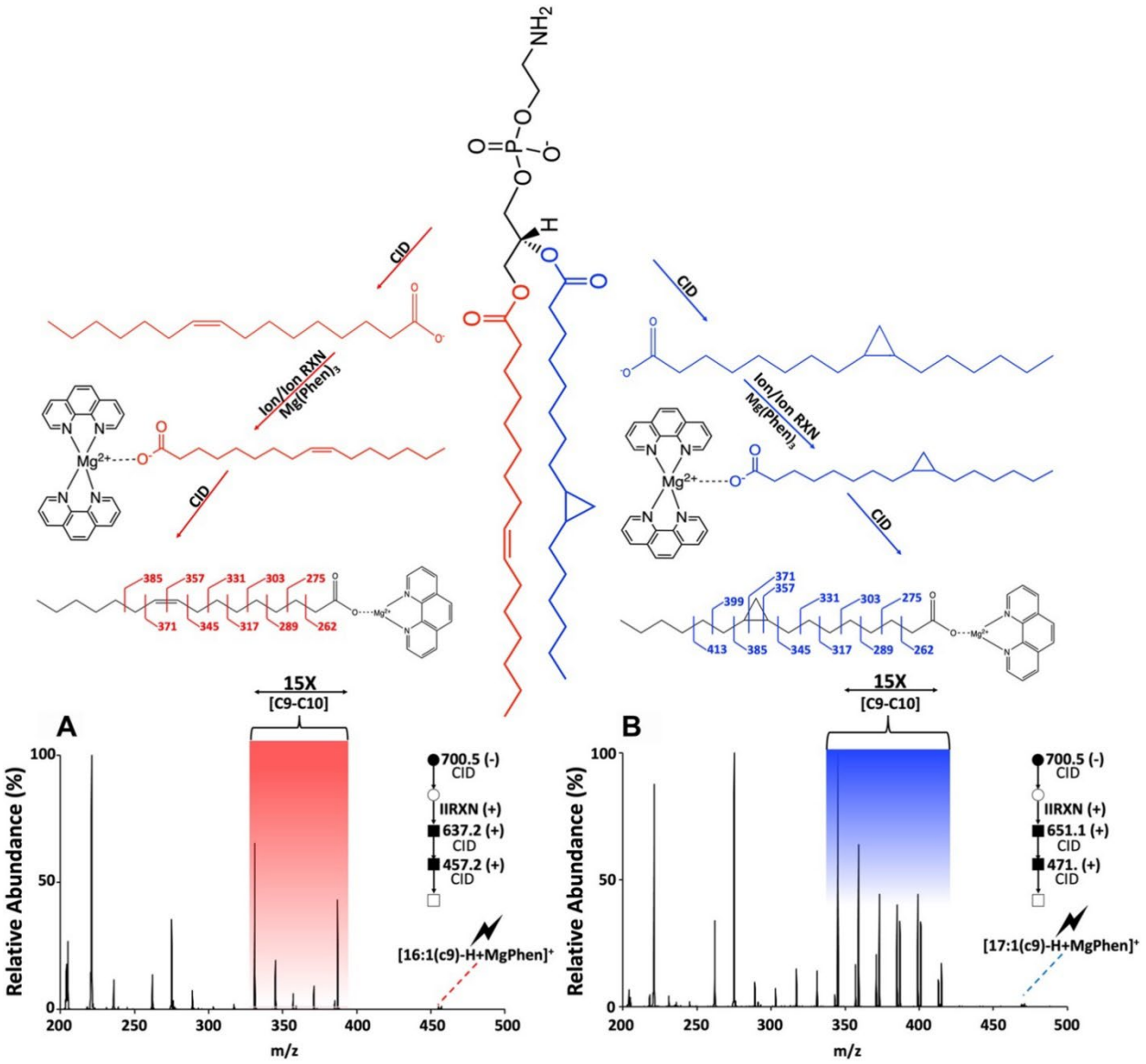

Figure 2.2 - Graphic representation of the approach to characterize fatty acyl chains in GPs. Anionic glycerophospholipids, [GP − H]− subjected to CID generate fatty acyl anions, [FA − H]−. The fatty acid anions undergo ion/ion reactions with tris-phenanthroline magnesium dictations, [MgPhen3]2+, resulting in a complex that spontaneously loses one of the phenanthroline ligands to yield [FA − H + MgPhen2]+ cations. Following an additional CID step to drive off a second phenanthroline ligand, CID of the resulting [FA − H + MgPhen]+ cations generate product ion spectra that allow for the localization of a double bond or cyclopropyl group. Filled and open circles (●/○) represent selected/unselected anions, respectively, and filled and open squares (■/□) represent selected and unselected cations. Lightning bolts (↯) indicate the precursor ion subjected to collisional activation.

An illustration of the process that allows for the C=C double bond and/or cyclopropane group characterization of the fatty acyl chains of GP anions is provided in **Figure 2.2** using PE 16:1(9Z)/17:1(c9) as a model GP. In brief, $[\text{PE } 16{:}1(9Z)/17{:}1(c9) - \text{H}]^-$ (*m/z* 728.5) was mass-selected in Q1 and transferred to q2 where it was stored and subjected to CID to form the fatty acyl chain fragment ions, $[16{:}1(9Z) - \text{H}]^-$ (*m/z* 457) and $[17{:}1(c9) - \text{H}]^-$ (*m/z* 471). Next, $[\text{Mg(Phen)}_3]^{2+}$ (*m/z* 282) was mass-selected in Q1 and stored with the fatty acid anions in q2 to allow for an ion/ion reaction. Attachment of $[\text{Mg(Phen)}_3]^{2+}$ to the fatty acyl anions resulted in the spontaneous loss of one phenanthroline, giving rise to two distinct product peaks $[16{:}1(9Z) - \text{H} + \text{Mg(Phen)}_2]^+$ (*m/z* 637) and $[17{:}1(c9) - \text{H} + \text{MgPhen}_2]^+$ (*m/z* 651). Ion-trap CID of the ions at *m/z* 637 and *m/z* 651 resulted in the loss of an additional phen, yielding ions at *m/z* 457 ($[16{:}1(9Z) - \text{H} + \text{MgPhen}]^+$) and *m/z* 471 ($[17{:}1(c9) - \text{H} + \text{MgPhen}]^+$). Consistent with previous work,[33] CID of $[16{:}1(9Z) - \text{H} + \text{MgPhen}]^+$ gives rise to a spectral pattern that is indictive of a double bond (12 Da spacing) in the 9th position (**Figure 2.2A**, highlighted in red). In contrast, CID of $[17{:}1(c9) - \text{H} + \text{MgPhen}]^+$ gives rise to a distinctive fragmentation pattern arising from the cyclopropyl ring in the 9th position (c9), displaying doublets between C9-C14, as highlighted in blue and shown in **Figure 2.2B**.

2.4.2 Characterization of GP species in E. Coli Total Lipid Extraction

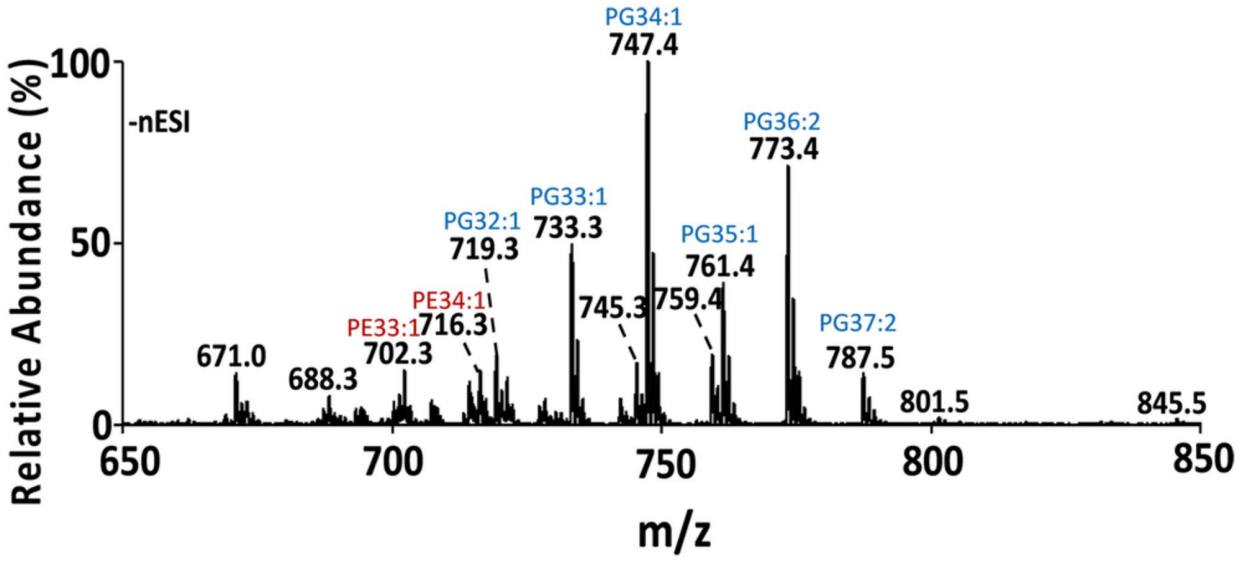

Figure 2.3 - Negative ion mode nano-ESI MS spectrum of lipid total extract from E. coli. Some of the mixture components that were subjected to characterization (see Table 1.1) are also indicated by head group, total FA carbon number and degree of unsaturation.

The workflow described above was applied to an *E. coli* total lipid extract for the structural elucidation of cyclopropyl and double bond-containing GPs. The vendor quoted lipid profile of 57.5% PE; 15.1% PG; 9.8% cardiolipin; 17.6% unknown provides a suitable matrix for demonstration of ion/ion reactions and MS/MS in shotgun lipid characterization. **Figure 2.3** shows the negative ion mass spectrum of the *E. coli* total lipid extract over the *m/z* range of 650–850, which is dominated by PE and PG anions. The most abundant PE and PG anions that were characterized in this work are indicated in red and blue, respectively.

Figure 2.4 illustrates the application of the ion/ion reaction approach to characterize the ion at *m/z* 733.3, tentatively identified as a PG 33:1 based on the mass.[38] **Figure 2.4A** shows the CID product ion spectrum of the *m/z* 733.5 anion, which shows the two most abundant fragment ions to be at *m/z* 267.2 and *m/z* 255.2. The former corresponds to the fatty acyl chain $[17{:}1 - H]^-$ while the latter corresponds to the fatty acyl chain $[16{:}0 - H]^-$, identifying PG 33:1 as PG 17:1_16:0. We note that there was no evidence of an isomeric species of PG 17:0_16.1 (or any other FA combination that corresponds to 33:1) due to the absence of FA signals consistent with other FA anions. The charge inversion reaction using $[Mg(Phen)_3]^{2+}$ produced two abundant product ion peaks consistent with $[16{:}0 - H + Mg(Phen)_2]^+$ (*m/z* 638.9) and $[17{:}1 - H + Mg(Phen)_2]^+$ (*m/z* 650.9) (**Figure 2.4B**). Isolation and CID of the *m/z* 650.9 ion resulted in the additional loss of a phenanthroline (180 Da), forming the fragment ion $[17{:}1 - H + MgPhen]^+$ (*m/z* 471.0). Isolation and activation of the $[17{:}1 - H + MgPhen]^+$ ion resulted in a spectrum similar to that of the 17:1 standard described above in the discussion of **Figures 2.1** and **2.2**. The diagnostic product ion doublets at *m/z* 357.2/359.2, 371.2/373.2, 385.0/387.0, 399.0/401.2, and 411.2/413.0 are consistent with the FA 17:1(c9) structure characterizing the species as PG 17:1(c9)_16:0.

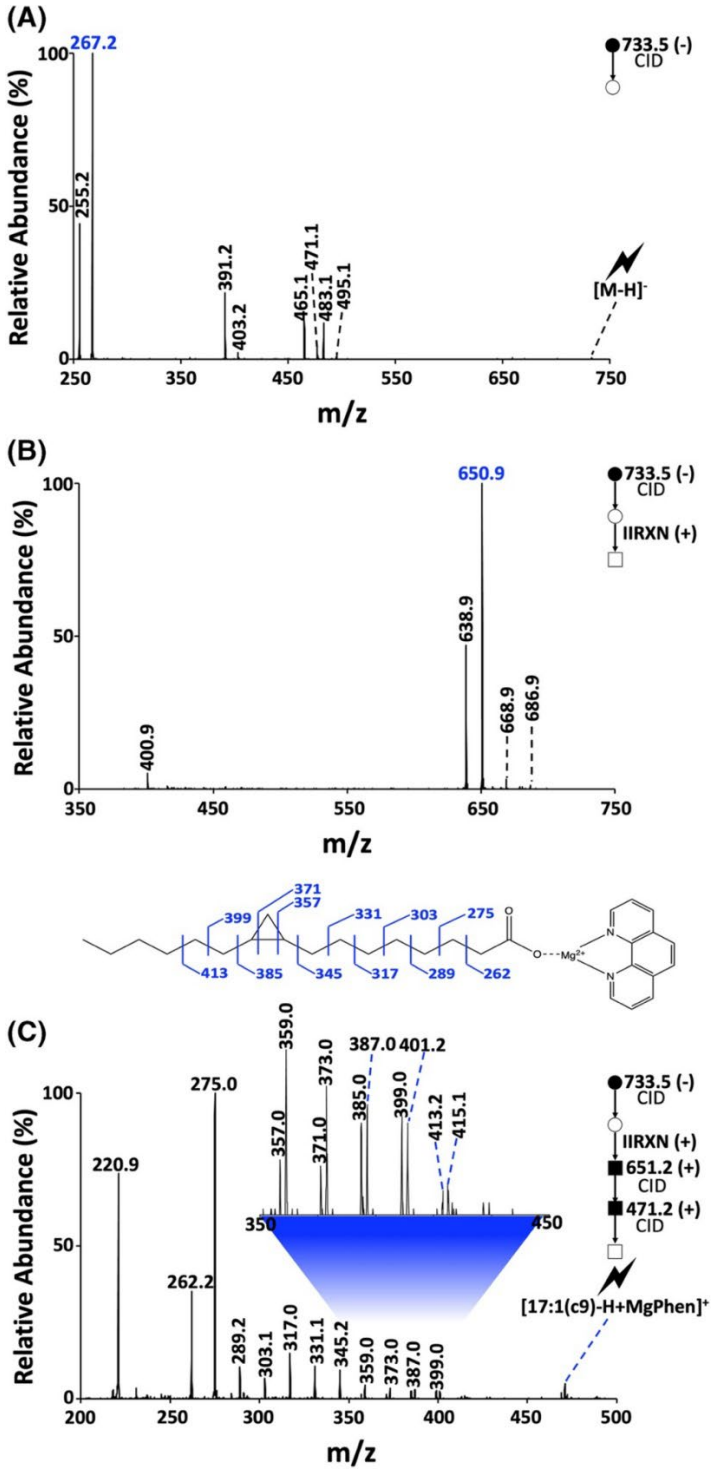

Figure 2.4 - (A) CID product ion spectrum of the PG 33:1 anion at m/z 733.3 (from Figure 3). (B) Ion/ion reaction of the ions in panel (A). CID of the ion at m/z 650.9 generates an abundant ion at m/z 471.2 (phenanthroline loss), the CID product ion spectrum of which is given in (C). Filled and open circles (●/○) represent selected/unselected anions, respectively, and filled and open squares (■/□) represent selected and unselected cations. Lightning bolts (↯) indicate the precursor ion subjected to collisional activation.

An example of a PE is provided by the ion at *m/z* 728.5 from **Figure 2.3** consistent with the presence of PE 35:2. **Figure 2.5A** shows the CID spectrum of the ion at *m/z* 728.5, which resulted in four product anions that correspond the complementary pairs 17:1(*m/z* 267.2)_18:1(*m/z* 281.2) and 16:1(*m/z* 253.2)_19:1(*m/z* 295.3). The CID spectrum therefore suggests the presence of a major isomer (i.e., PE 17:1_18:1) and a minor isomer (i.e., PE 16:1_19:1). After the anions of **Figure 2.5A** were subjected to ion/ion reactions with $[Mg(Phen)_3]^{2+}$, the fatty acyl anions were charge inverted resulting in $[16:1 - H + Mg(Phen)_2]^+$ (*m/z* 637.2), $[17:1 - H + Mg(Phen)_2]^+$ (*m/z* 651.2), $[18:1 - H + Mg(Phen)_2]^+$ (*m/z* 665.2), $[19:1 - H + Mg(Phen)_2]^+$ (*m/z* 679.1) (**Figure 2.5B**).

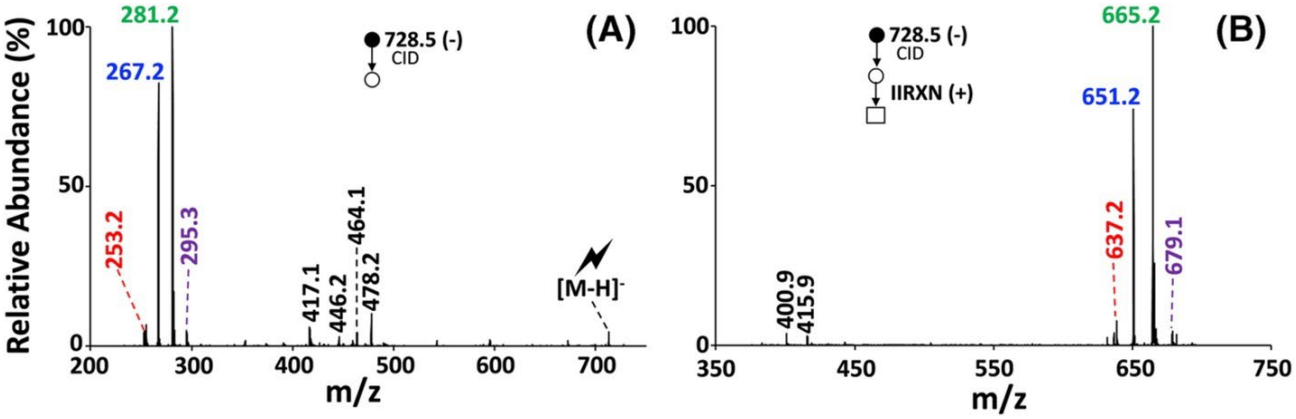

Figure 2.5 - (A) CID product ion spectrum of the PE 35:2 ions at m/z 728.5. (B) Product ion spectrum after reaction of the anions in (a) with [Mg(Phen)3]2+. Filled and open circles (●/○) represent selected/unselected anions, respectively, and filled and open squares (■/□) represent selected and unselected cations. Lightning bolts (↯) indicate the precursor ion subjected to collisional activation.

Ion-trap CID of the ions at *m/z* 637.2, 651.2, 665.2, and 679.1 resulted in an additional loss of a phenanthroline ligand resulting in the $[16:1 - H + MgPhen]^+$ (*m/z* 457.2), $[17:1 - H + MgPhen]^+$ (*m/z* 471.2), $[18:1 - H + MgPhen]^+$ (*m/z* 485.1), and $[19:1 - H + MgPhen]^+$ (*m/z* 499.0) ions. The CID product ion spectra of the four $[FA - H + MgPhen]^+$ cations listed above are provided in **Figure 2.6**. Consistent with **Figure 2.1B**, the $[16:1 - H + MgPhen]^+$ precursor ion **(Figure 2.6A**; *m/z* 457.2) gives rise to a spectral pattern with 12 Da spacing between *m/z* 345.1 and *m/z* 357.1 indicating a double bond at the C9 position. A similar spectral pattern was obtained from CID of the $[18:1 - H + MgPhen]^+$ ion (**Figure 2.6C;** *m/z* 485.1), with the tell-tale 12 Da spacing between *m/z* 373.1 and *m/z* 385.1 indicating

a double bond at the C11 position. Note that it is possible for there to be mixtures of ions with different positions of unsaturation but that, in these cases, a single isomer appears to be present.

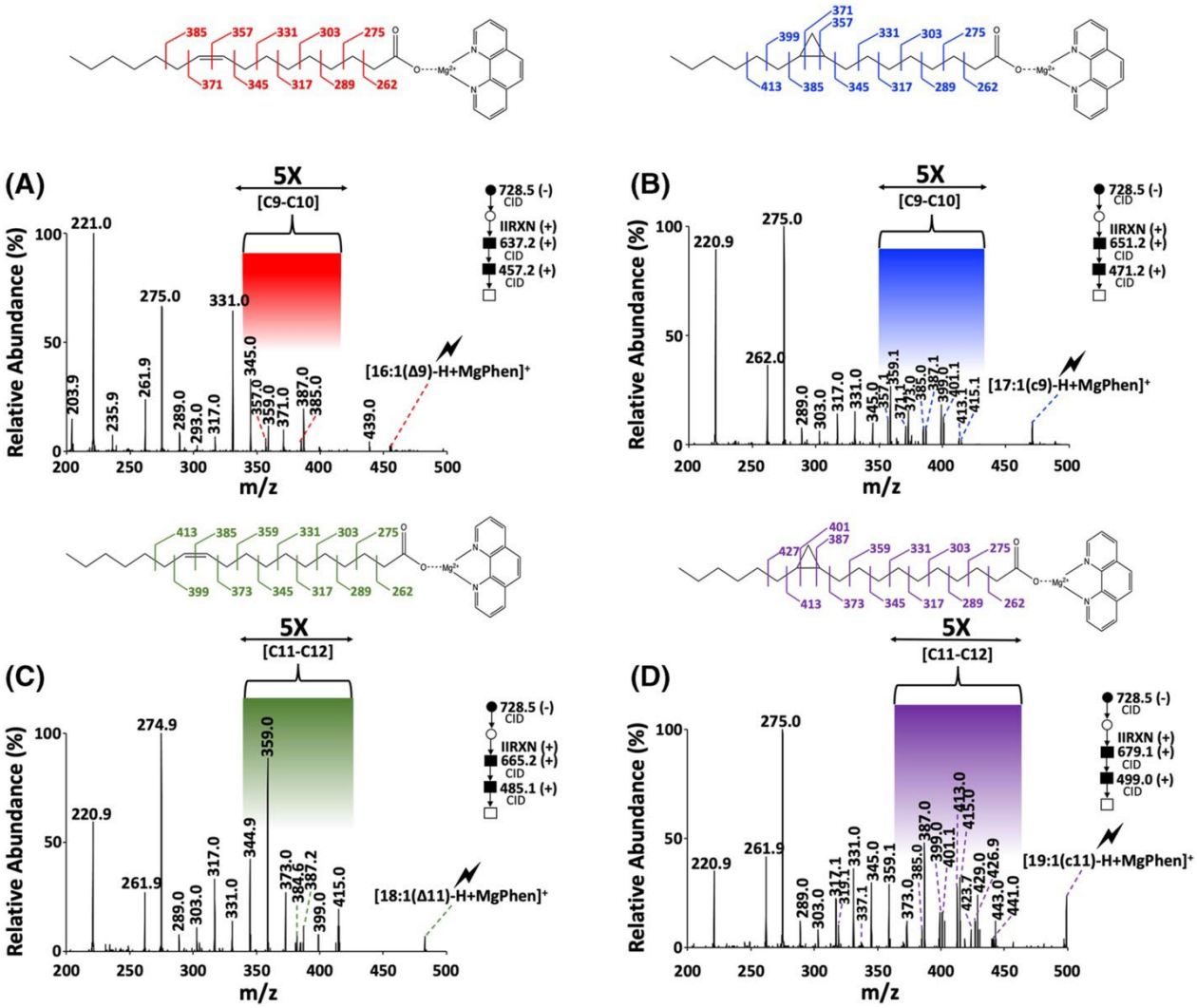

Figure 2.6 - (A) CID of the ion population at m/z 637.2 followed by activation of the ions at m/z 457.2. (B) CID of the ion population at m/z 637.2 followed activation of the ions at m/z 471.2. (C) CID of the ion population at m/z 637.2 followed by activation of the ions at m/z 485.1. (D) CID of the ion population at m/z 637.2 followed by activation of the ions at m/z 499.0. Filled and open circles (●/○) represent selected/unselected anions, respectively, and filled and open squares (■/□) represent selected and unselected cations. Lightning bolts (↯) indicate the precursor ion subjected to collisional activation.

The CID spectra from both $[17{:}1 - H + MgPhen]^+$ (**Figure 2.6B**; *m/z* 471.2) and $[19{:}1 - H + MgPhen]^+$ (**Figure 2.6D**; *m/z* 499.0) ions show characteristic doublet patterns, sug-

gesting the presence of a cyclopropyl ring at the C9 and C11 positions, respectively. A deprotonated phytomonic acid standard ($[19:1(c11) - H]^-$) was charge inverted with $[Mg(Phen)_3]^{2+}$, followed by CID to produce the $[19:1(c11) - H + MgPhen]^+$ ion at *m/z* 499.0. Another round of CID was then employed resulting in similar doublet patterns at 385.0/387.0, 399.0/401.1, 413.0/415.0, 426.9/429.1, and 441.0/443.0 to the profiled 19:1 fatty acyl chain (compare **Figure 2.7** and **Figure 2.6D).** In contrast, cis-10-nonadecanoic acid (FA 19:1 (10Z)) was subjected to the same process and the resulting product ion spectrum of $[19:1(10Z) - H + MgPhen]^+$ (*m/z* 499.0) shows the expected fragmentation pattern for an FA with a double bond at C10 and distinct from that of the profiled 19:1(c9) fatty acyl chain (compare **Figure 2.8** with **Figure 2.6D**). A $[17:1(9Z) - H]^-$ anion could be generated from a lyso-PC 17:1(9Z) standard (see Figure **2.8**) to compare with the data for the profiled *m/z* 471.2 ion (compare **Figure 2.9** with **Figure 2.6B**). The CID product ion spectrum of the *m/z* 471.2 generated from the lyso-PC 17:1(9Z) standard shows the expected pattern and 12 Da spacing for a double bond at the C9 position, in contrast with the behavior noted for the profiled *m/z* 471 ion.

Table 2.1 summarizes unsaturated GPs represented in the negative ion ESI mass spectrum of the *E. coli* total lipid extract (**Figure 2.3**) that were subjected characterization using the MS^n workflow outlined in **Figure 2.2**. Many of the GP anions derived from the *E. coli* extract were found to be composed of mixtures of FA compositions, as illustrated above for the PE 35:2 ions. In a few cases, FA anions from minor components were apparent upon CID of the GP precursor anions but were too low in abundance (<2% of the most abundant FA anion generated by CID of the GP anion) to allow for subsequent isolation and CID to localize the unsaturation. These cases are indicated with an asterisk in **Table 2.1**.

Table 2.1 - The PGs and PEs in an E. coli total lipid extract characterized via MSn involving CID of the deprotonated GP, ion/ion charge inversion of the FA product anions using tris-phenanthroline magnesium dictations, and CID of the [FA − H + MgPhen]+ ions. Asterisks indicate cases in which the FA anions could be observed from minor GP components but were too low in abundance for further characterization via MS/MS.

Headgroup	Sum composition	Combination	m/z $[M - H]^-$	Ring position	Double bond position
Standards					
PE	33:1	16:0/17:1	702.9	$[17:1(c9) - H]^-$	
PC	17:1	17:1 Lyso	542.0		$[17:1(\Delta10) - H]^-$
Fatty acid	19:1	19:1	295.6		$[19:1(\Delta10) - H]^-$
Fatty acid	19:1	19:1	295.6	$[19:1(c11) - H]^-$	
E. coli					
PE	33:2	16:1_17:1	700.5	$[17:1(c9) - H]^-$	$[16:1(\Delta9) - H]^-$
	33:2	15:1_18:1	700.5	*	$[18:1(\Delta11) - H]^-$
	33:1	16:0_17:1	702.5	$[17:1(c9) - H]^-$	
	33:1	17:0_16:1	702.5		$[16:1(\Delta9) - H]^-$
	34:2	17:1_17:1	714.5	$[17:1(c9) - H]^-$	
	34:2	16:1_18:1	714.5		$[18:1(\Delta11) - H] - [16:1(\Delta9) - H]^-$
	34:2	15:1_19:1	714.5	$[19:1(c11) - H]^-$	*
	34:1	16:0_18:1	716.4		$[18:1(\Delta11) - H]^-$
	34:1	16:1_18:0	716.4		$[16:1(\Delta9) - H]^-$
	34:1	17:0_17:1	716.4	$[17:1(c9) - H]^-$	
	35.2	18:1_17:1	728.5	$[17:1(c9) - H]^-$	$[18:1(\Delta11) - H]^-$
	35.2	16:1_19:1	728.5	$[19:1(c11) - H]^-$	$[16:1(\Delta9) - H]^-$
	35:1	16:0_19:1	730.5	$[19:1(c11) - H]^-$	
	35:1	18:0_17:1	730.5	$[17:1(c9) - H]^-$	
	36:2	19:1_17:1	742.5	$[19:1(c11) - H] - [17:1(c9) - H]^-$	
	36:2	18:1_18:1	742.5		$[18:1(\Delta11) - H]^-$
	37:2	17:1_20:1	756.5	$[17:1(c9) - H]^-$	
	37:2	18:1_19:1	756.5	$[19:1(c11) - H]^-$	$[18:1(\Delta11) - H]^-$
	37:2	19:0_18:2	756.5	*	*
PG	32:1	16:0_16:1	719.4		$[16:1(\Delta9) - H]^-$
	32:1	14:0_18:1	719.4		$[18:1(\Delta11) - H]^-$
	33:1	16:0_17:1	733.4	$[17:1(c9) - H]^-$	
	33:2	16:1_17:1	731.4	$[17:1(c9) - H]^-$	$[16:1(\Delta9) - H]^-$
	33:2	14:1_19:1	731.4	$[19:1(c11) - H]^-$	*
	34:2	16:1_18:1	745.4		$[16:1(\Delta9) - H] - [18:1(\Delta11) - H]^-$
	34:2	17:1_17:1	745.4	$[17:1(c9) - H]^-$	
	34:1	16:0_18:1	747.5		$[18:1(\Delta11) - H]^-$
	35.2	18:1_17:1	759.5	$[17:1(c9) - H]^-$	$[18:1(\Delta11) - H]^-$
	35.2	16:1_19:1	759.5	$[19:1(c11) - H]^-$	$[16:1(\Delta9) - H]^-$
	35:1	18:0_17:1	761.5	$[17:1(c9) - H]^-$	
	35:1	17:0_18:1	761.5		$[18:1(\Delta11) - H]^-$
	35:1	16:0_19:1	761.5	$[19:1(c11) - H]^-$	
	36:2	18:1_18:1	773.5		$[18:1(\Delta11) - H]^-$
	37:2	18:1_19:1	787.5	$[19:1(c11) - H]^-$	$[18:1(\Delta11) - H]^-$

2.5 Conclusion

In this work, we demonstrate for the first time the localization of both double bonds and cyclopropane sites in GPs using ion/ion charge inversion reactions. GP anions were fragmented generating FA anions in high relative abundance, which enables the identification of carbon number and the number of alkene/cyclopropyl groups. CID of deprotonated FAs, however, neither distinguishes cyclopropyl groups from double bonds nor allows for the localization of the sites of such groups. We therefore charge invert the FA anions via reaction with $[MgPhen_3]^{2+}$ initially to produce $[FA - H + Mg(Phen)_2]^+$ cations. CID of $[FA - H + Mg(Phen)_2]^+$ leads to loss of one Phen ligand, generating a $[FA - H + MgPhen]^+$ cation. CID of the $[FA - H + MgPhen]^+$ cation yields distinct fragmentation patterns for FA anions with double bonds and cyclopropyl groups. In each case, it is possible to identify whether the FA modification is a double bond or cyclopropane group as well as to localize the modification site. The phenomenology is demonstrated here with standards and is extended to GP anions generated from a *E. coli* total extract. The 16:1 and 18:1 fatty acyl chains in the *E. coli* total extract were found to be 16:1 (Δ9) and 18:1 (Δ11), respectively, whereas 17:1 and 19:1 fatty acyl chains were found to be 17:1 (c9) and 19 (c11), respectively. The demonstrated workflow offers extensive GP structural characterization using gas-phase ion/ion reactions and tandem mass spectrometry.

2.6 Author Contribution

De'Shovon M. Shenault: Investigation, data curation, methodology, visualization, writing—original draft preparation. **Scott A. McLuckey:** Methodology, resources, supervision, visualization, writing—review and editing. **Elissia T. Franklin:** Conceptualization, methodology, project administration, visualization, writing—review and editing.

2.7 Acknowledgement

This work was supported by the U.S. National Institute of Health (NIH) under Grants GM R37-45372 and GM R01-118484.

2.8 Conflict of Interest Statement

The authors declare no competing financial interests.

2.9 Data Availability

The data that support the findings of this study are available from the corresponding author upon reasonable request.

2.10 Supporting Information

Additional supporting information can be found online in the Supporting Information section at the end of this article.

2.11 References

(1) Naudí A, Cabré R, Jové M, et al. Chapter five—lipidomics of human brain aging and Alzheimer's disease pathology. Int Rev Neurobiol. 2015;122:133-189. doi:10.1016/bs.irn.2015.05.008

(2) Messias MCF, Mecatti GC, Priolli DG, de Oliveira Carvalho P. Plasmalogen lipids: functional mechanism and their involvement in gastrointestinal cancer. Lipids Health Dis. 2018;17(1):41. doi:10.1186/ s12944-018-0685-9

(3) Dean JM, Lodhi IJ. Structural and functional roles of ether lipids. Protein Cell. 2018;9(2):196-206.doi:10.1007/s13238-017-0423-5
4. De Siervo AJ. Alterations in the phospholipid composition of

(4) Escherichia coli B during growth at different temperatures. J Bacteriol. 1969;100(3):1342-1349. doi:10.1128/jb.100.3.1342- 1349.1969

(5) Tao BY. Chapter 24—industrial applications for plant oils and lipids. In: Yang S-T, ed. Bioprocessing for Value-Added Products from Renew- able Resources. Amsterdam: Elsevier; 2007:611-627. doi:10.1016/ B978-044452114-9/50025-6

(6) Blanco A, Blanco G. Chapter 5—lipids. In: Blanco A, Blanco G, eds. Medical biochemistry. Academic Press; 2017:99-119. doi:10.1016/ B978-0-12-803550-4.00005-7

(7) Garrett TA, Raetz CRH, Richardson T, Kordestani R, Son JD, Rose RL. Identification of phosphatidylserylglutamate: a novel minor lipid in Escherichia coli. J Lipid Res. 2009;50(8):1589-1599. doi:10.1194/jlr. M800549-JLR200

(8) Hsu F-F, Turk J. Electrospray ionization with low-energy collisionally activated dissociation tandem mass spectrometry of glycerophospho- lipids: mechanisms of fragmentation and structural characterization. J Chromatogr B. 2009;877(26):2673-2695. doi:10.1016/j.jchromb. 2009.02.033

(9) Hsu F-F, Turk J. Electrospray ionization/tandem quadrupole mass spectrometric studies on phosphatidylcholines: the fragmentation processes. J Am Soc Mass Spectrom. 2003;14(4):352-363. doi:10. 1016/S1044-0305(03)00064-3

(10) Blevins MS, Klein DR, Brodbelt JS. Localization of cyclopropane modi- fications in bacterial lipids via 213 nm ultraviolet photodissociation mass spectrometry. Anal Chem. 2019;91(10):6820-6828. doi:10.1021/acs.analchem.9b01038

(11) Hancock SE, Poad BLJ, Batarseh A, Abbott SK, Mitchell TW. Advances and unresolved challenges in the structural characterization of isomeric lipids. Anal Biochem. 2017;524:45-55. doi:10.1016/j.ab. 2016.09.014

(12) Grogan DW, Cronan JE. Cyclopropane ring formation in membrane lipids of bacteria. Microbiol Mol Biol Rev. 1997;61(4):429-441.

(13) Poger D, Mark AE. A ring to rule them all: the effect of cyclopropane fatty acids on the fluidity of lipid bilayers. J Phys Chem B. 2015; 119(17):5487-5495. doi:10.1021/acs.jpcb.5b00958

(14) Wang AY, Grogan DW, Cronan JE. Cyclopropane fatty acid synthase of Escherichia coli: deduced amino acid sequence, purification, and studies of the enzyme active site. Biochemistry. 1992;31(45): 11020-11028. doi:10.1021/bi00160a011

(15) Zhang Y-M, Rock CO. Membrane lipid homeostasis in bacteria. Nat Rev Microbiol. 2008;6(3):222-233. doi:10.1038/nrmicro1839

(16) Glickman MS, Cahill SM, Jacobs WR. The mycobacterium tuberculosis cmaA2 gene encodes a mycolic acid trans-cyclopropane synthetase. J Biol Chem. 2001;276(3):2228-2233. doi:10.1074/jbc.C000652200

(17) Chang YY, Cronan JE. Membrane cyclopropane fatty acid content is a major factor in acid resistance of Escherichia coli. Mol Microbiol. 1999; 33(2):249-259. doi:10.1046/j.1365-2958.1999.01456.x

(18) Xu C, Wang S, Ren H, Lin X, Wu L, Peng X. Proteomic analysis on the expression of outer membrane proteins of Vibrio alginolyticus at different sodium concentrations. Proteomics. 2005;5(12):3142-3152. doi:10.1002/pmic.200401128

(19) Wehrli PM, Angerer TB, Farewell A, Fletcher JS, Gottfries J. Investigating the role of the stringent response in lipid modifications during the stationary phase in E. coli by direct analysis with time-of-flight-secondary ion mass spectrometry. Anal Chem. 2016; 88(17):8680-8688. doi:10.1021/acs.analchem.6b01981

(20) Harvey DJ. Picolinyl derivatives for the characterization of cyclopropane fatty acids by mass spectrometry. Biomed Mass Spectrom. 1984;11(4):187-192. doi:10.1002/bms.1200110410

(21) Oursel D, Loutelier-Bourhis C, Orange N, Chevalier S, Norris V, Lange CM. Identification and relative quantification of fatty acids in Escherichia coli membranes by gas chromatography/mass spectrometry. Rapid Commun Mass Spectrom. 2007;21(20):3229- 3233. doi:10.1002/rcm.3177

(22) Ma X, Xia Y. Pinpointing double bonds in lipids by Paternò-Büchi reactions and mass spectrometry. Angew Chem Int Ed. 2014;53(10): 2592-2596. doi:10.1002/anie.201310699

(23) Pham HT, Maccarone AT, Thomas MC, Campbell JL, Mitchell TW, Blanksby SJ. Structural characterization of glycerophospholipids by combinations of ozone- and collision-induced dissociation mass spectrometry: the next step towards "top-down" lipidomics. Analyst. 2013;139(1):204-214. doi:10.1039/C3AN01712E

(24) Campbell JL, Baba T. Near-complete structural characterization of phosphatidylcholines using electron impact excitation of ions from organics. Anal Chem. 2015;87(11):5837-5845. doi:10.1021/acs. analchem.5b01460

(25) Jones JW, Thompson CJ, Carter CL, Kane MA. Electron-induced dissociation (EID) for structure characterization of glycerophosphati- dylcholine: determination of double bond positions and localization of acyl chains. J Mass Spectrom. 2015;50(12):1327-1339. doi:10.1002/ jms.3698

(26) Baba T, Campbell JL, Le Blanc JCY, Baker PRS. Distinguishing cis and trans isomers in intact complex lipids using electron impact excitation of ions from organics mass spectrometry. Anal Chem. 2017;89(14): 7307-7315. doi:10.1021/acs.analchem.6b04734

(27) Born MEN, Prentice BM. Structural elucidation of phosphatidylcholines from tissue using electron induced dissociation. Int J Mass Spectrom. 2020;452:11638. doi:10.1016/j.ijms.2020.116338

(28) Macias LA, Feider CL, Eberlin LS, Brodbelt JS. Hybrid 193 nm ultraviolet photodissociation mass spectrometry localizes cardiolipin unsaturations. Anal Chem. 2019;91(19):12509-12516. doi:10.1021/acs.analchem.9b03278

(29) Randolph CE, Blanksby SJ, McLuckey SA. Toward complete structure elucidation of glycerophospholipids in the gas phase through charge inversion ion/ion chemistry. Anal Chem. 2020;92(1):1219-1227. doi: 10.1021/acs.analchem.9b04376

(30) Randolph CE, Shenault DM, Blanksby SJ, McLuckey SA. Structural elucidation of ether glycerophospholipids using gas-phase ion/ion charge inversion chemistry. J Am Soc Mass Spectrom. 2020;31(5): 1093-1103. doi:10.1021/jasms.0c00025

(31) Randolph CE, Shenault DM, Blanksby SJ, McLuckey SA. Localization of carbon-carbon double bond and cyclopropane sites in cardiolipins via gas-phase charge inversion reactions. J Am Soc Mass Spectrom. 2021;32(2):455-464. doi:10.1021/jasms.0c00348

(32) Randolph CE, Foreman DJ, Blanksby SJ, McLuckey SA. Generating fatty acid profiles in the gas phase: fatty acid identification and rela- tive quantitation using ion/ion charge inversion chemistry. Anal Chem. 2019;91(14):9032-9040. doi:10.1021/acs.analchem.9b01333

(33) Liebisch G, Fahy E, Aoki J, et al. Update on LIPID MAPS classification, nomenclature, and shorthand notation for MS-derived lipid structures. J Lipid Res. 2020;61(12):1539-1555. doi:10.1194/jlr. S120001025

(34) Xia Y, Wu J, McLuckey SA, Londry FA, Hager JW. Mutual storage mode ion/ion reactions in a hybrid linear ion trap. J Am Soc Mass Spectrom. 2005;16(1):71-81. doi:10.1016/j.jasms.2004.09.017

(35) Xia Y, Liang X, McLuckey SA. Pulsed dual electrospray ionization for ion/ion reactions. J Am Soc Mass Spectrom. 2005;16(11):1750-1756. doi:10.1016/j.jasms.2005.07.013

(36) Londry FA, Hager JW. Mass selective axial ion ejection from a linear quadrupole ion trap. J Am Soc Mass Spectrom. 2003;14(10): 1130-1147. doi:10.1016/S1044-0305(03)00446-X

(37) Randolph CE, Foreman DJ, Betancourt SK, Blanksby SJ, McLuckey SA. Gas-phase ion/ion reactions involving tris-phenanthroline alkaline earth metal complexes as charge inversion reagents for the identification of fatty acids. Anal Chem. 2018; 90(21):12861-12869. doi:10.1021/acs.analchem.8b03441

(38) https://www.lipidmaps.org/databases/lmsd/browse

2.12 Supporting Information

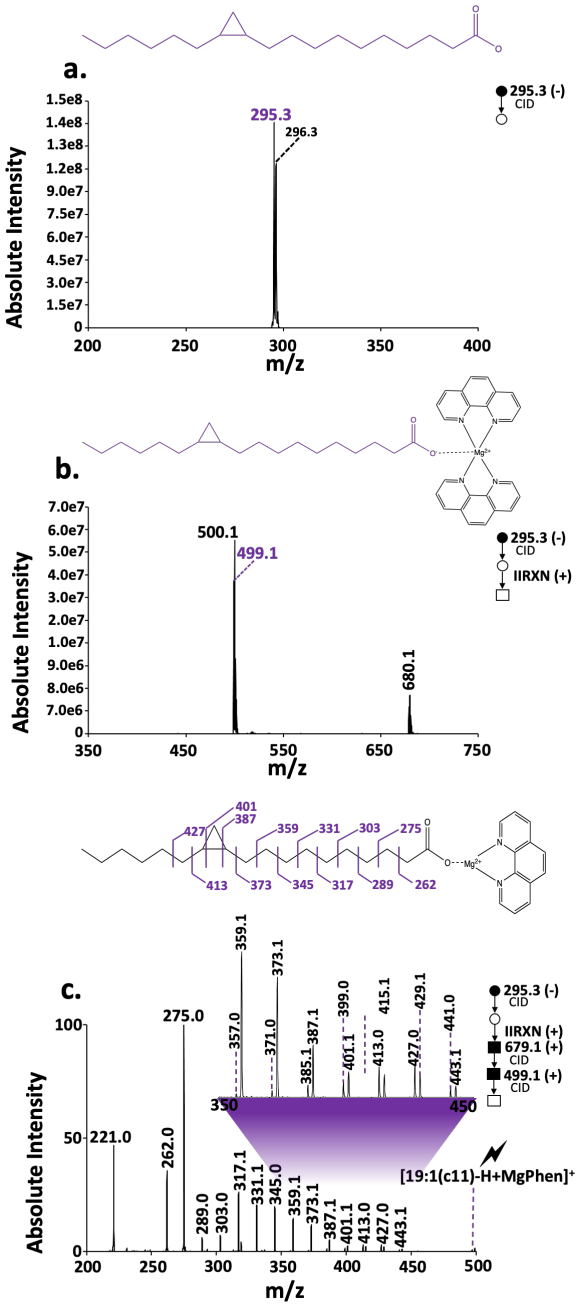

Figure 2.7 - Distinguishing the GP structures; a) CID of Phytomonic Acid 19:1(c11), b) Charge inversion ion/ion reaction of ions in panel a), c) Ion trap CID of [C19:1(c11) - H + MgPhen]−. Filled and open circles (●/○) represent selected/unselected anions, respectively, and filled and open squares (■/□) represent selected and unselected cations. Lightning bolts (🗲) indicate the precursor ion subjected to collisional activation. Absolute abundances are provided in a. and b. but these cannot be compared directly as the detector gain may not be the same for positive and negative ions.

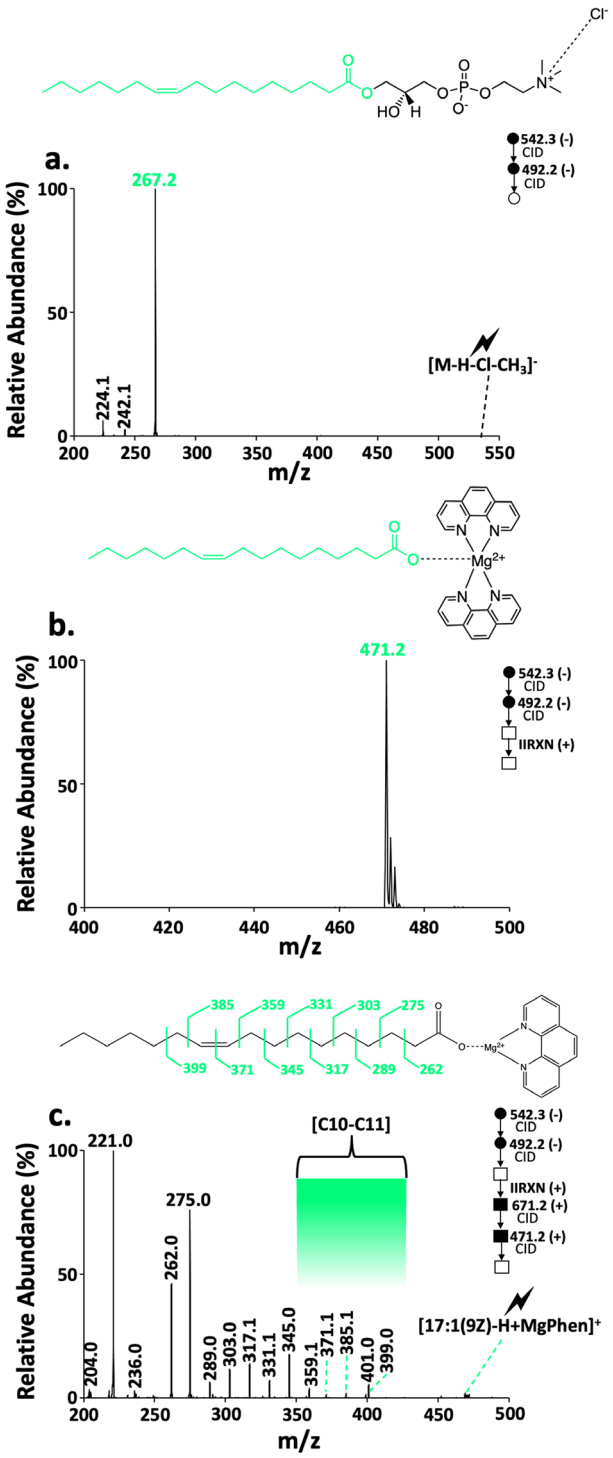

Figure 2.8 - Distinguishing the GP structures; a) CID of chloride adduct of PC lyso-17:1(9Z) b) Charge inversion ion/ion reaction of ions in panel a), c) Ion trap CID of [C17:1(9Z) - H + MgPhen]$^{-}$. Filled and open circles (●/○) represent selected/unselected anions, respectively, and filled and open squares (■/□) represent selected and unselected cations. Lightning bolts (↯) indicate the precursor ion subjected to collisional activation.

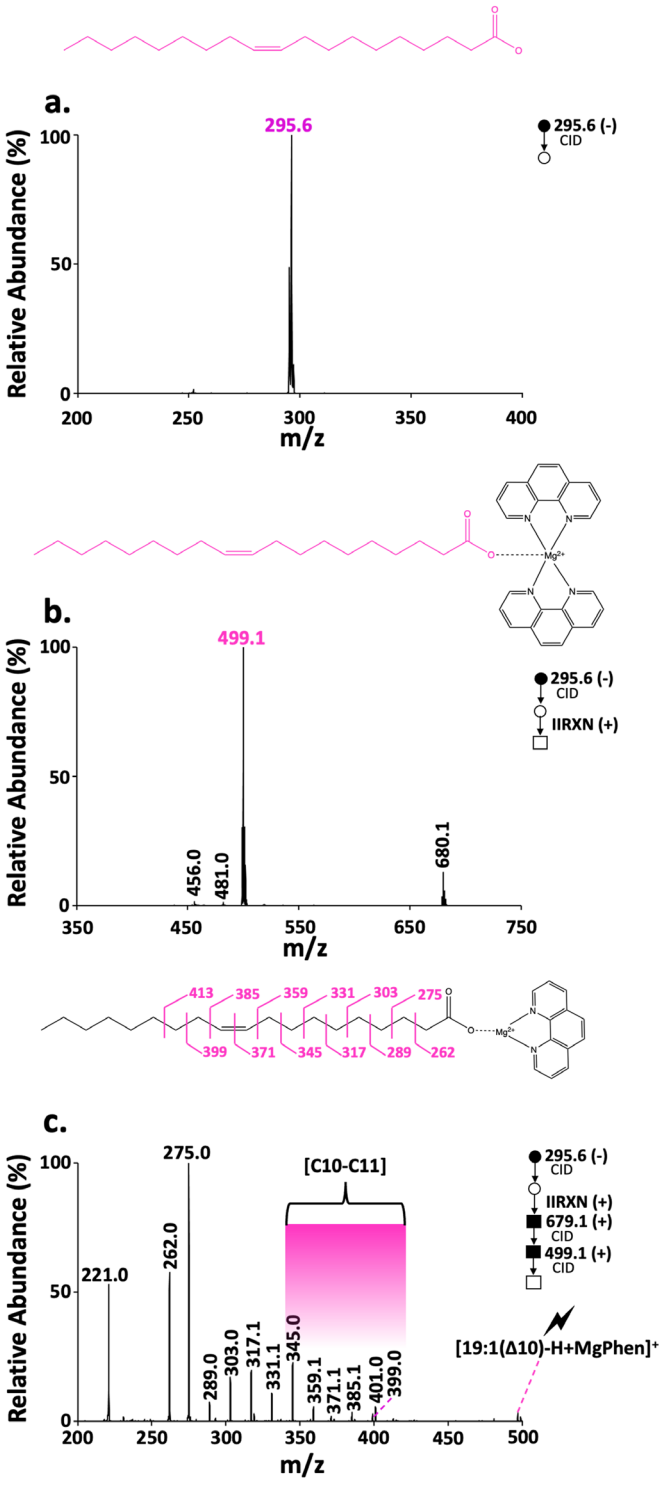

Figure 2.9 - Distinguishing the GP structures; a) CID of Cis-10 Nonadecenoic Acid 19:1(10Z), b) Charge inversion ion/ion reaction of ions in panel a), c) Ion trap CID of [C19:1(10Z) - H + MgPhen]−. Filled and open circles (●/○) represent selected/unselected anions, respectively, and filled and open squares (■/□) represent selected and unselected cations. Lightning bolts (🗲) indicate the precursor ion subjected to collisional activation.

CHAPTER 3. LOCALIZATION OF METHYL BRANCHING SITES ON FATTY ACIDS BY COMBINING RADICAL DIRECTED DISSOCIATION AND GAS-PHASE ION/ION CHEMISTRY

A portion of this manuscript will be published at a later date.

3.1 Abstract

Branched chain fatty acids (BCFA) are unique structural fatty acid consisting of methyl branching located on the carbon chain of the fatty acid. BCFAs are found naturally in vernix caseosa, sebum, and other bacterial making them important to characterization. Straight chain FA and BCFA are isomeric with each other, proving to be an analytical challenge which is further complexed due to varying orientations of the methyl site while sharing similar mass spectra. gas chromatography mass spectrometry (GC-MS) and liquid chromatography mass spectrometry (LC/MS) are common approach for the separation of lipid species at sum compositional levels. However, mass spectra of both branched (iso and/or anteiso FAs) and SCFAs are identical with separation only possible with longer retention time, high concentrations, and reference standard, gives minimal localization the branching moieties. Herein, we couple gas-phase ion/ion chemistry to charge invert BCFA anions and further interrogate with radical directed dissociation (RDD). The incorporation of the RDD, differentiate lipid isomers while producing a rich fragmentation pinpointing the site of branching. This charge inversion approach was useful in identifying site of saturation and unsaturation of branched chain moieties, without the aid of reference samples and any separation techniques.

Keywords: Methyl Branching, Ion/Ion reaction, RDD, Saturated fatty acids, Gas-Phase Charge Inversion Reaction.

3.2 Introduction

Branched chain fatty acids (BCFAs), commonly found in bacteria (*Bacillus subtilis*) are saturated fatty acids (FA) with one or more methyl branching ordinarily located on the terminal end of the carbon chain.[1,2,3] BCFAs can be classified as iso-, anteiso-, multi-methyl-, or ω-alicyclic BCFAs.[4,5,6] In *Bacillus subtilis,* BCFAs regulates the biophysical properties of membrane in a

similar fashion as the *cis*-double bond: where both increase fluidity, form rigidity of saturated fatty acids, and lower the phase transition temperature (T_m).[7,8] 95% of *Bacillus subtilis* membrane are composed of BCFAs.[9,10] While BCFAs are found majority in different genera of bacteria, 25% wt of BCFA can be found naturally in vernix caseosa (secretion covering newborn children) on human tissue, meibum, sebum, and dairy products.[11,12,13] In many studies in the Journal of Nutrition and Agricultural Science, illuminates' the importance of BCFAs found in food sources. BCFAs constitutes around 500 mg/d found in the American diet from beef and dairy, while in other fermented foods showed a fraction of BCFAs found.[14,15] Compared to other milk products, Yak-milk (Qinghai-Tibet plateau) per cup yields 777 mg of BCFAs versus US whole milk (158 mg), with an estimated <5,000 mg of BCFAs found in yak yogurt.[16] In humans, BCFAs can be found in tissue, brain, blood and/or cancer cells, making them important to study.[17] Numerous studies on BCFAs (such as, phytanic acid, pristanic acid and valproic acid (VPA)) focus on understanding there biochemical and physiological role that BCFAs play in human.[18,19,20] Investigators have reported, VPA (which is used as a mood-stabilizing and antiepileptic drug) can induce oxidative stress, neurodegenerative diseases which leads to damage to nervous system and human fetal growth.[21,22]

Amongst most BCFAs are isomeric straight chain fatty acids (SCFAs), that have proving to be an analytical challenge due to varying positions of the branching location along the FA.[23] Historically, gas chromatography mass spectrometry (GC-MS) facilitates a high resolution separation of both BCFAs and SCFAs for quantitation.[24,25] The analysis approach allows the conversion of the fatty acid from its natural lipid class into methyl esters (FAME), which increase analyte volatility. However, one limitation of GC-MS approach allows coelution of FAMEs with branched-chain fatty acid methyl esters (BCFAMEs) and other normal saturates. With the addition of highly polar columns and longer time, baseline resolution can readily be achieved with GC-MS.[26,27,28] Liquid chromatography mass spectrometry (LC/MS) is a common approach for the separation of lipid species at sum compositional levels. However, mass spectra of both branched (iso and/or anteiso FAs) and SCFAs are identical and separation is only possible with reversed-phase high performance liquid chromatography (RP-HPLC) with the addition of a longer retention time and is unable to localize the branching site.[29,30] Recently, Chopra and co-workers have combined ion/ion charge inversion reaction (IIRXN) with LC-MS/MS method, which allows post-column charge switching derivatization of online isomeric branched and straight chain acyl chain, with

identification of methyl-branching site of unsaturation. However, this method cannot be utilized for intact methyl-branched lipids and require hour long elution times.[31]

There are several methods that induce structural information of fatty acyl chain; however, methods incorporate additional instrumentation modification to achieve informative information. Photodissociation (PD) and ultraviolet photodissociation (UVPD) with LC-MS, utilize a laser-based dissociation with the aid of FA derivation reagents for the discrimination of isomers that differ in site(s) of unsaturation and saturation.[23,32,33] Other approaches from Xia and coworkers have pinpointed the site(s) of methyl branching, cyclopropanes and/or carbon-carbon double bond (C=C) location found in bacteria (Escherichia Coli and Bacillus subtilis), sphingomyelin (sphingoid base and N-Acyl Chain), phosphatidylcholines (PCs) and lysophosphatidylcholines (LPCs) found in human plasma.[34,35,36]

Previous, we have shown the utility of gas-phase IIRXN for the structural elucidation of fatty acyls from varying subclass of lipids in biological matrices.[37383940414243444 5] In this work, we couple Briefly, singly deprotonated BCFA, $[BCFA\text{-}H]^-$ reacted with a doubly charged magnesium complex, $[(TEMPO\text{-}Terpy)_2\text{-}Mg]^{+2}$, to form cations, $[BCFA - H + (TEMPO\text{-}Terpy)\text{-}Mg]^+$. Ion-trap CID of $[BCFA - H + (TEMPO\text{-}Terpy)\text{-}Mg]^+$, resulted in a homolytic cleavage and loss of the TEMPO moiety leaving behind a nascent free radical, which is further interrogated with CID, resulting in the localization of the site(s) of branching.

3.3 Experimental Section

3.3.1 Nomenclature

The proposed shorthand notation for lipid structures were recommended by Liebisch et al., is illustrated throughout this work.[46] Considering fatty acyl (FA) chains, who are represented by the total number of carbons before the colon, followed by the position of the double(s) bond to trailed after the colon. To signify methyl branching sites, "Me" is symbolized after the position of the branching, which are illustrated by parentheses.[31] For example 14-methyl palmitic acid, also known by formal name 14-methyl-hexadecanoic acid, can be demonstrated as FA 16:0(14Me). Another example, phytanic acid, commonly referred by 3,7,11,15-Tetramethylhexadecanoic acid, can be represented as 16:0(3Me,7Me,11Me,15Me).

3.3.2 Chemicals

Heptadecanoic acid, 14-methyl palmitic acid (16:0 (14Me)), 15-methyl palmitic acid (16:0 (15Me)), Stearic acid, 17-methyl stearic acid methyl ester (18:0 (17Me)), Phytanic acid (16:0 (3Me,7Me,11Me,15Me)) and Arachidic acid standards were purchased from Cayman Chemical Company (Ann Arbor, MI). Magnesium chloride, HPLC Grade methanol, HPLC Grade water and chloroform were purchased from Thermo Fisher Scientific (Waltham, MA). Tert-Butyl methyl ether (MTBE) were purchased from Sigma-Aldrich, Inc. (St. Louis, MO). 2, 2':6', 2" terpyridine (terpy) (Tempo-Terpy) was synthesized by Dr. Jinshan Gao laboratory.

3.3.3 MTBE Lipid Extraction and Preparation of nESI Solution

All lipid standards were dissolved in methanol and dilute to a final concentration of 10 μM. Lipids were extracted from pooled human plasma using MTBE extraction protocol in an identical fashion as previously described.[47] A solution of pooled human plasma extract was diluted to a final concentration of 50 μM in methanol. Details for the synthesis are described in the **Appendix I Section** of the dissertation. 2, 2':6', 2" terpyridine(terpy) (Tempo-Terpy) magnesium complex were prepared but mixing 3:1 (mol/mol) magnesium chloride with 2, 2':6', 2" terpyridine(terpy) (Tempo-Terpy) in methanol and diluted with methanol to a final concentration of 10 μM.

3.3.4 Mass Spectrometry

Experiments were performed on a Sciex QTRAP 4000 hybrid triple quadrupole/linear ion trap mass spectrometer (Sciex, Concord, ON, Canada), modified to perform ion/ion reactions. As previously reported,[48] anionic and cationic species were stored simultaneously, on the modified instrument. Opposing charged ions were generated from separate nano-ESI emitters in an alternately-pulsed style.[49] Lipid anions, $[FA - H]^-$, were generated as an anion using nano-ESI (-1700 V), mass selected in Q1, and transferred to q2 for storage. Next, $MgCl_2$ and 2,2':6',2"terpyridine (Tempo-Terpy) was prepared in a methanolic solution to form a doubly charged complex $[(TEMPO\text{-}Terpy)_2\text{-}Mg]^{+2}$, were produced by nano-ESI (+1400 V), mass isolated by Q1, and transferred to q2 to be mutually stored with the $[FA - H]^-$ anion, resulting in a charge-inverted $[FA – H + (TEMPO\text{-}Terpy)\text{-}Mg]^+$ for 0.5 s.[49] Ion-trap CID of $[FA – H + (TEMPO\text{-}Terpy)\text{-}Mg]^+$, results in homolytic cleavage and loss of the TEMPO moiety leaving behind a nascent free radical which is

further interrogated with CID, resulting products are mass analyzed to determine localization of branching site.

3.4 Results and Discussion

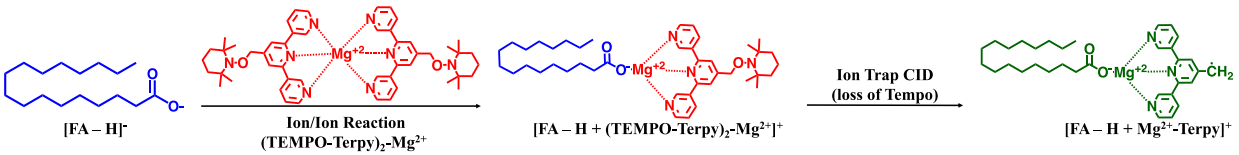

Scheme 3.1 - Demonstration of the gas-phase charge inversion ion/ion reaction for the analysis of BCFAs and SCFAs. The reaction scheme details the ion selection of the anion $[FA\text{-}H]^-$, which undergoes charge inversion chemistry with cation $[(TEMPO\text{-}Terpy)_2\text{-}Mg]^{+2}$ to form $[FA–H+(TEMPO\text{-}Terpy)_2\text{-}Mg^{2+}]^+$ cationic complex. CID of $[FA–H+(TEMPO\text{-}Terpy)_2\text{-}Mg^{2+}]^+$ complex, results in a homolytic cleavage and loss of the TEMPO moiety, leaving a free radical complex, $[FA–H+Terpy\text{-}Mg^{2+}]^+$ for further localization of the methyl branching or saturated site. Closed and open circles (●/○) signify selected/unselected anions, respectively, and closed and open squares (■/□) signify selected/unselected cations. Lightning bolts (↯) indicate the precursor ion subjected to collisional activation.

3.4.1 Distinguishing branched chain fatty acid moieties from saturated fatty acyl chains.

Scheme 3.1 exemplifies the creation of $[FA–H+(Terpy)\text{-}Mg^{2+}]^+$ cationic complex. As described, mutual storage of branched and straight chain FA anions with $[(TEMPO\text{-}Terpy)_2\text{-}Mg]^{+2}$ cation, underwent charge inversion reaction in a high-pressure collision cell, q2. The resulting ion/ion reaction, convert the singly deprotonated BCFAs and SCFAs anion into $[FA–H+(TEMPO\text{-}Terpy)\text{-}Mg^{2+}]^+$ cations. Ion trap CID of $[FA–H+(TEMPO\text{-}Terpy)\text{-}Mg^{2+}]^+$ gave rise to the loss of TEMPO moiety, leaving $[FA–H+Mg^{2+}Terpy\text{-}CH_2{\cdot}]^+$ to later promote radical-directed dissociation (RDD) fragmentation. As mentioned, upon CID of $[FA–H+(TEMPO\text{-}Terpy)\text{-}Mg^{2+}]^+$, results in a neutral loss of TEMPO, leaving a radical precursor ion $[FA–H+ Mg^{2+}Terpy\text{-}CH_2{\cdot}]^+$. Additional CID of radical precursor $[FA–H+ Mg^{2+}Terpy\text{-}CH_2{\cdot}]^+$, results in rich RDD fragmentation of either SCFAs or BCFAs. **Figure 3.1** highlights the region of the CID product ion spectra of (a) $[17:0–H+ Mg^{2+}Terpy\text{-}CH_2{\cdot}]^+$, (b) $[16:0(14Me)\text{-}H+ Mg^{2+}Terpy\text{-}CH_2{\cdot}]^+$, and (c) $[16:0(15Me)–H+ Mg^{2+}Terpy\text{-}CH_2{\cdot}]^+$ that shows distinctive behaviors similar of a straight chain FA, a FA with a branching site at the 14^{th} position and FA with a branching site at the 15^{th} position.

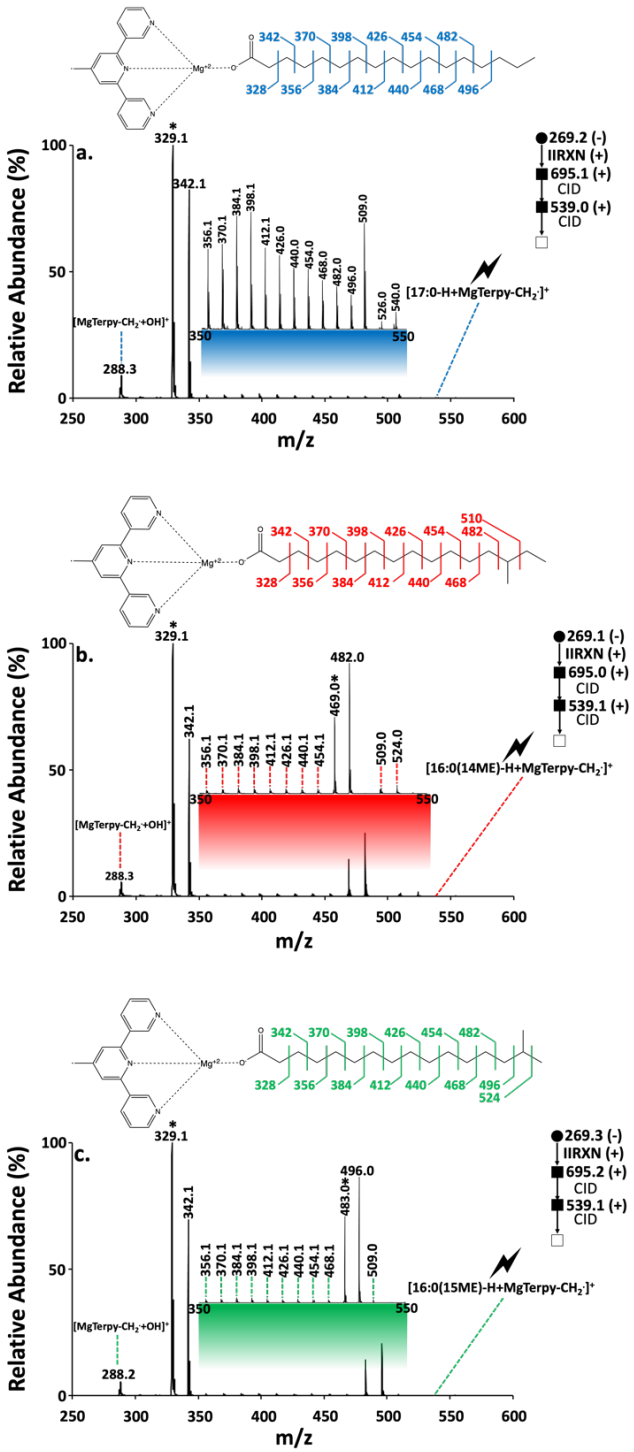

Figure 3.1 - Ion Trap CID product ion spectra of (a) [17:0−H+ Mg2+Terpy-CH2.]+, (b) [16:0(14Me)-H+ Mg2+Terpy-CH2.]+, and (c) [16:0(15Me)−H+ Mg2+Terpy-CH2.]+. Closed and open circles (●/○) signify selected/unselected anions, respectively, and closed and open squares (■/□) signify selected/unselected cations. Lightning bolts (🗲) indicate the precursor ion subjected to collisional activation. Asterisk (*) indicates the odd-electron fragment product peaks developed from the RDD fragmentation.

Additionally, *m/z* 288 $[Mg^{2+}Terpy\text{-}CH_2{\cdot}+OH]^+$ and *m/z* 314 $[Mg^{2+}Terpy\text{-}CH_2{\cdot}+CO_2{\cdot}^-]^+$ (no evidence shown) are common to product ion spectra for all $[FA–H+ Mg^{2+}Terpy\text{-}CH_2{\cdot}]^+$ ions. Given that irradiation of the radical precursor with CID, yields a radical driven fragmentation pattern, causing an even- and odd-electrons fragments displayed amongst the product ions. In this case, an odd-electron product peak *m/z* 329 $[Mg^{2+}Terpy\text{-}CH_2{\cdot}+CH_3O{=}CO^-]^+$ is present for all $[FA–H+ Mg^{2+}Terpy\text{-}CH_2{\cdot}]^+$ ion spectra. In the instance of straight chain FA cation $[17:0–H+ Mg^{2+}Terpy\text{-}CH_2{\cdot}]^+$, all the product ions between m/z 342 and 496 generates a series of evenly spaced product ions 14 Da apart, which corresponds to the carbon-carbon (C-C) single bond cleavage along the aliphatic chain (**Figure 3.1a**.). Ion trap CID of $[16:0(14Me)\text{-}H+ Mg^{2+}Terpy\text{-}CH_2{\cdot}]^+$, shown in **Figure 3.1b.**, illustrates a series of evenly spaced product ions 14 Da apart, indicating C-C single bond cleavage, beginning at C2-C3 (*m/z* 329.1), and ending at C11-C12 (*m/z* 454). However, as the fragmentation approaches the methyl branching site, two dramatic relative abundant product ions; odd-electron product ion at C12-C13, *m/z* 469.0 (indicating the radical ion) and even-electron product ion C13-C14 at *m/z* 482.0. In comparison with **Figure 3.1b.**, CID spectrum of $[16:0(15Me)\text{-}H+ Mg^{2+}Terpy\text{-}CH_2{\cdot}]^+$ (**Figure 3.1c.**), displaying a series of even-electron ions spaced 14 Da apart, starting at C2-C3 (*m/z* 329.1) and ending at C13-C14 (*m/z* 468.1). However, an interrupted even-electron series towards the methyl branching site, causing an increase in the relative abundance to the two adjacent peaks C13-C14 at *m/z* 483.0 (indicating the radical ion) and even-electron product ion C14-C15 at *m/z* 496.0. It is evident that CID produce a rich RDD fragmentation that can differentiate methyl branching site from straight chain isomers. Therefore, this method will be utilized to distinguish other isomers.

To demonstrate the utility of this approach further, we examined another pair of isomers; (a) stearic acid $[18:0\text{-}H]^-$ and 17-methyl stearic acid methyl ester $[18:0(17Me)\text{-}H]^-$, shown in **Figure S3.3**. Briefly, ion trap CID of $[18:0–H+ Mg^{2+}Terpy\text{-}CH_2{\cdot}]^+$ (**Figure S3.3a.**), displays similar features to **Figure 3.1a.**, giving rise to a series of evenly spaced products ion 14 Da apart, corresponding to the C-C single bond cleavage along the aliphatic chain, from product ions *m/z* 342.0 to 524.0. Nevertheless, ion trap CID of $[18:0(17Me)\text{-}H+ Mg^{2+}Terpy\text{-}CH_2{\cdot}]^+$, shown in **Figure S3.3b.**, exhibits unique features that identifies with a branched chain fatty acid. The product ion spectrum of $[18:0(17Me)\text{-}H+ Mg^{2+}Terpy\text{-}CH_2{\cdot}]^+$, illustrates a C-C single bond cleavage, with a series of even electron product ions beginning at *m/z* 342 and ending at 496, 14 Da spaced. Ironically, as the RDD fragmentation continues down the chain, two relative higher peaks, one odd-

electron product ion at C15-C16, *m/z* 511 (indicating the radical peak) and second, even-electron product ion at C16-C17 at m/z 524. The resulting product spectra allows for the localization of the branching or straight chain moiety.

3.4.2 Characterizing isoprenoids fatty acids from saturated fatty acyl chains.

Isoprenoids, derived from isoprene, are a class of branched chain fatty acids (IFA), commonly found in plants, microalgae, marine food, bacteria, and/or fungi, that form the backbone of archaeal membrane of phospholipids. Often considered as the "transportation fuel", isoprenoids can enhance, stabilize, and structure the membrane. While there are several types of Isoprenoids, such as 4,8,12-trimethyltridecanoic acid (TMTD), 3,7,11,15 tetramethylhexadecanoic acid (phytanic acid) and/or 2,6,10,14-tetramethylpentadecanoic acid (pristanic acid), they serve as important biomarkers for understanding oxidase deficiency in humans, can be an analytical challenge with differentiating isomers. [50,51,52,53] In this work, we have shown the utility of the gas-phase charge inversion reaction for identifying the BCFA/SCFA anion with $[(\text{TEMPO-Terpy})_2\text{-Mg}]^{+2}$ cation to form a RDD driven fragmentation pattern for localization of branching or straight chain fatty acids.

In brief, isolation, and storage of $[20{:}0{-}\text{H}]^-$ anion with $[(\text{TEMPO-Terpy})_2\text{-Mg}]^{+2}$ cation in a high-pressure collision cell, resulted in a gas-phase charge inversion ion/ion reaction. The subsequent product, $[20{:}0 - \text{H} + \text{TEMPO-Terpy-Mg}]^+$, was formed by a neutral loss (NL) of one TEMPO-Terpy ligand. Ion trap CID of $[20{:}0 - \text{H} + \text{TEMPO-Terpy-Mg}]^+$, resulted in the TEMPO moiety undergoing homolytic cleavage and leaving behind a nascent free radical on the terpy, $[20{:}0 - \text{H} + \text{Mg-Terpy-CH}_2\cdot]^+$. Further, ion trap CID of $[20{:}0 - \text{H} + \text{Mg-Terpy-CH}_2\cdot]^+$ cations undergo RDD, resulting in a series of charge remote fragmentation (CRFs) spaced +14 Da apart, signifying sequential C-C single bond cleavage along the aliphatic chain (shown in **Figure 3.2a**.).

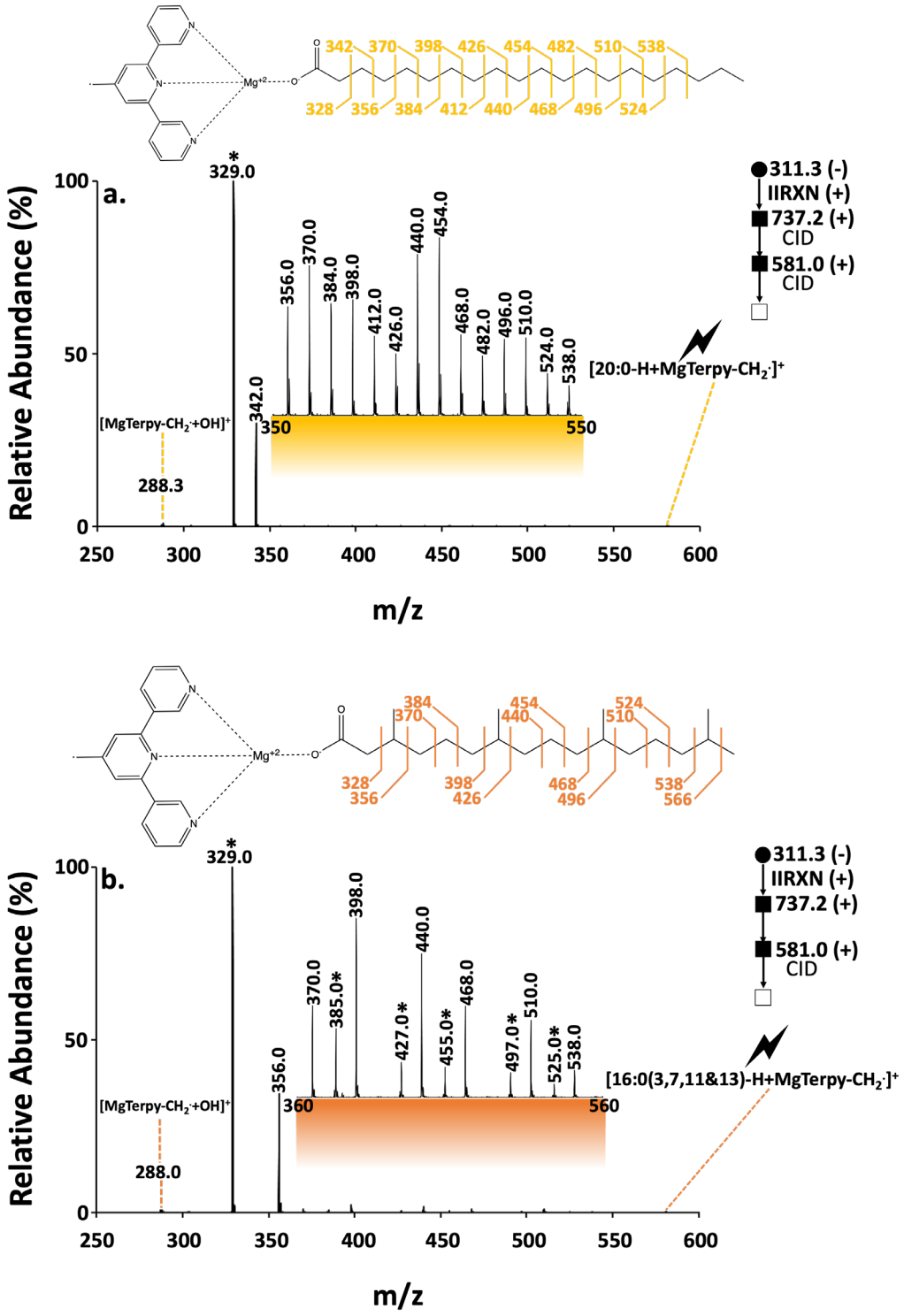

Figure 3.2 - The CID product ion spectra of (a) [20:0−H+ Mg2+Terpy-CH2.]+ and (b) [16:0(3,7,11,15Me)-H+ Mg2+Terpy-CH2.]+. Closed and open circles (●/○) signify selected/unselected anions, respectively, and closed and open squares (■/□) signify selected/unselected cations. Lightning bolts (🗲) indicate the precursor ion subjected to collisional activation. Asterisk (*) indicates the odd-electron fragment product peaks developed from the RDD fragmentation.

In contrast, BCFA [16:0(3,7,11,15ME – H + Mg-Terpy-CH_2·]$^+$ CID spectrum (**Figure 3.2b.**), shows a 28 Da spacing consistent with radical-directed cleavage of the acyl chain backbone on either side of the methyl-branch point, thus providing evidence of a methyl branching site. Ion trap CID of [16:0(3,7,11,15ME – H + Mg-Terpy-CH_2·]$^+$, demonstrates distinctive characteristics that identifies the branching site at multiple points, displaying a consistent loss of the branching fragment peak down the acyl chain. Different from the single branching site, shown in **Figure 3.1b., Figure 3.1c.,** and **Figure S3.3b.,** at each branching location of 16:0(3,7,11,15ME), results in the loss of the fragment production ion at (3) *m/z* 342.0, (7) *m/z* 412.0, (11) *m/z* 482.0 and (15) *m/z* 552.0. Also, the spectrum features even-electron and odd electron product ions before each loss of the branching fragment product ion, starting at (3) odd-electron product ion C2-C3 m/z 329.0 (indicating the radical peak) and ending at even-electron C3-C4 m/z 356.0. Next, (7) starting with odd-electron product ion C5-C6 *m/z* 385.0 (indicating the radical peak) and ending with even-electron product ion C6-C7 *m/z* 398.0. Continuing down the acyl chain, (11) starting odd-electron product ion C9-C10 m/z 455.0 (indicating the radical peak) and ending at even-electron product ion C10-C11 *m/z* 468.0. Lastly, starting odd-electron product ion C13-C14 *m/z* 525.0 and ending at even-electron C14-C15 m/z 538.0. Also note, there are several radical peaks present in the spectrum after each fragment of sites 7 and 11, shown at *m/z* 427.0 and 497.0, shown in **Figure 3.2b.**

3.5 Conclusion

We developed a RDD method for structural elucidation of BCFAs and SCFAs isomers. This approach encompasses the utility of the charge inversion reaction with CID to prompt a free radical for further interrogation of branching location. In the gas-phase, deprotonated FAs anion are transposed via the ion/ion reaction with doubly charged magnesium TEMPO-Terpy complex, to produce a [FA – H + (TEMPO-Terpy)-Mg^{2+}]$^+$ cationic complex. Ion trap CID of cationic complex, resulted in a homolytic cleavage and loss of the TEMPO moiety leaving behind a nascent free radical site, [FA – H + Mg^{2+}-Terpy-CH_2^-]$^+$. Further interrogation with CID of [FA – H + Mg^{2+}-Terpy-CH_2^-]$^+$ results in localization of the site(s) of saturation or branching. The utility of the ion/ion reaction is able to identify whether the FA modification is a straight chain or branching moiety as well as to localize the modification site. This approach was demonstrated on standards but can be extended to other bacteria or human plasma anion generated in the gas-phase. Further studies will focus development of isomer quantitation to determine the fraction of isomer present

in a biological matrix. This approach could utilize different ratios of isomers FA 17:0, 16:0 (14Me) and 16:0 (15Me), (for example, 80:20, 20:80, 50:50, 30:70 and 70:30) to generate a measured value to measure against a corresponding m/z to determine the amount of isomer present in a given m/z.

3.6 Acknowledgement

This work was supported by the U.S. National Institute of Health (NIH) under Grants GM R37-45372 and GM R01-118484.

3.7 Data availability statement

The data that support the findings of this study are available from the corresponding author upon reasonable request.

3.8 Supporting Information

Additional supporting information can be found online in the Supporting Information section at the end of this article.

3.9 Notes

The authors declare no competing financial interests.

3.10 Author Information

Corresponding Author

Scott A. McLuckey - *Department of Chemistry, Purdue University, West Lafayette, Indiana 47907-2084, United States;* orcid.org/0000-0002-1648-5570

Jinshan Gao – *Department of Chemistry and Biochemistry, Center for Quantitative Obesity Research, Montclair State University, Montclair, NJ 07043*

Authors

De'Shovon M. Shenault - *Department of Chemistry, Purdue University, West Lafayette, Indiana 47907-2084, United States*; orcid.org/0000-0002-9208-0655

Kimberly Fabijanczuk - *Department of Chemistry, Purdue University, West Lafayette, Indiana 47907-2084, United States*

Rayan Murtada - *Department of Chemistry and Biochemistry, Center for Quantitative Obesity Research, Montclair State University, Montclair, NJ 07043*

Shane Finn - *Department of Chemistry and Biochemistry, Center for Quantitative Obesity Research, Montclair State University, Montclair, NJ 07043*

3.11 References

(1) Kaneda, T. Biosynthesis of Branched Chain Fatty Acids. *J. Biol. Chem.* **1963**, *238* (4), 1229–1235. https://doi.org/10.1016/S0021-9258(18)81168-1.

(2) Saito, K. Note on the Chemical Structure of 'Subtilopentadecanoic' and 'Subtiloheptadecanoic'Acids. *J. Biochem. (Tokyo)* **1966**, *59* (2), 186–188.

(3) Su, X.; Magkos, F.; Zhou, D.; Eagon, J. C.; Fabbrini, E.; Okunade, A. L.; Klein, S. Adipose Tissue Monomethyl Branched-Chain Fatty Acids and Insulin Sensitivity: Effects of Obesity and Weight Loss. *Obesity* **2015**, *23* (2), 329–334. https://doi.org/10.1002/oby.20923.

(4) Kaneda, T. Fatty Acids in the Genus Bacillus I. Iso- and Anteiso-Fatty Acids as Characteristic Constituents of Lipids in 10 Species. *J. Bacteriol.* **1967**, *93* (3), 894–903. https://doi.org/10.1128/jb.93.3.894-903.1967.

(5) Bishop, D. G.; Rutberg, L.; Samuelsson, B. The Chemical Composition of the Cytoplasmic Membrane of Bacillus Subtilis. *Eur. J. Biochem.* **1967**, *2* (4), 448–453. https://doi.org/10.1111/j.1432-1033.1967.tb00158.x.

(6) Suutari, M.; Laakso, S. Unsaturated and Branched Chain-Fatty Acids in Temperature Adaptation of Bacillus Subtilis and Bacillus Megaterium. *Biochim. Biophys. Acta BBA - Lipids Lipid Metab.* **1992**, *1126* (2), 119–124. https://doi.org/10.1016/0005-2760(92)90281-Y.

(7) Kaneda, T. Iso- and Anteiso-Fatty Acids in Bacteria: Biosynthesis, Function, and Taxonomic Significance. *Microbiol. Rev.* **1991**, *55* (2), 288–302. https://doi.org/10.1128/mr.55.2.288-302.1991.

(8) Oku, H.; Kaneda, T. Biosynthesis of Branched-Chain Fatty Acids in Bacillus Subtilis. A Decarboxylase Is Essential for Branched-Chain Fatty Acid Synthetase. *J. Biol. Chem.* **1988**, *263* (34), 18386–18396. https://doi.org/10.1016/S0021-9258(19)81371-6.

(9) Huang, H.-Y.; Huang, S.-Y.; Chen, P.-Y.; King, V. A.-E.; Lin, Y.-P.; Tsen, J.-H. Basic Characteristics of Sporolactobacillus Inulinus BCRC 14647 for Potential Probiotic Properties. *Curr. Microbiol.* **2007**, *54* (5), 396–404. https://doi.org/10.1007/s00284-006-0496-5.

(10) Ran-Ressler, R. R.; Devapatla, S.; Lawrence, P.; Brenna, J. T. Branched Chain Fatty Acids Are Constituents of the Normal Healthy Newborn Gastrointestinal Tract. *Pediatr. Res.* **2008**, *64* (6), 605–609. https://doi.org/10.1203/PDR.0b013e318184d2e6.

(11) Sherman, D. J.; Ross, M. G.; Day, L.; Ervin, M. G. Fetal Swallowing: Correlation of Electromyography and Esophageal Fluid Flow. *Am. J. Physiol.-Regul. Integr. Comp. Physiol.* **1990**, *258* (6), R1386–R1394. https://doi.org/10.1152/ajpregu.1990.258.6.R1386.

(12) Hoeger, P. H.; Schreiner, V.; Klaassen, I. A.; Enzmann, C. C.; Friedrichs, K.; Bleck, O. Epidermal Barrier Lipids in Human Vernix Caseosa: Corresponding Ceramide Pattern in Vernix and Fetal Skin. *Br. J. Dermatol.* **2002**, *146* (2), 194–201. https://doi.org/10.1046/j.1365-2133.2002.04584.x.

(13) Taormina, V. M.; Unger, A. L.; Schiksnis, M. R.; Torres-Gonzalez, M.; Kraft, J. Branched-Chain Fatty Acids—An Underexplored Class of Dairy-Derived Fatty Acids. *Nutrients* **2020**, *12* (9), 2875. https://doi.org/10.3390/nu12092875.

(14) Ran-Ressler, R. R.; Sim, D.; O'Donnell-Megaro, A. M.; Bauman, D. E.; Barbano, D. M.; Brenna, J. T. Branched Chain Fatty Acid Content of United States Retail Cow's Milk and Implications for Dietary Intake. *Lipids* **2011**, *46* (7), 569–576. https://doi.org/10.1007/s11745-011-3530-8.

(15) Ran-Ressler, R. R.; Bae, S.; Lawrence, P.; Wang, D. H.; Brenna, J. T. Branched-Chain Fatty Acid Content of Foods and Estimated Intake in the USA. *Br. J. Nutr.* **2014**, *112* (4), 565–572. https://doi.org/10.1017/S0007114514001081.

(16) Sun, W.; Luo, Y.; Wang, D. H.; Kothapalli, K. S. D.; Brenna, J. T. Branched Chain Fatty Acid Composition of Yak Milk and Manure during Full-Lactation and Half-Lactation. *Prostaglandins Leukot. Essent. Fatty Acids* **2019**, *150*, 16–20. https://doi.org/10.1016/j.plefa.2019.09.002.

(17) Lheureux, P. E.; Penaloza, A.; Zahir, S.; Gris, M. Science Review: Carnitine in the Treatment of Valproic Acid-Induced Toxicity – What Is the Evidence? *Crit. Care* **2005**, *9* (5), 431. https://doi.org/10.1186/cc3742.

(18) SCHÖNFELD, P.; KAHLERT, S.; REISER, G. In Brain Mitochondria the Branched-Chain Fatty Acid Phytanic Acid Impairs Energy Transduction and Sensitizes for Permeability Transition. *Biochem. J.* **2004**, *383* (1), 121–128. https://doi.org/10.1042/BJ20040583.

(19) Wanders, R. J. A.; Jansen, G. A.; Lloyd, M. D. Phytanic Acid Alpha-Oxidation, New Insights into an Old Problem: A Review. *Biochim. Biophys. Acta BBA - Mol. Cell Biol. Lipids* **2003**, *1631* (2), 119–135. https://doi.org/10.1016/S1388-1981(03)00003-9.

(20) Rönicke, S.; Kruska, N.; Kahlert, S.; Reiser, G. The Influence of the Branched-Chain Fatty Acids Pristanic Acid and Refsum Disease-Associated Phytanic Acid on Mitochondrial Functions and Calcium Regulation of Hippocampal Neurons, Astrocytes, and Oligodendrocytes. *Neurobiol. Dis.* **2009**, *36* (2), 401–410. https://doi.org/10.1016/j.nbd.2009.08.005.

(21) Chaudhary, S.; Parvez, S. An in Vitro Approach to Assess the Neurotoxicity of Valproic Acid-Induced Oxidative Stress in Cerebellum and Cerebral Cortex of Young Rats. *Neuroscience* **2012**, *225*, 258–268. https://doi.org/10.1016/j.neuroscience.2012.08.060.

(22) Nanau, R. M.; Neuman, M. G. Adverse Drug Reactions Induced by Valproic Acid. *Clin. Biochem.* **2013**, *46* (15), 1323–1338. https://doi.org/10.1016/j.clinbiochem.2013.06.012.

(23) Pham, H. T.; Trevitt, A. J.; Mitchell, T. W.; Blanksby, S. J. Rapid Differentiation of Isomeric Lipids by Photodissociation Mass Spectrometry of Fatty Acid Derivatives: Photodissociation of Derivatized Fatty Acids. *Rapid Commun. Mass Spectrom.* **2013**, *27* (7), 805–815. https://doi.org/10.1002/rcm.6503.

(24) Ran-Ressler, R. R.; Lawrence, P.; Brenna, J. T. Structural Characterization of Saturated Branched Chain Fatty Acid Methyl Esters by Collisional Dissociation of Molecular Ions Generated by Electron Ionization. *J. Lipid Res.* **2012**, *53* (1), 195–203. https://doi.org/10.1194/jlr.D020651.

(25) Wang, Z.; Wang, D. H.; Park, H. G.; Tobias, H. J.; Kothapalli, K. S. D.; Brenna, J. T. Structural Identification of Monounsaturated Branched Chain Fatty Acid Methyl Esters by Combination of Electron Ionization and Covalent Adduct Chemical Ionization Tandem Mass Spectrometry. *Anal. Chem.* **2019**, *91* (23), 15147–15154. https://doi.org/10.1021/acs.analchem.9b03912.

(26) Harvey, D. J. Picolinyl Esters as Derivatives for the Structural Determination of Long Chain Branched and Unsaturated Fatty Acids. *Biomed. Mass Spectrom.* **1982**, *9* (1), 33–38. https://doi.org/10.1002/bms.1200090107.

(27) Ran-Ressler, R. R.; Lawrence, P.; Brenna, J. T. Structural Characterization of Saturated Branched Chain Fatty Acid Methyl Esters by Collisional Dissociation of Molecular Ions Generated by Electron Ionization [S]. *J. Lipid Res.* **2012**, *53* (1), 195–203. https://doi.org/10.1194/jlr.D020651.

(28) Zirrolli, J. A.; Murphy, R. C. Low-Energy Tandem Mass Spectrometry of the Molecular Ion Derived from Fatty Acid Methyl Esters: A Novel Method for Analysis of Branched-Chain Fatty Acids. *J. Am. Soc. Mass Spectrom.* **1993**, *4* (3), 223–229. https://doi.org/10.1016/1044-0305(93)85085-C.

(29) Palyzová, A.; Řezanka, T. Separation and Identification of Diacylglycerols Containing Branched Chain Fatty Acids by Liquid Chromatography-Mass Spectrometry. *J. Chromatogr. A* **2021**, *1635*, 461708. https://doi.org/10.1016/j.chroma.2020.461708.

(30) Tanno, H.; Sassa, T.; Sawai, M.; Kihara, A. Production of Branched-Chain Very-Long-Chain Fatty Acids by Fatty Acid Elongases and Their Tissue Distribution in Mammals. *Biochim. Biophys. Acta BBA - Mol. Cell Biol. Lipids* **2021**, *1866* (1), 158842. https://doi.org/10.1016/j.bbalip.2020.158842.

(31) Randolph, C. E.; Beveridge, C. H.; Iyer, S.; Blanksby, S. J.; McLuckey, S. A.; Chopra, G. Identification of Monomethyl Branched-Chain Lipids by a Combination of Liquid Chromatography Tandem Mass Spectrometry and Charge-Switching Chemistries. *J. Am. Soc. Mass Spectrom.* **2022**, *33* (11), 2156–2164. https://doi.org/10.1021/jasms.2c00225.

(32) Narreddula, V. R.; Boase, N. R.; Ailuri, R.; Marshall, D. L.; Poad, B. L. J.; Kelso, M. J.; Trevitt, A. J.; Mitchell, T. W.; Blanksby, S. J. Introduction of a Fixed-Charge, Photolabile Derivative for Enhanced Structural Elucidation of Fatty Acids. *Anal. Chem.* **2019**, *91* (15), 9901–9909. https://doi.org/10.1021/acs.analchem.9b01566.

(33) Narreddula, V. R.; Sadowski, P.; Boase, N. R. B.; Marshall, D. L.; Poad, B. L. J.; Trevitt, A. J.; Mitchell, T. W.; Blanksby, S. J. Structural Elucidation of Hydroxy Fatty Acids by Photodissociation Mass Spectrometry with Photolabile Derivatives. *Rapid Commun. Mass Spectrom.* **2020**, *34* (9), e8741. https://doi.org/10.1002/rcm.8741.

(34) Zhao, X.; Wu, G.; Zhang, W.; Dong, M.; Xia, Y. Resolving Modifications on Sphingoid Base and N-Acyl Chain of Sphingomyelin Lipids in Complex Lipid Extracts. *Anal. Chem.* **2020**, *92* (21), 14775–14782. https://doi.org/10.1021/acs.analchem.0c03502.

(35) Zhao, X.; Xia, Y. Characterization of Fatty Acyl Modifications in Phosphatidylcholines and Lysophosphatidylcholines via Radical-Directed Dissociation. *J. Am. Soc. Mass Spectrom.* **2021**, *32* (2), 560–568. https://doi.org/10.1021/jasms.0c00407.

(36) Lin, Q.; Li, P.; Jian, R.; Xia, Y. Localization of Intrachain Modifications in Bacterial Lipids Via Radical-Directed Dissociation. *J. Am. Soc. Mass Spectrom.* **2022**, *33* (4), 714–721. https://doi.org/10.1021/jasms.2c00011.

(37) Randolph, C. E.; Foreman, D. J.; Betancourt, S. K.; Blanksby, S. J.; McLuckey, S. A. Gas-Phase Ion/Ion Reactions Involving Tris-Phenanthroline Alkaline Earth Metal Complexes as Charge Inversion Reagents for the Identification of Fatty Acids. *Anal. Chem.* **2018**, *90* (21), 12861–12869. https://doi.org/10.1021/acs.analchem.8b03441.

(38) Randolph, C. E.; Foreman, D. J.; Blanksby, S. J.; McLuckey, S. A. Generating Fatty Acid Profiles in the Gas Phase: Fatty Acid Identification and Relative Quantitation Using Ion/Ion Charge Inversion Chemistry. *Anal. Chem.* **2019**, *91* (14), 9032–9040. https://doi.org/10.1021/acs.analchem.9b01333.

(39) Randolph, C. E.; Blanksby, S. J.; McLuckey, S. A. Toward Complete Structure Elucidation of Glycerophospholipids in the Gas Phase through Charge Inversion Ion/Ion Chemistry. *Anal. Chem.* **2020**, *92* (1), 1219–1227. https://doi.org/10.1021/acs.analchem.9b04376.

(40) Chao, H.-C.; McLuckey, S. A. Differentiation and Quantification of Diastereomeric Pairs of Glycosphingolipids Using Gas-Phase Ion Chemistry. *Anal. Chem.* **2020**, *92* (19), 13387–13395. https://doi.org/10.1021/acs.analchem.0c02755.

(41) Randolph, C. E.; Shenault, D. M.; Blanksby, S. J.; McLuckey, S. A. Structural Elucidation of Ether Glycerophospholipids Using Gas-Phase Ion/Ion Charge Inversion Chemistry. *J. Am. Soc. Mass Spectrom.* **2020**, *31* (5), 1093–1103. https://doi.org/10.1021/jasms.0c00025.

(42) Randolph, C. E.; Marshall, D. L.; Blanksby, S. J.; McLuckey, S. A. Charge-Switch Derivatization of Fatty Acid Esters of Hydroxy Fatty Acids via Gas-Phase Ion/Ion Reactions. *Anal. Chim. Acta* **2020**, *1129*, 31–39. https://doi.org/10.1016/j.aca.2020.07.005.

(43) Chao, H.-C.; McLuckey, S. A. In-Depth Structural Characterization and Quantification of Cerebrosides and Glycosphingosines with Gas-Phase Ion Chemistry. *Anal. Chem.* **2021**, *93* (19), 7332–7340. https://doi.org/10.1021/acs.analchem.1c01021.

(44) Randolph, C. E.; Shenault, D. M.; Blanksby, S. J.; McLuckey, S. A. Localization of Carbon–Carbon Double Bond and Cyclopropane Sites in Cardiolipins via Gas-Phase Charge Inversion Reactions. *J. Am. Soc. Mass Spectrom.* **2021**, *32* (2), 455–464. https://doi.org/10.1021/jasms.0c00348.

(45) Shenault, D. S. M.; McLuckey, S. A.; Franklin, E. T. Localization of Cyclopropyl Groups and Alkenes Within Glycerophospholipids Using Gas-Phase Ion/Ion Chemistry. *J. Mass Spectrom. n/a* (n/a), e4913. https://doi.org/10.1002/jms.4913.

(46) Liebisch, G.; Vizcaíno, J. A.; Köfeler, H.; Trötzmüller, M.; Griffiths, W. J.; Schmitz, G.; Spener, F.; Wakelam, M. J. O. Shorthand Notation for Lipid Structures Derived from Mass Spectrometry. *J. Lipid Res.* **2013**, *54* (6), 1523–1530. https://doi.org/10.1194/jlr.M033506.

(47) Matyash, V.; Liebisch, G.; Kurzchalia, T. V.; Shevchenko, A.; Schwudke, D. Lipid Extraction by Methyl-Tert-Butyl Ether for High-Throughput Lipidomics. *J. Lipid Res.* **2008**, *49* (5), 1137–1146. https://doi.org/10.1194/jlr.D700041-JLR200.

(48) Xia, Y.; Wu, J.; McLuckey, S. A.; Londry, F. A.; Hager, J. W. Mutual Storage Mode Ion/Ion Reactions in a Hybrid Linear Ion Trap. *J. Am. Soc. Mass Spectrom.* **2005**, *16* (1), 71–81. https://doi.org/10.1016/j.jasms.2004.09.017.

(49) Xia, Y.; Liang, X.; McLuckey, S. A. Pulsed Dual Electrospray Ionization for In/In Reactions. *J. Am. Soc. Mass Spectrom.* **2005**, *16* (11), 1750–1756. https://doi.org/10.1016/j.jasms.2005.07.013.

(50) Jordan, S. F.; Nee, E.; Lane, N. Isoprenoids Enhance the Stability of Fatty Acid Membranes at the Emergence of Life Potentially Leading to an Early Lipid Divide. *Interface Focus* **2019**, *9* (6), 20190067. https://doi.org/10.1098/rsfs.2019.0067.

(51) Cramp, L.; Evershed, R. P. 14.20 - Reconstructing Aquatic Resource Exploitation in Human Prehistory Using Lipid Biomarkers and Stable Isotopes. In *Treatise on Geochemistry (Second Edition)*; Holland, H. D., Turekian, K. K., Eds.; Elsevier: Oxford, 2014; pp 319–339. https://doi.org/10.1016/B978-0-08-095975-7.01225-0.

(52) Malik, S.; Liu, C.-G.; Zhao, X.-Q.; Mehmood, M. A. 3.08 - Long-Chain Liquid Biofuels. In *Comprehensive Biotechnology (Third Edition)*; Moo-Young, M., Ed.; Pergamon: Oxford, 2019; pp 101–109. https://doi.org/10.1016/B978-0-444-64046-8.00485-7.

(53) Koga, Y. Early Evolution of Membrane Lipids: How Did the Lipid Divide Occur? *J. Mol. Evol.* **2011**, *72* (3), 274–282. https://doi.org/10.1007/s00239-011-9428-5.

3.12 Supporting Information

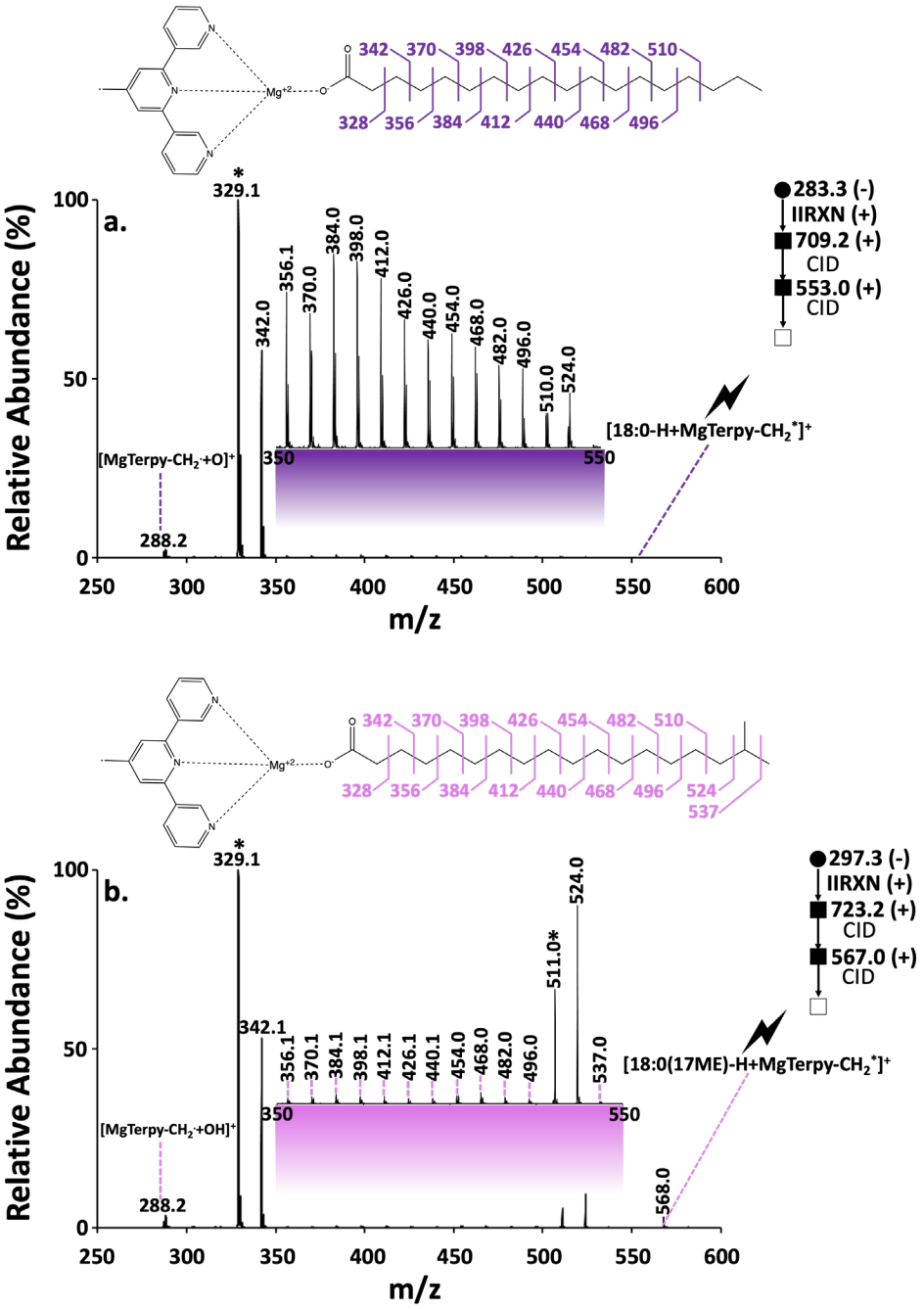

Figure 3.3 - The CID product ion spectra of (a) [18:0−H+ Mg^{2+}Terpy-CH_2·]$^+$ and (b) [18:0(17Me)-H+ Mg^{2+}Terpy-CH_2·]$^+$. Closed and open circles (●/○) signify selected/unselected anions, respectively, and closed and open squares (■/□) signify selected/unselected cations. Lightning bolts (↯) indicate the precursor ion subjected to collisional activation. Asterisk (*) indicates the odd-electron fragment product peaks developed from the RDD fragmentation.

CHAPTER 4. GAS-PHASE ION/ION STRATEGY FOR THE DIFFERENTIATION OF ISOMERIC BIS(MONOACYLGLYCERO)PHOSPHATE AND PHOSPHATIDYLGLYCEROL SPECIES BY SHOTGUN LIPIDOMICS.

A portion of this manuscript will be published at a later date.

4.1 Abstract

Bis(monoacylglycerol)phosphate (BMPs) commonly found in the late endosomal and lysosomal vesicles, are key component in lysosomal stability and vesicle trafficking. Similar to phosphatidylglycerol (PGs), BMP and PGs are a unique class of regioisomers, with different structural features and biochemical roles in the cell. Due to the complexity and these isomeric species, PG and BMP pose an analytical challenge in the separation and quantitation of isomeric ions. Approaches such as liquid chromatography mass spectrometry (LC-MS), hydrophilic interaction liquid chromatography mass spectrometry (HILIC-MS), and/or reverse-phase liquid chromatography tandem mass spectrometry (RPLC-MS/MS), for the quantification and separation of phospholipids classes; CLs, BMP, and/or PGs found in varying human tissue, cancer cells and mouse samples. However, these techniques require long elution time, high degree of samples, and reference standards to accurately identify. Herein, we propose a gas-phase charge inversion ion/ion reaction to discriminate intact PG and BMP isomeric species. In addition, pinpoint the site(s) of unsaturation in acyl chain constituents. This approach utilizes a doubly charged magnesium tri-tert-butyl-terpyridine complex, denoted $[Mg(TTBT)_2]^{2+}$to differentiate constitutional isomer in the gas-phase without additional offline derivation methods.

Keywords: Bis(monoacylglycero)phosphate, Phosphatidylglycerol, Isomers, Ion/Ion Reaction, Shotgun Lipidomics,

4.2 Introduction

Phospholipids (PLs), also known as glycerophospholipids (GPLs), are one of the major component of the lipid bilayer, that aid in cellular structure and stability to form protection against environmental attacks.[1] PLs are a group of polar lipids that consist of two fatty acids moieties at

the sn-1 and sn-2 position, a glycerol backbone esterified to a phosphate group with an organic molecule consisting of either choline, ethanolamine, serine, inositol, glycerol, and/or etc..[2,3] The classification of PL is based on the diversity of the head group, which is linked to the phosphate group varies by chain length, degree of saturation and unsaturation.[4] In an organism, PLs perform a variety of essential biological roles. PLs serve as physical element of the respiratory chain in the mitochondria, acts as the precursor molecules for second messengers in the membrane and modifies the cancer cell from oxidative destruction. [5,6,7]

Of the PLs classes, bis(monoacylglycerol)phosphate (BMPs) and phosphatidylglycerol (PGs) are a unique class of regioisomers, with different structural features and biochemical roles in the cell.[8] In the bacterial membrane, PGs are the most abundant PLs class found and the major component of the lung surfactant.[9] Synthetized in the mitochondria with cardiolipins (CLs); acts as the predecessor for glycophospholipids, bacterial proteolipids, lipoteichoic acids, BMPs and other biological molecules.[10,11,12,13] Having a net negative charge, PGs introduce negative polarity in the membrane surface to allow for biological processes, such as: transporting, signaling and other protein interactions.[14]

Similarly, BMPs are the second most abundant lipid found in mammalian cells and tissues. A negatively charged PLs class lipid, BMPs are crucial to lysosomal stability and vesicle trafficking bis(monoacylglycerol)phosphate (BMPs).[15,16] BMPs originally named lysobisphophatidic acid (LBPA), have shown to promote degradation of glycosphingolipids by targeting the multivesicular; which provides suitable nature for interaction glycosphingolipid hydrolases to the lipid substrate.[17,18] PGs and BMPs present a unique example of sn-positional isomers where both share acyl chains connected to the glycerol-backbone. In the case of PGs and other PLs, acyl chains are esterified to the glycerol backbone, represented as sn-1:sn-2 position, however, BMP differs with one acyl-chain connected at both the glycerol backbone and headgroup, resulting in an sn-1:sn-1′ orientation.[19,20,21,22] Although recent reports suggest BMPs serve as biomarkers for metastatic cancer, lysosomal storage diseases (LSDs), and drug-induced phospholipidosis, BMP are understudied compared to its PG counterpart.[23,24,25,26]

Since PGs and BMPs are constitutional isomers, accurate measurements are needed to separate isomeric species from biological matrices. In recent studies, utilization of liquid chromatog-

raphy mass spectrometry (LC-MS), hydrophilic interaction liquid chromatography mass spectrometry (HILIC-MS), and/or reverse-phase liquid chromatography tandem mass spectrometry (RPLC-MS/MS), for the quantification and separation of phospholipids classes; CLs, BMP, and/or PGs found in varying human tissue, cancer cells and mouse samples. However, these methods require reference standards to confirm retention time, higher degree of samples and solvents, long analysis time and/or etc. than other shotgun approaches, but fail to fully separate isomeric species.[27,28,29,30,31,32] The integration Ion mobility with tandem mass spectrometry were employed for the separation of regioisomeric species, but similar to chromatography methods, ion mobility require reference standards, long analysis time and suffers from low sensitivity, while struggle to fully probe intact BMPs and PGs species.[33,34,35]

Other techniques involving condensed phase derivatization strategies have been utilized to methylate the phosphate group of the phospholipid (phosphatidylinositol (PPIs), PGs, and BMP isomers for identification in a biological sample, but this method is time consuming due to a neutral loss scan (NLS) of methylated head groups a head of time to identify lipid species, however, technique is not able to quantify isomers at varing chain lengths.[36,37,38] Utilization of tandem mass spectrometry can be useful for separating isomeric species.[39] Electrospray ionization (ESI) in negative ion mode has been widely used to examine PG species but isomeric BMP cannot be differentiate from PG, due to similar mass to charge (m/z) and relative abundances. With the aid of ammonium adducts, positive ESI can differentiate both PG and BMP at a higher degree of sensitivity compared to typical tandem mass spectrometry (MS/MS) negative ion mode. Which produce diverse product spectrum that identify isomer species but cannot provide complete separation of coeluted isomer type.[40,41]

Herein, we demonstrate the use of a gas-phase charge inversion ion/ion reaction to discriminate intact PG and BMP isomeric species. In addition, pinpoint the site(s) of unsaturation in acyl chain constituents. In previous work, charge inversion reaction has been used for the localization of saturated and unsaturated species, present in biological matrices.[42–47] In brief, via nESI negative ion mode, single deprotonated BMP/PG, $[BMP/PG - H]^-$, was mass selected during transit and transferred to high pressure collision cell, q2 for storage.

Next, in positive ion mode, doubly charged magnesium tri-tert-butyl-terpyridine complex, denoted $[Mg(TTBT)_2]^{2+}$, was mass selected and transferred to high pressure collision cell, q2 to undergo charge inversion reaction (IIRXN). To facilitate the ion/ion reaction, magnesium complex

dictations and lipid anions were simultaneously stored in q2, resulting in the formation of two charge inverted species: $[BMP/PG - H + Mg(TTBT)_2]^+$ and $[BMP/PG - H + Mg(TTBT)]^+$. Ion-trap collisional induced dissociation (CID) of dominate ion peak, $[BMP/PG - H + Mg(TTBT)]^+$ resulted in distinctive fragmentation corresponding to isomer constituent, facilitating differentiation of BMP/PG isomers and localization of unsaturation sites in acyl chain constituents. Explicitly, standards of PLs with PGs and BMPs are used to demonstrate capability of the ion/ion reaction.

4.3 Experimental Section

4.3.1 Nomenclature

We have adapted the shorthand lipid nomenclature recommended by Liebisch et al., which is demonstrated throughout this work.[48] For example, bis(monoacylglycero)phosphate and phosphatidylglycerol are represented as BMP and PG, respectively. In short, PG 16:0/18:1(Δ9) categorizes the phosphatidylglycerol (PG), by glycerol head group, two fatty acyl chains at the sn-1 and sn-2 position, esterified to the glycerol backbone, having a carbon number (represented before the colon, 16 and 18), degree of unsaturation, carbon-carbon double bond (C=C), and stereo-orientation (represented after the colon as 0 and 1). The separator "/" indicating that the *sn*-positions are known. The separator "_" is used when the *sn*-positions are not known. Geometry and C=C position is specified using "9Z" nomenclature meaning that the double bond is at the 9th carbon of the fatty acyl chain with cis geometry. When the C=C geometry is unknown, Δ-nomenclature followed by the carbon position number is used, i.e., PG 16:0/18:1(Δ9). However, in the case of BMP RR 18:1(Δ9) /18:1(Δ9) identifies the bis(monoacylglycero)phosphate (BMP), by two monoacylglycerols bound to a phosphate group at the sn:1/sn:1 configuration.[49] RR represents the stereochemistry of the acyl chain connected to both sides of the phosphate group.

4.3.2 Chemicals

18:1(Δ9-Cis) BMP (R,R), 14:0 Hemi BMP (S,R), 18:1 (Δ9-Cis) PG, 16:0-18:1 PG, and 18:0-18:1 PG standards were purchased from Avanti Polar Lipids (Alabaster, AL). 1,2-Dilauroyl-sn-glycero-3-PG (sodium salt) (PG 12:0/12:0), 1,2-Dimyristoyl-sn-glycero-3-PG (sodium salt)

(PG 14:0/14:0), 1,2-Dipalmitoyl-sn-glycero-3-PG (sodium salt) (PG 16:0/16:0), and 1,2-Distearoyl-rac-glycero-3-PG (sodium salt) (PG 18:0/18:0) standards were all purchased from Cayman Chemical Company (Ann Arbor, MI). 4,4′,4″-Tri-tert-Butyl-2,2′:6′,2″-terpyridine were purchased from Sigma-Aldrich, Inc. (St. Louis, MO). Magnesium chloride, HPLC Grade methanol, HPLC Grade water and chloroform were purchased from Thermo Fisher Scientific (Waltham, MA).

4.3.3 Mass Spectrometry

All data were collected on modified a Sciex QTRAP4000 hybrid triple quadrupole/linear ion trap mass spectrometer. Briefly, alternately, pulsed nano-electrospray ionization (nESI) was used for ion generation. Deprotonated lipid anions $[BMP/PG - H]^-$, were generated via negative ion mode nESI, mass selected during transit through Q1, and transferred to q2 for storage. Next, the charge inversion (IIRXN) reagent doubly charged magnesium tri-tert-butyl-terpyridine complex cations, denoted $[Mg(TTBT)_2]^{2+}$, were generated via positive ion mode nESI. To facilitate the ion/ion reaction, magnesium complex dictations and lipid anions were simultaneously stored in q2, resulting in the formation of charge-inverted lipid cations $[BMP/PG - H + Mg(TTBT)_2]^+$. Ion-trap CID of charge-inverted lipid anion isomer resulted in distinctive fragmentation, facilitating differentiation of BMP/PG isomers and localization of unsaturation sites in acyl chain constituents.

4.4 Results and Discussion

4.4.1 Distinguishing bis(monoacylglycerol)phosphate moieties from regioisomeric phosphatidylglycerol species.

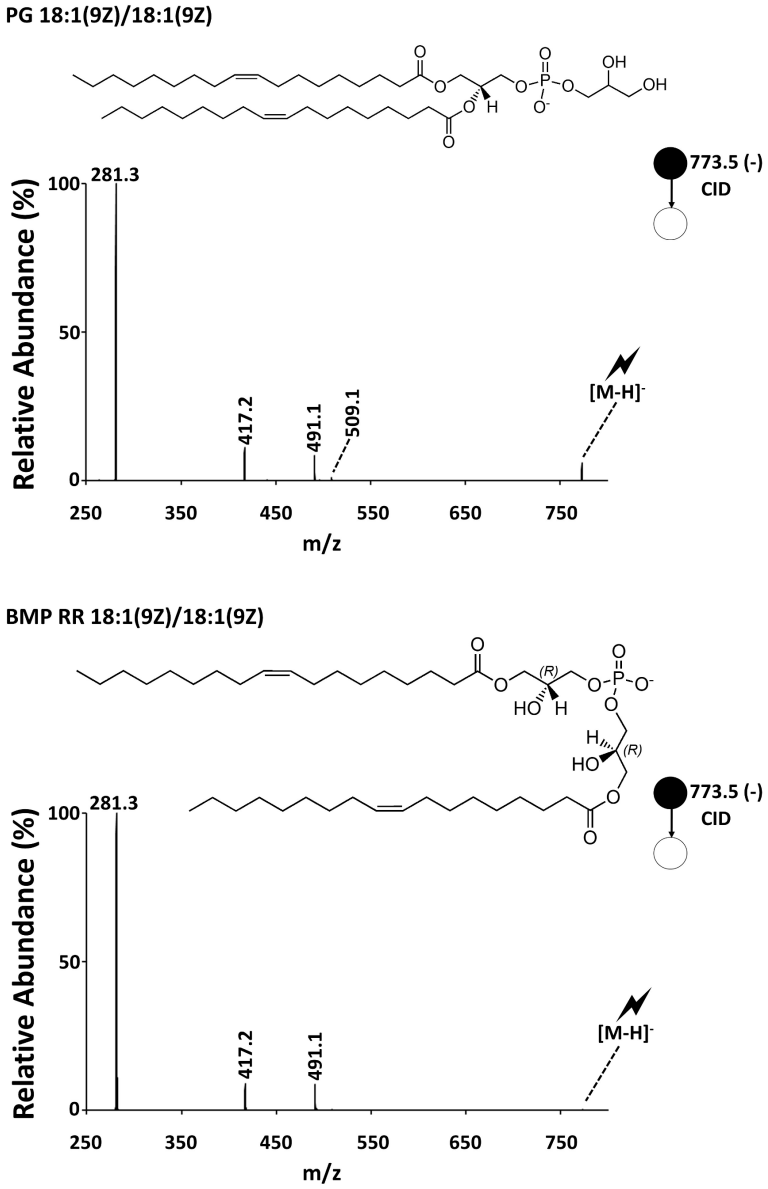

Figure 4.1 - MS^2 CID product spectra of constitutional isomers. (a) [PG 18:1(9Z)/18:1(9Z) - H]$^-$ (m/z 773.5) and (b) [BMP 18:1(9Z)/18:1(9Z) - H]$^-$ (m/z 773.5) in negative ion mode. CID spectra of [PG 18:1(9Z)/18:1(9Z) - H]$^-$ and [BMP 18:1(9Z)/18:1(9Z) - H]$^-$ exhibiting identical fragmentation patterns, corresponding to the fatty acyl chain [18:1 – H]$^-$ (m/z 281.3), neutral loss of sn1 or sn2 (m/z 491.1) and neutral loss of sn1 or sn2 group and glycerol (m/z 417.2). Closed and open circles (●/○) signify selected/unselected anions, respectively. Lightning bolts (↯) indicate the precursor ion subjected to collisional activation.

Tandem mass spectrometry (MS/MS) technique are commonly used in the detection of lipid species, due to its high sensitivity, robustness, and dependability. In conjunction with MS/MS experiment, collisional induced dissociation (CID) is normally employed to aid in the characterization and quantitation of lipid species. As mentioned above, constitutional isomers PGs and BMPs are unique lipid classes of PLs, that pose an analytical challenge due to common mischaracterization in the gas-phase. In positive ion mode, ammonium adducted PGs and BMPs $[M + NH_4^-]^+$ are detected. While PGs are favored more in the negative ion mode, both lipid classes $[M - H]^-$ are found, sharing similar spectra.

In positive ion mode, CID spectra of $[M + NH_4^-]^+$, produce product fragments corresponding to headgroup dictation. While in negative mode, CID spectra of $[M - H]^-$ produce identical fragment spectra. For example, shown in **Figure 4.1**, negative ion mode CID product ion spectra of both [PG 18:1(9Z)/18:1(9Z) - H]- and $[BMP 18:1(9Z)/18:1(9Z) - H]^-$. Ironically, both MS/MS CID spectra of **Figure 4.1(a)**. $[PG 18:1(9Z)/18:1(9Z) - H]^-$ and **Figure 4.1(b).** $[BMP 18:1(9Z)/18:1(9Z) - H]^-$ illustrates identical fragmentation patterns, corresponding to acyl chain composition (m/z 281.3), neutral loss of sn1 or sn2 (m/z 491.1) and neutral loss of sn1 or sn2 group and glycerol (m/z 417.2) moieties.

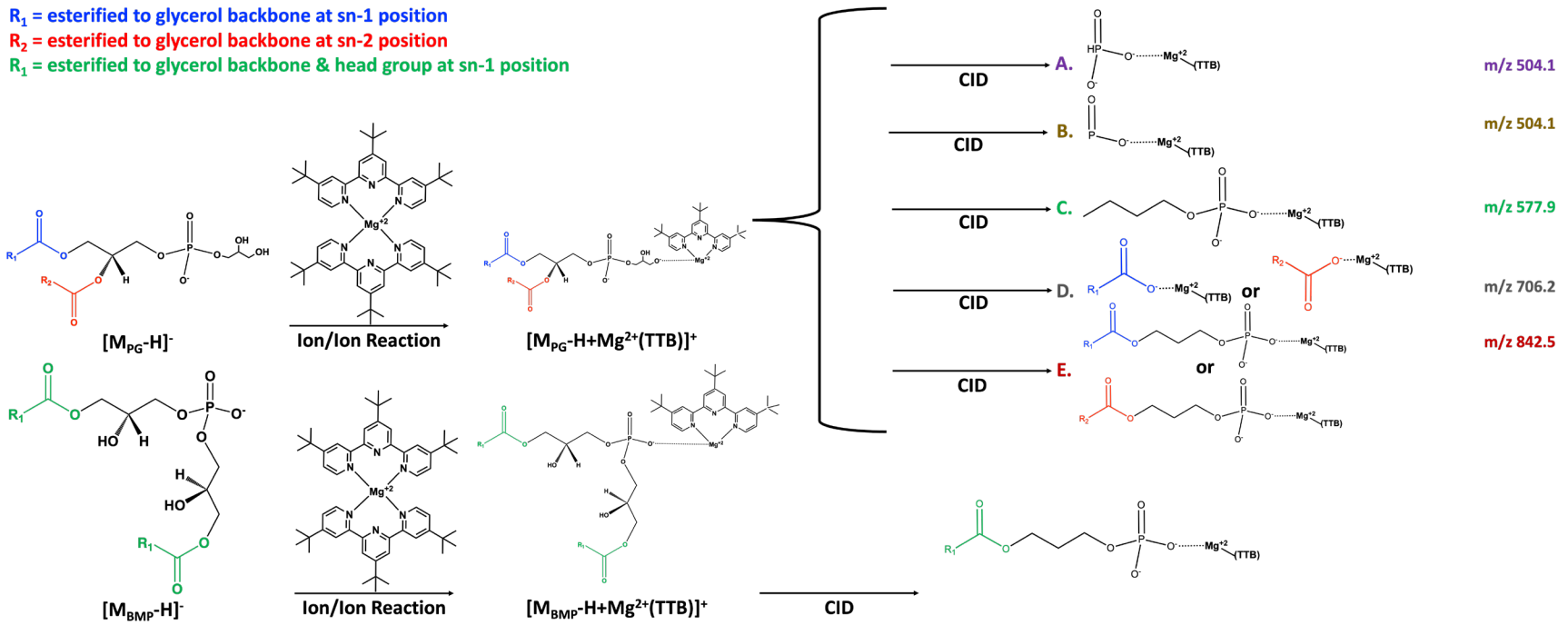

Scheme 4.1 - Demonstration of the gas-phase charge inversion ion/ion reaction for the analysis Of BMPs and PGs. The reaction scheme details the ion selection of the singly deprotonated PG and BMP anion ($[M_{PG} –H]^-$ and $[M_{BMP} –H]^-$), which undergoes a charge inversion reaction with cation $[Mg(TTBT)_2]^{2+}$, to form $[M_{PG/BMP}\text{-}H+Mg^{2+}(TTBT)_2]^+$ and $[M_{PG/BMP}\text{-}H+Mg^{2+}(TTBT)]^+$ cationic complexes. CID of $[M_{PG}\text{-}H+Mg^{2+}(TTBT)]^+$ complex cation, yields structurally informative product ions indicating: $[M_{PG} – H + MgTTBT – sn1/sn2)]^+$, $[M_{PG} - H + MgTTBT – sn1/sn2 -C_3H_7O_3]^+$, $[sn1/sn2 – H + MgTTBT]^+$ and amongst other peaks. Ion-trap CID of $[M_{BMP} - H + Mg(TTBT)]^+$ resulted in single product ion $[M_{BMP} - H + MgTTBT – sn1/sn2 - C_3H_7O_3]^+$.

To distinguish constitutional isomers from its isomeric counterparts without the aid of chromatography and/or derivation techniques, the ion/ion reaction was employed. Charge inversion of intact PG/BMP anions via reaction with divalent metal complexes, such as $[Mg(TTBT)_2]^{2+}$, followed by CID enables the distinction between PLs classes. Further interrogation of fatty acyl allowed localization of carbon-carbon double bond. An illustration of this process allows distinction of PG/BMP isomer, shown in **Scheme 4.1**. In brief, $[M_{PG/BMP} - H]^-$ was mass-selected in Q1 and transferred to q2 for storage. Next, $[Mg(TTBT)_2]^{2+}$ (m/z 413.2), was mass-selected in Q1 and stored with the $[M - H]^-$ anions in q2, to allow ion/ion reaction to occur.

The consequential ion/ion reaction, caused in a charge-inverted complex $[M_{PG/BMP}-H+Mg^{2+}(TTBT)_2]^+$, where the FA chains complexed to the alkaline earth metal reagent, resulting two product ions: $[M_{PG} - H + Mg\ TTBT]^+$ and $[M_{PG} - H + (Mg(TTBT)_2]^+$ or $[M_{BMP} - H + Mg\ TTBT]^+$ and $[M_{BMP} - H + (Mg(TTBT)_2]^+$. In the case of PGs, ion-trap CID of $[M_{PG} - H + Mg\ TTBT]^+$ complex cation yields structurally informative product ions indicating: $[M_{PG} – H + MgTTTB – sn1/sn2]^+$, $[M_{PG} - H + Mg\ TTBT - sn1/sn2 -C_3H_7O_3]^+$, $[sn1/sn2 – H + Mg\ TTBT]^+$ amongst other fragments. Following the similar workflow, ion/ion reaction of BMP anion with $[Mg(TTBT)_2]^{2+}$ resulted in similar product spectra of PGs; $[M_{BMP} - H + Mg\ TTBT]^+$ and $[M_{BMP} - H + (Mg(TTBT)_2]^+$. Ion-trap CID of [BMP RR - H + Mg(TTBT)]$^+$ resulted in single product ion [BMP RR - H + Mg TTBT – sn1/sn2 - $C_3H_7O_3]^+$, shown in **Scheme 4.1**. MS^4 of [BMP RR - H + Mg TTBT – sn1/sn2) - $C_3H_7O_3]^+$ gave rise to [sn1/sn2 - H + Mg TTBT]$^+$, while MS^n of [sn1/sn2 - H + Mg TTBT]$^+$ allowed C=C localization.

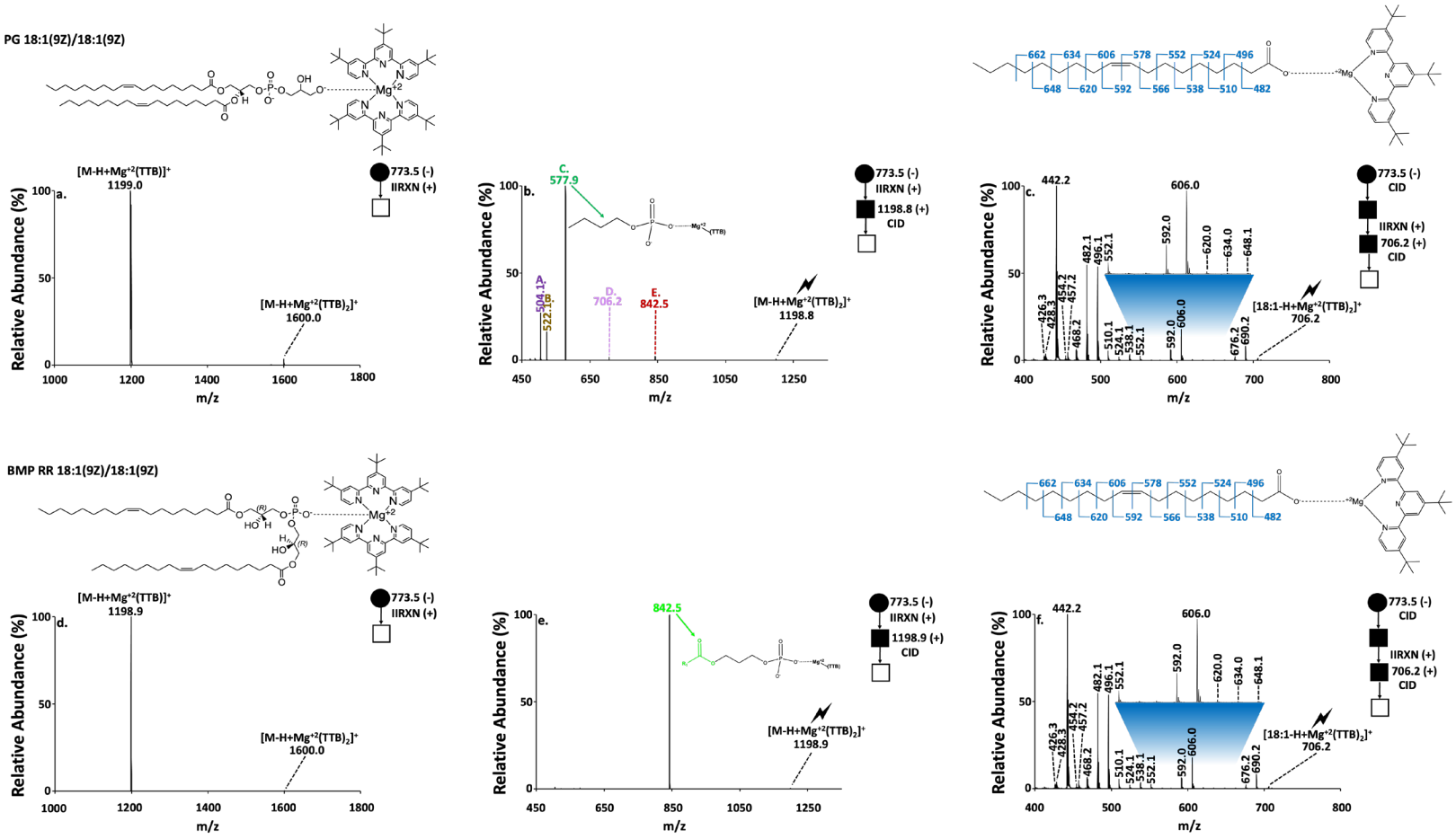

Figure 4.2 - Demonstration of the gas-phase charge inversion reaction for the analysis of PGs and BMPs. (a) Ion/ion reaction of PG 18:1(9Z)/18:1(9Z) with [Mg(TTTB)2]2+, yielding two dominating product ions: [MPG-H+Mg2+(TTTB)2]+ and [MPG-H+Mg2+(TTB)]+. (b) Ion trap CID of MPG-H+Mg2+(TTB)]+ yield fragment ion corresponding to head group and acyl chain ions. (c) CID of [18:1 – H + MgTTTB]+, yields the spectra pattern indicative of double bond location. (d) In a similar fashion, ion/ion reaction of BMP RR 18:1(9Z)/18:1(9Z) with [Mg(TTTB)2]2+, gave rise to two dominating product ions: [MBMP-H+Mg2+(TTTB)2]+ and [MBMP-H+Mg2+(TTTB)]+. (e) However, CID product spectra of MBMP-H+Mg2+(TTTB)]+ gave rise to only one ion, corresponding to the MBMP - H + MgTTTB - 18:1(9Z) - C3H7O3]+. (f) CID of [18:1 – H + MgTTTB]+ , yields the spectra pattern indicative of double bond location.

To demonstrate the utility of IIRXNs for the differentiation and detailed identification of BMP and PG isomers, we examined isomeric PG 18:1(9*Z*)/18:1(9*Z*) and BMP RR 18:1(9*Z*)/18:1(9*Z*), illustrated in **Figure 4.2**. In **Figure 4.2a and Figure 4.2d**., IIRXN of PG and BMP resulted in the same spectra. However, in **Figure 2b**., IIRXN between $[PG - H]^-$ anions and $[Mg(TTBT)_2]^{2+}$ dictations resulted in the formation of two product ions: $[PG - H + Mg\ TTBT]^+$ and $[PG - H + (Mg(TTBT)_2]^+$. CID of the $[PG – H + Mg\ TTBT]^+$ complex cation yields structurally informative product ions indicating: $[PG – H + MgTTBT - 18:1(9Z)]^+$ (m/z 916.63), $[PG - H + MgTTBT - 18:1(9Z) -C_3H_7O_3]^+$ (m/z 842.5), $[18:1 – H + MgTTBT]^+$ (m/z 706.2) including other product ions corresponding to the headgroup rearrangement, shown in **Figure 4.2b**. To determine the site(s) of unsaturation in the acyl chains, a secondary step of CID was employed. Specifically, the CID spectrum of $[18:1(9Z) - H + MgTTBT]^+$ generated an isomer-specific fragmentation pattern dictated by carbon-carbon double bond position (C=C) (**Figure 4.2c.).** To establish the effectiveness of IIRXN reaction for the discrimination of isomeric BMP and PG lipid molecular structures, BMP RR (18:1(9Z)/18:1(9Z)) anions were charged inverted in an identical manner with MgTTBT cation complex, **Figure 4.2d**. Resulting in two product ions: $[BMP\ RR - H + MgTTBT]^+$ and $[BMP\ RR - H + (Mg(TTBT)_2]^+$. Ion-trap CID of $[BMP\ RR - H + Mg(TTBT)]^+$ resulted in single product ion $[BMP\ RR - H + MgTTBT - 18:1(9Z) - C_3H_7O_3]^+$ (m/z 842.57) (**Figure 4.2e.**). Reisolation and CID of $[BMP\ RR - H + MgTTBT - 18:1(9Z) - C_3H_7O_3]^+$ gave rise to $[18:1(9Z) - H + MgTTBT]^+$ and an additional step of CID of $[18:1(9Z) - H + MgTTBT]^+$ permitted C=C localization, shown in **Figure 4.2f.**

Another example of the effectiveness of the charge inversion reaction to distinguish regioisomers species, **Figure S14.3(a).** PG 14:0/14:0 and **Figure S4.3(b)**. BMP SR 14:0/14:0, shown in Supporting Information, **Figure S4.3**. Briefly, ion trap CID of PG 14:0/14:0 resulted in $[PG – H + MgTTBT – 14:0]^+$ (m/z 789.4), $[14:0– H + MgTTBT]^+$ (m/z 653.2) product ions and other dominate ions corresponding to the headgroup rearrangement. While BMP SR 14:0/14:0 resulted in one peak corresponding to $[BMP\ SR - H + MgTTBT – 14:0 - C_3H_7O_3]^+$ (m/z) (shown in **Figure S4.3(a)**.) Additionally, isolation and CID of $BMP\ SR - H + MgTTBT – 14:0 - C_3H_7O_3]^+$, gave rise to $[14:0 - H + MgTTBT]^+$ and an additional step of CID of $[14:0 - H + MgTTBT]^+$, shown in **Figure S4.3(b)**. In total, the combination of IIRXN reactions and MS^n enables in-depth structural

identification and differentiation of PG and BMP isomers, including the assignment of C=C position(s). Notably, the developed gas-phase ion/ion strategy is capable of distinguishing BMP/PG isomers without the aid of synthetic standards.

4.5 Conclusion

We developed a novel approach for the differentiation and structural elucidation of intact regioisomers PGs and BMPs species. In the negative ion mode, PG and BMP isomers share identical mass spectra, making them hard to differentiate from each other. To account for that, this method incorporates the utility of the gas-phase ion/ion reaction with alkaline earth metal reagent and low energy CID for separation of isomeric species without the aid of chromatography or other derivation techniques. In the negative ion mode, PG and BMP isomers share identical mass spectra, making them hard to differentiate from each other. In the gas-phase, deprotonated FAs anion are transformed via the ion/ion reaction with doubly charged magnesium tri-tert-butyl-terpyridine reagent, to produce $[M_{PG/BMP}\text{-}H+Mg^{2+}(TTBT)_2]^+$ cationic complex. Ion trap CID of $[M_{PG/BMP}\text{-}H+Mg^{2+}(TTBT)]^+$ yield two product peaks, corresponding to the PG and BMP: $[M_{PG}$ - H + Mg TTBT$]^+$ and $[M_{PG}$ - H + $(Mg(TTBT)_2]^+$ or $[M_{BMP}$ - H + Mg TTBT$]^+$ and $[M_{BMP}$ - H + $(Mg(TTBT)_2]^+$. For PG, CID spectra of $[M_{PG}$ - H + Mg TTBT$]^+$ reveals structural peaks that indicative of the fatty acyl loss, loss of glycerol headgroup with fatty acyl, and other dominate peaks corresponding to the headgroup rearrangement. Ironically in the case of BMP, CID spectra only reveals the loss of the fatty acyl moieties. With further interrogation of fatty acyl will reveal the carbon-carbon double bond. This approach was established on standards but can be extended to bacterium anion generated in the gas-phase. Further studies will focus development of isomer quantitation to determine the fraction of isomer present in a biological sample. This approach could utilize different ratios of isomers PG 18:1(9Z)/18:1(9Z) and BMP RR 18:1(9Z)/18:1(9Z) (for example, 75:25. 25:75, 50:50, 60:40 and 40:60), to generate a measured value to measure against a corresponding m/z to determine the amount of isomer present in a given m/z.

4.6 References

(1) Dowhan, W. The Role of Phospholipids in Cell Function. In *Advances in Lipobiology*; Elsevier, 1997; Vol. 2, pp 79–107. https://doi.org/10.1016/S1874-5245(97)80006-7.

(2) Zhou, D.-Y.; Rakariyatham, K. Phospholipids. In *Encyclopedia of Food Chemistry*; Melton, L., Shahidi, F., Varelis, P., Eds.; Academic Press: Oxford, 2019; pp 546–549. https://doi.org/10.1016/B978-0-08-100596-5.22357-3.

(3) El-Bacha, T.; Torres, A. G. Phospholipids: Physiology. In *Encyclopedia of Food and Health*; Caballero, B., Finglas, P. M., Toldrá, F., Eds.; Academic Press: Oxford, 2016; pp 352–359. https://doi.org/10.1016/B978-0-12-384947-2.00540-7.

(4) Bogdanov, M.; Mileykovskaya, E.; Dowhan, W. Lipids in the Assembly of Membrane Proteins and Organization of Protein Supercomplexes: Implications for Lipid-Linked Disorders. In *Lipids in Health and Disease*; Quinn, P. J., Wang, X., Eds.; Subcellular Biochemistry; Springer Netherlands: Dordrecht, 2008; pp 197–239. https://doi.org/10.1007/978-1-4020-8831-5_8.

(5) Lee, A. G. The Effects of Lipids on Channel Function. *J. Biol.* **2009**, *8* (9), 86. https://doi.org/10.1186/jbiol178.

(6) Cadenas, C.; Vosbeck, S.; Hein, E.-M.; Hellwig, B.; Langer, A.; Hayen, H.; Franckenstein, D.; Büttner, B.; Hammad, S.; Marchan, R.; Hermes, M.; Selinski, S.; Rahnenführer, J.; Peksel, B.; Török, Z.; Vígh, L.; Hengstler, J. G. Glycerophospholipid Profile in Oncogene-Induced Senescence. *Biochim. Biophys. Acta BBA - Mol. Cell Biol. Lipids* **2012**, *1821* (9), 1256–1268. https://doi.org/10.1016/j.bbalip.2011.11.008.

(7) Vigh, L.; Escribá, P. V.; Sonnleitner, A.; Sonnleitner, M.; Piotto, S.; Maresca, B.; Horváth, I.; Harwood, J. L. The Significance of Lipid Composition for Membrane Activity: New Concepts and Ways of Assessing Function. *Prog. Lipid Res.* **2005**, *44* (5), 303–344. https://doi.org/10.1016/j.plipres.2005.08.001.

(8) Scherer, M.; Schmitz, G. Metabolism, Function and Mass Spectrometric Analysis of Bis(Monoacylglycero)Phosphate and Cardiolipin. *Chem. Phys. Lipids* **2011**, *164* (6), 556–562. https://doi.org/10.1016/j.chemphyslip.2011.06.007.

(9) Uphoff, A.; Hermansson, M.; Haimi, P.; Somerharju, P. Chapter 11 - Analysis of Complex Lipidomes. In *Medical Applications of Mass Spectrometry*; Vékey, K., Telekes, A., Vertes, A., Eds.; Elsevier: Amsterdam, 2008; pp 223–249. https://doi.org/10.1016/B978-044451980-1.50013-6.

(10) Ridgway, N. D. Chapter 7 - Phospholipid Synthesis in Mammalian Cells. In *Biochemistry of Lipids, Lipoproteins and Membranes (Sixth Edition)*; Ridgway, N. D., McLeod, R. S., Eds.; Elsevier: Boston, 2016; pp 209–236. https://doi.org/10.1016/B978-0-444-63438-2.00007-9.

(11) Kobayashi, K.; Endo, K.; Wada, H. Specific Distribution of Phosphatidylglycerol to Photosystem Complexes in the Thylakoid Membrane. *Front. Plant Sci.* **2017**, *8*. https://doi.org/10.3389/fpls.2017.01991.

(12) Geiger, O.; Sohlenkamp, C.; López-Lara, I. M. Formation of Bacterial Glycerol-Based Membrane Lipids: Pathways, Enzymes, and Reactions. In *Biogenesis of Fatty Acids, Lipids and Membranes*; Geiger, O., Ed.; Handbook of Hydrocarbon and Lipid Microbiology; Springer International Publishing: Cham, 2019; pp 87–107. https://doi.org/10.1007/978-3-319-50430-8_8.

(13) Jorasch, P.; Warnecke, D. C.; Lindner, B.; Zähringer, U.; Heinz, E. Novel Processive and Nonprocessive Glycosyltransferases from Staphylococcus Aureus and Arabidopsis Thaliana Synthesize Glycoglycerolipids, Glycophospholipids, Glycosphingolipids and Glycosylsterols. *Eur. J. Biochem.* **2000**, *267* (12), 3770–3783. https://doi.org/10.1046/j.1432-1327.2000.01414.x.

(14) Sych, T.; Levental, K. R.; Sezgin, E. Lipid-Protein Interactions in Plasma Membrane Organization and Function. *Annu. Rev. Biophys.* **2022**, *51*, 135–156. https://doi.org/10.1146/annurev-biophys-090721-072718.

(15) Schulze, H.; Sandhoff, K. Lysosomal Lipid Storage Diseases. *Cold Spring Harb. Perspect. Biol.* **2011**, *3* (6), a004804. https://doi.org/10.1101/cshperspect.a004804.

(16) Meikle, P. J.; Duplock, S.; Blacklock, D.; Whitfield, P. D.; Macintosh, G.; Hopwood, J. J.; Fuller, M. Effect of Lysosomal Storage on Bis(Monoacylglycero)Phosphate. *Biochem. J.* **2008**, *411* (1), 71–78. https://doi.org/10.1042/BJ20071043.

(17) Kolter, T.; Sandhoff, K. PRINCIPLES OF LYSOSOMAL MEMBRANE DIGESTION: Stimulation of Sphingolipid Degradation by Sphingolipid Activator Proteins and Anionic Lysosomal Lipids. *Annu. Rev. Cell Dev. Biol.* **2005**, *21* (1), 81–103. https://doi.org/10.1146/annurev.cellbio.21.122303.120013.

(18) *Transacylase and Phospholipases in the Synthesis of Bis(monoacylglycero)phosphate | Biochemistry*. https://pubs.acs.org/doi/full/10.1021/bi961164o (accessed 2023-04-20).

(19) Chevallier, J.; Sakai, N.; Robert, F.; Kobayashi, T.; Gruenberg, J.; Matile, S. Rapid Access to Synthetic Lysobisphosphatidic Acids Using PIII Chemistry. *Org. Lett.* **2000**, *2* (13), 1859–1861. https://doi.org/10.1021/ol0059246.

(20) Matsuo, H.; Chevallier, J.; Mayran, N.; Le Blanc, I.; Ferguson, C.; Fauré, J.; Blanc, N. S.; Matile, S.; Dubochet, J.; Sadoul, R.; Parton, R. G.; Vilbois, F.; Gruenberg, J. Role of LBPA and Alix in Multivesicular Liposome Formation and Endosome Organization. *Science* **2004**, *303* (5657), 531–534. https://doi.org/10.1126/science.1092425.

(21) Chevallier, J.; Chamoun, Z.; Jiang, G.; Prestwich, G.; Sakai, N.; Matile, S.; Parton, R. G.; Gruenberg, J. Lysobisphosphatidic Acid Controls Endosomal Cholesterol Levels *. *J. Biol. Chem.* **2008**, *283* (41), 27871–27880. https://doi.org/10.1074/jbc.M801463200.

(22) Hullin-Matsuda, F.; Taguchi, T.; Greimel, P.; Kobayashi, T. Lipid Compartmentalization in the Endosome System. *Semin. Cell Dev. Biol.* **2014**, *31*, 48–56. https://doi.org/10.1016/j.semcdb.2014.04.010.

(23) Nakashima, S.; Nagata, K.; Banno, Y.; Sakiyama, T.; Kitagawa, T.; Miyawaki, S.; Nozawa, Y. A Mouse Model for Niemann-Pick Disease: Phospholipid Class and Fatty Acid Composition of Various Tissues. *J. Lipid Res.* **1984**, *25* (3), 219–227. https://doi.org/10.1016/S0022-2275(20)37817-2.

(24) Sleat, D. E.; Wiseman, J. A.; El-Banna, M.; Price, S. M.; Verot, L.; Shen, M. M.; Tint, G. S.; Vanier, M. T.; Walkley, S. U.; Lobel, P. Genetic Evidence for Nonredundant Functional Cooperativity between NPC1 and NPC2 in Lipid Transport. *Proc. Natl. Acad. Sci.* **2004**, *101* (16), 5886–5891. https://doi.org/10.1073/pnas.0308456101.

(25) Bouvier, J.; Zemski Berry, K. A.; Hullin-Matsuda, F.; Makino, A.; Michaud, S.; Geloën, A.; Murphy, R. C.; Kobayashi, T.; Lagarde, M.; Delton-Vandenbroucke, I. Selective Decrease of Bis(Monoacylglycero)Phosphate Content in Macrophages by High Supplementation with Docosahexaenoic Acids. *J. Lipid Res.* **2009**, *50* (2), 243–255. https://doi.org/10.1194/jlr.M800300-JLR200.

(26) Hullin-Matsuda, F.; Kawasaki, K.; Delton-Vandenbroucke, I.; Xu, Y.; Nishijima, M.; Lagarde, M.; Schlame, M.; Kobayashi, T. De Novo Biosynthesis of the Late Endosome Lipid, Bis(Monoacylglycero)Phosphates. *J. Lipid Res.* **2007**, *48* (9), 1997–2008. https://doi.org/10.1194/jlr.M700154-JLR200.

(27) *PII: 0005-2760(92)90281-Y | Elsevier Enhanced Reader*. https://doi.org/10.1016/0005-2760(92)90281-Y.

(28) Vosse, C.; Wienken, C.; Cadenas, C.; Hayen, H. Separation and Identification of Phospholipids by Hydrophilic Interaction Liquid Chromatography Coupled to Tandem High Resolution Mass Spectrometry with Focus on Isomeric Phosphatidylglycerol and Bis(Monoacylglycero)Phosphate. *J. Chromatogr. A* **2018**, *1565*, 105–113. https://doi.org/10.1016/j.chroma.2018.06.039.

(29) Baronas, E. T.; Lee, J.-W.; Alden, C.; Hsieh, F. Y. Biomarkers to Monitor Drug-Induced Phospholipidosis. *Toxicol. Appl. Pharmacol.* **2007**, *218* (1), 72–78. https://doi.org/10.1016/j.taap.2006.10.015.

(30) Scherer, M.; Schmitz, G.; Liebisch, G. Simultaneous Quantification of Cardiolipin, Bis(Monoacylglycero)Phosphate and Their Precursors by Hydrophilic Interaction LC−MS/MS Including Correction of Isotopic Overlap. *Anal. Chem.* **2010**, *82* (21), 8794–8799. https://doi.org/10.1021/ac1021826.

(31) Lecommandeur, E.; Baker, D.; Cox, T. M.; Nicholls, A. W.; Griffin, J. L. Alterations in Endo-Lysosomal Function Induce Similar Hepatic Lipid Profiles in Rodent Models of Drug-Induced Phospholipidosis and Sandhoff Disease. *J. Lipid Res.* **2017**, *58* (7), 1306–1314. https://doi.org/10.1194/jlr.M073395.

(32) Lee, J. C.; Yang, J. S.; Moon, M. H. Simultaneous Relative Quantification of Various Polyglycerophospholipids with Isotope-Labeled Methylation by Nanoflow Ultrahigh Performance Liquid Chromatography-Tandem Mass Spectrometry. *Anal. Chem.* **2019**, *91* (10), 6716–6723. https://doi.org/10.1021/acs.analchem.9b00800.

(33) Kliman, M.; May, J. C.; McLean, J. A. Lipid Analysis and Lipidomics by Structurally Selective Ion Mobility-Mass Spectrometry. *Biochim. Biophys. Acta BBA - Mol. Cell Biol. Lipids* **2011**, *1811* (11), 935–945. https://doi.org/10.1016/j.bbalip.2011.05.016.

(34) Damen, C. W. N.; Isaac, G.; Langridge, J.; Hankemeier, T.; Vreeken, R. J. Enhanced Lipid Isomer Separation in Human Plasma Using Reversed-Phase UPLC with Ion-Mobility/High-Resolution MS Detection [S]. *J. Lipid Res.* **2014**, *55* (8), 1772–1783. https://doi.org/10.1194/jlr.D047795.

(35) Showalter, M. R.; Berg, A. L.; Nagourney, A.; Heil, H.; Carraway, K. L.; Fiehn, O. The Emerging and Diverse Roles of Bis(Monoacylglycero) Phosphate Lipids in Cellular Physiology and Disease. *Int. J. Mol. Sci.* **2020**, *21* (21), 8067. https://doi.org/10.3390/ijms21218067.

(36) Cai, T.; Shu, Q.; Hou, J.; Liu, P.; Niu, L.; Guo, X.; Liu, C. C.; Yang, F. Profiling and Relative Quantitation of Phosphoinositides by Multiple Precursor Ion Scanning Based on Phosphate Methylation and Isotopic Labeling. *Anal. Chem.* **2015**, *87* (1), 513–521. https://doi.org/10.1021/ac503224j.

(37) Wang, M.; Wang, C.; Han, R. H.; Han, X. Novel Advances in Shotgun Lipidomics for Biology and Medicine. *Prog. Lipid Res.* **2016**, *61*, 83–108. https://doi.org/10.1016/j.plipres.2015.12.002.

(38) Kielkowska, A.; Niewczas, I.; Anderson, K. E.; Durrant, T. N.; Clark, J.; Stephens, L. R.; Hawkins, P. T. A New Approach to Measuring Phosphoinositides in Cells by Mass Spectrometry. *Adv. Biol. Regul.* **2014**, *54*, 131–141. https://doi.org/10.1016/j.jbior.2013.09.001.

(39) Hankin, J. A.; Murphy, R. C.; Barkley, R. M.; Gijón, M. A. Ion Mobility and Tandem Mass Spectrometry of Phosphatidylglycerol and Bis(Monoacylglycerol)Phosphate (BMP). *Int. J. Mass Spectrom.* **2015**, *378*, 255–263. https://doi.org/10.1016/j.ijms.2014.08.026.

(40) Hsu, F.-F.; Turk, J.; Williams, T. D.; Welti, R. Electrospray Ionization Multiple Stage Quadrupole Ion-Trap and Tandem Quadrupole Mass Spectrometric Studies on Phosphatidylglycerol from Arabidopsis Leaves. *J. Am. Soc. Mass Spectrom.* **2007**, *18* (4), 783–790. https://doi.org/10.1016/j.jasms.2006.12.012.

(41) Duffin, K.; Obukowicz, M.; Raz, A.; Shieh, J. J. Electrospray/Tandem Mass Spectrometry for Quantitative Analysis of Lipid Remodeling in Essential Fatty Acid Deficient Mice. *Anal. Biochem.* **2000**, *279* (2), 179–188. https://doi.org/10.1006/abio.1999.4452.

(42) Shenault, D. S. M.; McLuckey, S. A.; Franklin, E. T. Localization of Cyclopropyl Groups and Alkenes Within Glycerophospholipids Using Gas-Phase Ion/Ion Chemistry. *J. Mass Spectrom. n/a* (n/a), e4913. https://doi.org/10.1002/jms.4913.

(43) Randolph, C. E.; Foreman, D. J.; Blanksby, S. J.; McLuckey, S. A. Generating Fatty Acid Profiles in the Gas Phase: Fatty Acid Identification and Relative Quantitation Using Ion/Ion Charge Inversion Chemistry. *Anal. Chem.* **2019**, *91* (14), 9032–9040. https://doi.org/10.1021/acs.analchem.9b01333.

(44) Randolph, C. E.; Shenault, D. M.; Blanksby, S. J.; McLuckey, S. A. Structural Elucidation of Ether Glycerophospholipids Using Gas-Phase Ion/Ion Charge Inversion Chemistry. *J. Am. Soc. Mass Spectrom.* **2020**, *31* (5), 1093–1103. https://doi.org/10.1021/jasms.0c00025.

(45) Randolph, C. E.; Blanksby, S. J.; McLuckey, S. A. Toward Complete Structure Elucidation of Glycerophospholipids in the Gas Phase through Charge Inversion Ion/Ion Chemistry. *Anal. Chem.* **2020**, *92* (1), 1219–1227. https://doi.org/10.1021/acs.analchem.9b04376.

(46) Randolph, C. E.; Shenault, D. M.; Blanksby, S. J.; McLuckey, S. A. Localization of Carbon–Carbon Double Bond and Cyclopropane Sites in Cardiolipins via Gas-Phase Charge Inversion Reactions. *J. Am. Soc. Mass Spectrom.* **2021**, *32* (2), 455–464. https://doi.org/10.1021/jasms.0c00348.

(47) Randolph, C. E.; Beveridge, C. H.; Iyer, S.; Blanksby, S. J.; McLuckey, S. A.; Chopra, G. Identification of Monomethyl Branched-Chain Lipids by a Combination of Liquid Chromatography Tandem Mass Spectrometry and Charge-Switching Chemistries. *J. Am. Soc. Mass Spectrom.* **2022**, *33* (11), 2156–2164. https://doi.org/10.1021/jasms.2c00225.

(48) Liebisch, G.; Vizcaíno, J. A.; Köfeler, H.; Trötzmüller, M.; Griffiths, W. J.; Schmitz, G.; Spener, F.; Wakelam, M. J. O. Shorthand Notation for Lipid Structures Derived from Mass Spectrometry. *J. Lipid Res.* **2013**, *54* (6), 1523–1530. https://doi.org/10.1194/jlr.M033506.

(49) Matsuzawa, Y.; Hostetler, K. Y. Degradation of Bis(Monoacylglycero)Phosphate by an Acid Phosphodiesterase in Rat Liver Lysosomes. *J. Biol. Chem.* **1979**, *254* (13), 5997–6001. https://doi.org/10.1016/S0021-9258(18)50510-X.

4.7 Supporting Information

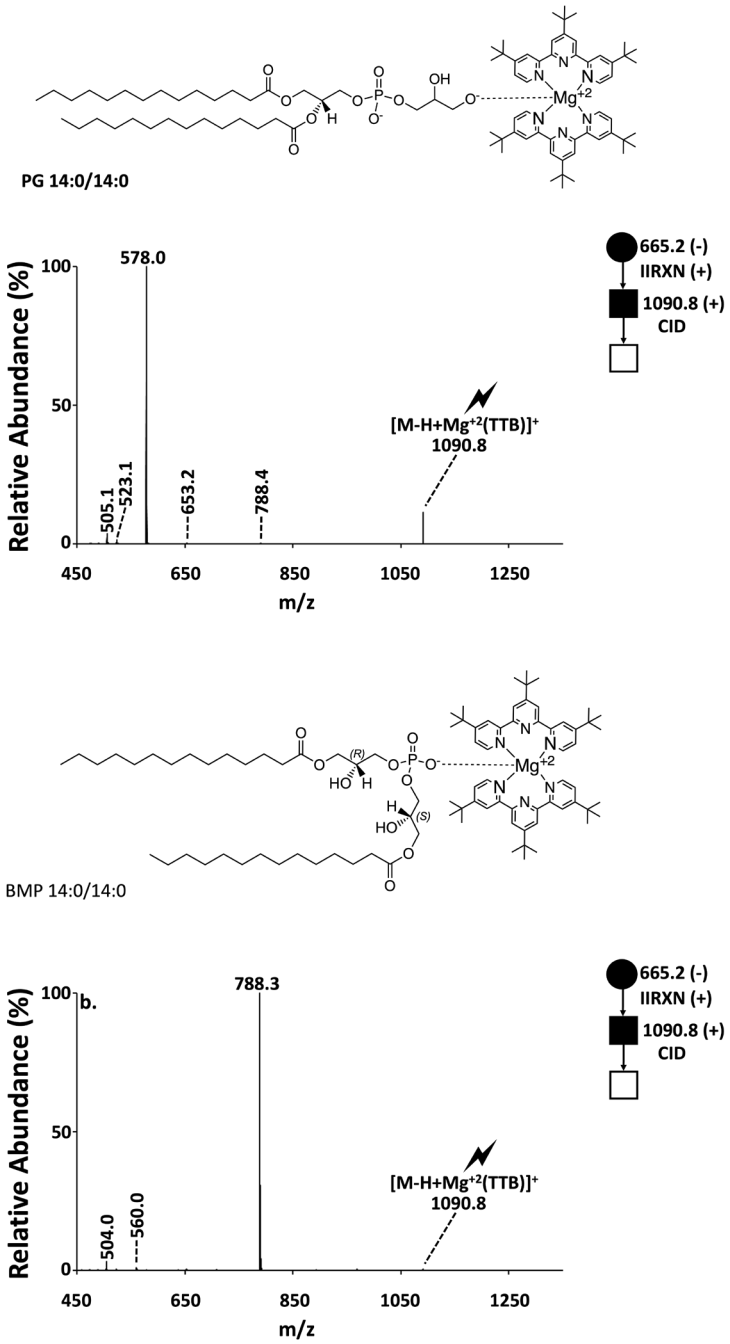

Figure 4.3 - Demonstration of the gas-phase charge inversion reaction for the analysis of PGs and BMPs. (a) Ion/ion reaction of cationic complex generated from ion/ion reaction of PG 14:0/14:0 with $[Mg(TTBT)_2]^{2+}$, to form $[M_{PG}\text{-}H+Mg^{2+}(\ TTBT)]^{+}$. Ion trap CID of $[M_{PG}\text{-}H+Mg^{2+}(\ TTBT)]^{+}$ yield product ions indicative of headgroup rearrangement, fatty acyl loss and acyl loss of glycerol backbone. (b) Ion trap CID of $M_{BMP}\text{-}H+Mg^{2+}(TTBT)]^{+}$ formed from the charge inversion reaction with metal alkaline earth metal complex, on single peak corresponding to the loss of a fatty acyl moiety.

CHAPTER 5. OH LIPIDS. THE PLACES WE HAVE GONE

As I close this chapter of lipid, I am reminded of the question posed to me by Dr. Graham Cooks during recruitment weekend; “how would you use mass spectrometry to solve this problem”. I believe this same question has boggled the mind of many scientists in the world of mass spectrometry and in the Lipidomics community. With the invention of the first mass spectrometer by Francis Aston and J.J. Thompson in the late 1912[123], this powerful analytical tool has changed the landscape of how we probe and detect lipids in a biological matrix.

On my quest to answer the question; I am reminded of the Dr. Seuss book, “Oh the places you'll go”. The childhood story that unravelled over the course my graduate career at Purdue University. Starting at page one with my introduction to the world of Lipidomics. It wasn’t at Scott McLuckey group poster but during my first session on the Sciex 4000 Triple Quadrupole in the wet lab. Watching how capillary tips were loaded with lipid and reagents solvents to the interface of the orifice of the mass spectrometer. Turning on duo pulsed nano-electrospray ionization (nESI) of positive and negative ions generate in the gas-phase. The mass analyzer ionizes the solvents into charge droplets to be mass selected during transit to a high-pressure collision cell, to undergo modifications before detection. Looking at the ions being formed and transferred during different segments, while developing spectrums, I was hooked. Like the lipid, I was generated and transformed into a new version of myself and detected. Leaving instrument time, the journey has started, and I am on my way.

In several ways, lipids have allowed me to surpass my limited understanding what a lipid is. Lipids are extraordinary molecules found in all living organisms, with so many different classes and subclasses of species, I am overwhelmed with the different roles and function that lipids process, but the question is still posed. How have I added to this sector of research? Over the course of the dissertation, I have explored new ways to evaluate and characterize various subclass of lipids in and out of a biological matrix. With the aid of the ion/ion reaction, I was able to add to a well-known technique, for the analysis of lipids, shown in **Chapters 2-4**. The utilization of organic and biochemistry to untangle surface and chemical compositions in the gas-phase. The incorporation of prior and future knowledge has made me successful in the new field of research. Like the little boy in the book, I was on a journey of uncertainty and creativity. I have arrived to the new me. Thank you, lipid, for open my eyes to a new horizon of science. For crafting technical skills and

empowering me to present you. Thank you for taking me on a journey that I will never forget. May I never forget the lessons taught and giving. I promise to take you to the next segment of research.

5.1 Reference

(1) *The Nobel Prize in Chemistry 1922*. NobelPrize.org. https://www.nobelprize.org/prizes/chemistry/1922/summary/ (accessed 2023-06-22).

(2) Thomson, J. J. XLVII. *On Rays of Positive Electricity*. *Lond. Edinb. Dublin Philos. Mag. J. Sci.* **1907**, *13* (77), 561–575. https://doi.org/10.1080/14786440709463633.

(3) Thomson, J. J. *Rays of Positive Electricity and Their Application to Chemical Analyses*; Longmans, Green and Company, 1921.

APPENDIX

2, 2':6', 2" terpyridine (terpy) (Tempo-Terpy) was synthesized by Dr. Jinshan Gao laboratory.

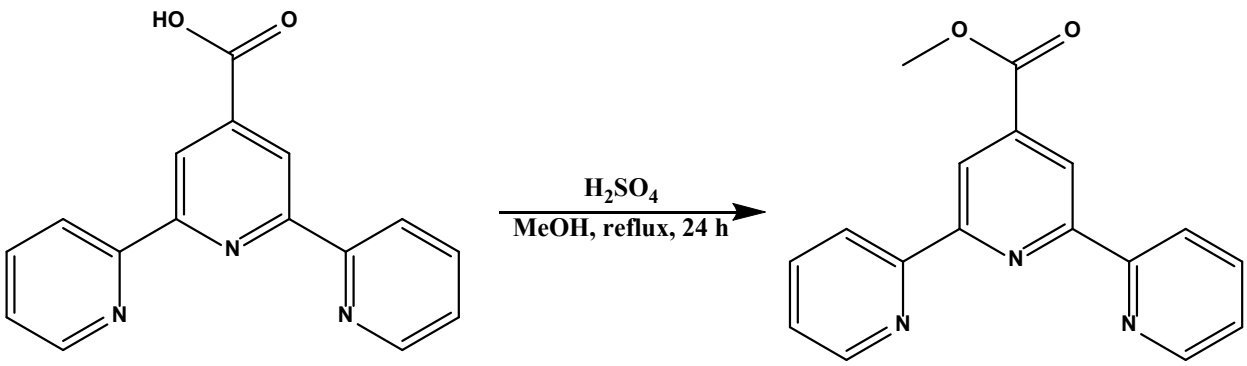

4′-Carboxylic acid-2,2′:6′,2″-terpyridine esterified to 4′-Methoxycarbonyl-2,2′:6′,2″-terpyridine.

1. Glassware was oven-dried and flame-dried prior to reaction.
2. 300 mg of Starting material suspended in 100-mL of HPLC-grade Methanol.
3. Sparged with argon for 15 minutes
4. Dropwise addition of 4 mL of concentrated sulfuric acid.
5. Stirred and refluxed for 24 hours.

Workup:

1. Reaction was cooled to room temperature and adjusted to pH 6-7 with 2M KOH and saturated sodium bicarbonate solution.
2. Solvent removed in vacuo.
3. Redissolved in ethyl acetate and washed thrice with 19.2 Mohm water.
4. Solvent removed and product isolated as white solid. 98.6% yield.

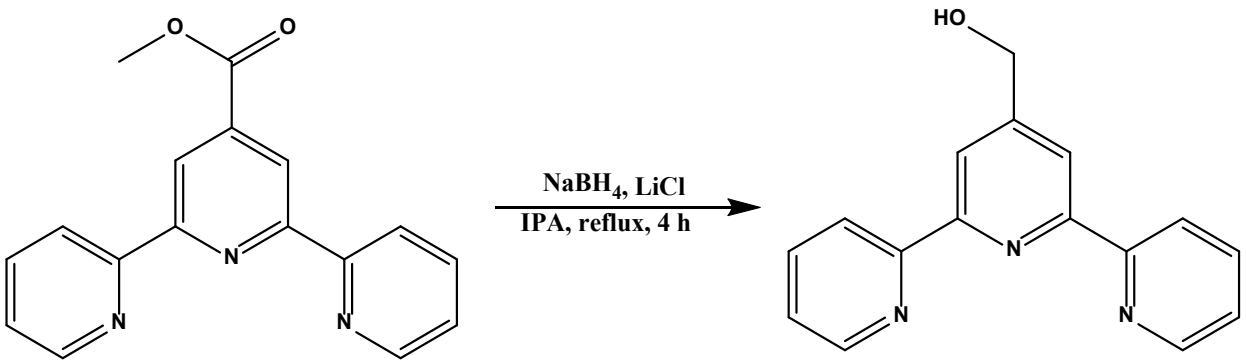

4′-Methoxycarbonyl-2,2′:6′,2″-terpyridine reduced to 4′-Methanol-2,2′:6′,2″-terpyridine.

1. Glassware was oven-dried and flame-dried prior to reaction.
2. Starting material dispersed in HPLC-grade Isopropanol.
3. Argon sparged for 15 minutes.
4. Sodium borohydride and lithium chloride in 3 times molar excess to the starting material added to reaction vessel.
5. Reflux while stirring for 4 hours.

Workup:

1. Allowed to reach room temperature.
2. Solvent removed in Vacuo.
3. Reconstituted in DCM and washed thrice with 18.2 Mohm water.
4. Dried over anhydrous sodium sulfate.
5. Solvent removed in Vacuo and product isolated as white solid. 95.6% yield.

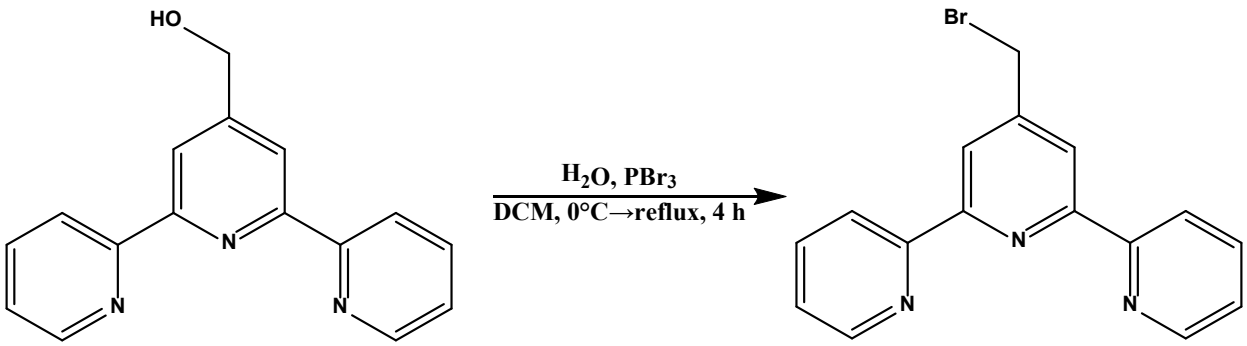

4′-Methanol-2,2′:6′,2″-terpyridine brominated to 4′-bromo-2,2′:6′,2″-terpyridine.

1. Starting material was switched between argon and vacuum thrice and left under argon (flask 1).
2. Separate flask (flask 2), oven and flame dried, contains 10mL of HPLC grade dichloromethane and twice as many moles of water as there are starting material in flask 1 (37 μL in this case).
3. Flask 2 was brought down to 0°C in ice bath while under vigorous stirring.
4. Phosphorous tribromide is added to flask 2 (equimolar to water, 2x moles of starting material).
5. The starting material is dissolved in flask 1 with dichloromethane and transferred to flask 2 in a dropwise fashion.
6. Flask 2 is allowed to reach room temperature before being refluxed for 4 hours while stirring.

Workup:

1. Allowed to reach room temperature.
2. pH adjusted to 7 with saturated sodium bicarbonate solution.
3. The organic layer was separated, and aqueous layer subjected to two extractions with DCM.
4. The organic layer was dried over anhydrous sodium sulfate.
5. Solvent removed in vacuo to isolate a pale brown solid.

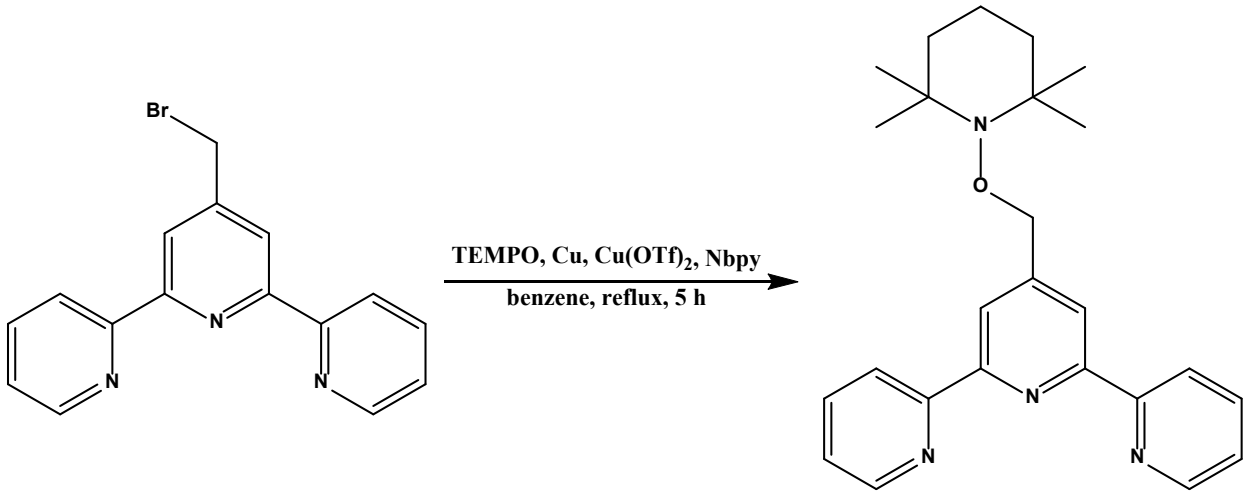

4′-bromo-2,2′:6′,2″-terpyridine to 4’-(2,2,6,6-Tetramethylpiperidine 1-oxy)-2,2′:6′,2″-Terpyridine.

Glassware oven and flame dried.

1. Starting Material switched between vacuum and argon thrice, and left under argon.
2. TEMPO, copper, copper(II) trifluoromethanesulfonate, and 4,4′-Dinonyl-2,2′-dipyridyl were added to the reaction flask.
3. The molar ratios are as follows:
4. Starting material : TEMPO : Cu : $Cu(Otf)_2$: Nbpy = 1 : 1.2 : 1.2 : 0.1 : 0.4
5. Reaction flask if switched between vacuum and argon thrice, then left under argon.
6. All reactants were dissolved or suspended in anhydrous benzene.
7. Refluxed while stirring for 5 hours.

Workup

1. Mixture was allowed to reach room temperature.
2. The mixture was filtered through a short pad of silica.
3. The organic layer was rinsed with saturated ammonium chloride (NH_4Cl), 1 M ammonium hydroxide (NH_4OH), and saturated sodium chloride solution.
4. Organic layer was dried over sodium sulfate.
5. The product was isolated via flash chromatography, using a 12g silica gel column. The mobile phase increased from 100% hexane to 70% ethyl acetate in a stepwise manner over the course of 70 minutes.

6. Fractions containing product were confirmed via MS and dried to isolate the product as a white solid.

VITA

EDUCATION

Ph.D. Candidate in Chemistry **2023**

Purdue University

B.S.A in Chemistry **2016**

Chicago State University

B.S.A in Environmental Science **2014**

Illinois State University

A.A.S in Culinary Arts and Hospitality Management **2012**

Washburne Culinary Institute

RESEARCH EXPERIENCE

Purdue University **2018-2023**

Thesis title: Utilizing Gas-Phase Ion/Ion Reactions for Localization of Cyclopropyl and Methyl Branched Fatty Acids using Alkaline Earth Metal Complexes

Developed a novel gas-phase charge inversion ion/ion reaction in conjunction with activation and fragmentation to identify cyclopropane and double-bond sites in glycerophospholipids (GPLs). This work enables the characterization of GPLs species at the headgroup, and fatty acyl sum compositional levels leaving the location(s) of carbon-carbon double bond and cyclopropane ring.

Established approach couples' gas-phase ion/ion chemistry to charge invert branched chain fatty acids (BCFA) anions, which are further interrogate with radical directed dissociation (RDD) cation to determine the site of branching. This work allows the use of collaboration from other groups and new methodologies to determine the distinction of BCFA in comparison to the straight chain isomer. As the lead investigator, this project brought many challenges and new training methods to educate younger students on the new techniques on the characterization and quantitative analysis of lipid isomers with unique branching moieties.

Chicago State University **2014-2017**

Undergraduate proposal title: A Comparison of the Organic Composition and Morphological Structure of Prosthetic and Natural Human Hair Fibers

Revolutionized and developed innovative schemes to investigate the composition and morphological structure of synthetic versus human hair. Structural elucidation of keratin proteins from known human hair samples, observed cuticle and medulla formations that are indicative to humans.

Characterized samples using nuclear magnetic resonance (NMR), Ultraviolet-Visible Spectrometry (UV-VIS), Scanning Electron Microscopic (SEM) and Inverted Microscopic gave rise to qualitative and quantitative analysis to determine the concentration and known structures to govern counterfeit products sold as human hair.

Undergraduate Research Experience: Training in Interdisciplinary Laboratory Techniques (TILT)

Conducted various comprehensive experiments to develop laboratory techniques in the areas of Chemistry, Physics and Biology.

Trained on various equipment found in laboratories, such as: Extraction and isolation techniques of natural products, Polymerase Chain Reaction (PCR), Isolation of DNA from cells, Microscopy techniques, IR/NMR techniques, Gas chromatography (GC), High-performance liquid chromatography (HPLC), UV/VIS Spectrophotometry and Fluorometry, Growing cells in culture, Protein analysis, Organic synthesis, and Research ethics and responsible conduct of research.

Center of STEM Education and Research: REU Experience

Designed environmental research projects for undergraduate students to develop research skills from low poverty sectors. Identifying unique challenges that affects the plants and water supply within the University Prairie Garden. Forming hypothesis and building teams to conduct series of test, using extraction and NMR techniques to determine inmediation protocols to save native plants.

PUBLICATIONS

Shenault, D. S. M., McLuckey, S. A., & Franklin, E. T. (2023). Localization of cyclopropyl groups and alkenes within glycerophospholipids using gas-phase ion/ion chemistry. Journal of Mass Spectrometry, 58(4), e4913.

Randolph, C. E., Shenault, D. S. M., Blanksby, S. J., & McLuckey, S. A. (2020). Localization of Carbon–Carbon Double Bond and Cyclopropane Sites in Cardiolipins via Gas-Phase Charge Inversion Reactions. Journal of the American Society for Mass Spectrometry, 32(2), 455-464.

Randolph, C. E.; Shenault, D. M.; Blanksby, S. J.; McLuckey, S. A. Structural Elucidation of Ether Glycerophospholipids Using Gas-Phase Ion/Ion Charge Inversion Chemistry. Journal of the American Society of Mass Spectrometry. 2020. https://doi.org/10.1021/jasms.0c00025.

PRESENTATIONS

(7) Shenault, D., Nsiah, S., Randolph, C., and McLuckey, S., *"Gas-Phase Ion/Ion Strategy for the Differentiation of Isomeric Bis(monoacylglycero)phosphate and Phosphatidylglycerol Species by Shotgun Lipidomics".* American Society of Mass Spectrometry (ASMS), Houston, Texas Convention Center, June 2023

(6) Shenault, D., Fabijanczuk, K., Murtada, R., Finn, S., Gao, J. and McLuckey, S., *"Localization of Methyl Branching Sites on Fatty Acids by Combining Radical Directed Dissociation and Gas-Phase Ion/Ion Chemistry".* National Organization for the Professional Advancement of Black Chemists and Chemical Engineers (NOBCChE), The Rosen Shingle Creek. Orlando, Florida, October 2022

(5) Shenault, D., Fabijanczuk, K., Murtada, R., Finn, S., Gao, J. and McLuckey, S., *"Localization of Methyl Branching Sites on Fatty Acids by Combining Radical Directed Dissociation and Gas-Phase Ion/Ion Chemistry".* American Society of Mass Spectrometry (ASMS), Minneapolis, Minnesota Convention Center, June 2022

(4) Shenault, D., McLuckey, S. and Franklin, E., "*Cyclopropyl Glycerophospholipid Distinction Using Gas-Phase Ion/Ion Chemistry".* ACT-SO Teen Program, Argonne National Laboratory, January 2022

(3) Shenault, D., McLuckey, S. and Franklin, E., "*Cyclopropyl Glycerophospholipid Distinction Using Gas-Phase Ion/Ion Chemistry".* American Society of Mass Spectrometry (ASMS), Philadelphia, Pennsylvania Conference Center, October 2021

(2). Shenault, D. and Goss, V., *"A Comparison of the Organic Composition and Morphological Structure of Prosthetic and Natural Human Hair Fibers"*. Undergraduate Thesis Presentation, Chicago State University, November 2016.

(1) Shenault, D.; Byrns, G., *"Heritage Health Emergency Control Policy"*. REU Experience, Illinois State University, July 2014.

TEACHING EXPERIENCE

Teaching Assistant (General Chemistry 1 & 2) 2018-2020

Purdue University/Department of Chemistry, Lafayette IN

Created/presented lectures and answered questions to ensure student understanding of laboratory experiments while ensuring lab safety by instructing students on proper safety procedures and being vigilant while monitoring students. Evaluating and developing new methods to be a better teacher while participating in weekly teaching assistant meeting to provide feedback on methods use and communicate students' progress.

Student Coordinator **2017-2018**

Chicago State University/Center of STEM Education and Research, Chicago, IL

Facilitated STEM research workshops for college students developing platform/presentation skills. Worked in collaboration with CSU Administration providing secondary education students college experience with the intent to create a retention plan.

Served as a Business Administrator processing vendor invoices, sub-contracts with surround universities, and purchase orders chemical and technical companies.

EXTRA-CURRICULAR ACTIVITIES

Division of Diversity and Inclusion (DTA) – Outreach Board Member 2018-2024

Organized, trained and established Big 10 University liaison to draft minority students into Higher Education STEM related programs.

National Organization for the Professional Advancement of Black Chemists and Chemical Engineers (NOBCChE) **– Purdue University Graduate Chapter – Overseer**

Supervising all student organization meetings; overseeing the process of student organization event planning and securing funding for events and community engagements.

Iota Sigma Pi – Outreach Committee Board Member 2019-2020

Identified and created strategic plans for community projects, member gathering and/or socials, while developing experimental design and framework for national chemistry week across the Tippecanoe County.

American Chemical Society and NOBCChE CSU Chapter - President 2015-2017

Supervising all student organization meetings and increasing student engagement

VOLUNTEERISM

HeadsUP Program, West-Lafayette & Lafayette Locations, Program Site-Director 2019-2024

Overseeing preservice teacher volunteers and reporting while training volunteers in culturally responsive homework help. Providing K-12 students with homework help and academic skill advancement while rewarding students for positive behavior and challenging students to improve maladaptive behaviors

Developed seminars to train parents on “how to in vision and execute goals and pertaining to self, family, and social dynamics”.

Breakthrough Urban Ministries, The Way Christian Ministries 2012-2018

Designed menus and execute meals for homeless shelter called Breakthrough Urban Ministries through Way Christian Ministries.

Academic Awards & Honors:

National Honor Society for Woman in Chemistry - Iota Sigma Pi. 2019-2010

Chicago State University, Chicago, IL 2015-2017

Graduate Chemistry Honor

Student Leadership Award (out of 350 students)

Dean's List (out of 750 students)

PROFESSIONAL MEMBERSHIPS

American Society of Mass Spectrometry 2019-2023

National Honor Society for Woman in Chemistry 2019-2024

American Chemical Society (ACS) 2014-2024

National Organization for the Professional Advancement of Black Chemists and Chemical 2014-2024

PUBLICATIONS

1. Shenault, D., Fabijanczuk, K., Murtada, R., Finn, S., Gao, J. and McLuckey, S., Localization of Methyl Branching Sites on Fatty Acids by Combining Radical Directed Dissociation and Gas-Phase Ion/Ion Chemistry. Manuscript in preparation.
2. Shenault, D. S., Nsiah, S. T., Randolph, C. E., & McLuckey, S. A. (2023). Gas-Phase Ion/Ion Strategy for the Differentiation of Isomeric Bis(monoacylglycero)phosphate and Phosphatidylglycerol Species by Shotgun Lipidomics. Manuscript in preparation.
3. Shenault, D. S. M., McLuckey, S. A., & Franklin, E. T. (2023). Localization of cyclopropyl groups and alkenes within glycerophospholipids using gas-phase ion/ion chemistry. Journal of Mass Spectrometry, 58(4), e4913.
4. Adeoye, T. F., Burch, M., Glenn, T., Scarlett, R., & Shenault, D. S. M. (2021). Mentoring Black Teens during National Pandemics: Mutually Beneficial Service. Purdue Journal of Service-Learning and International Engagement, 8(1), 15.
5. Randolph, C. E., Shenault, D. S. M., Blanksby, S. J., & McLuckey, S. A. (2020). Localization of carbon–carbon double bond and cyclopropane sites in cardiolipins via gas-phase charge inversion reactions. Journal of the American Society for Mass Spectrometry, 32(2), 455-464.
6. Randolph, C. E., Shenault, D. S. M., Blanksby, S. J., & McLuckey, S. A. (2020). Structural elucidation of ether glycerophospholipids using gas-phase ion/ion charge inversion chemistry. Journal of the American Society for Mass Spectrometry, 31(5), 1093-1103.